Understanding functional interplay between PARP-1 and PARP-2 in T cell development and function

Judith Navarro Serer

TESIS DOCTORAL UPF / 2016

Thesis director: Dr. José Yélamos López

Thesis co-director: Dr. Juan Martín Caballero (PRBB)

Grup Poli (ADP-ribosa) polimerases. Programa de Recerca en Càncer, IMIM (Institut Hospital del Mar d'Investigacions Mèdiques)

upf. Universitat Pompeu Fabra Barcelona

IMIM Parc de Salut MAR Barcelona

Institut Hospital del Mar d'Investigacions Mèdiques

A la meva família

ACKNOWLEDGEMENTS

Gràcies,

Al Dr. José Yélamos, mentor y director de este proyecto, por brindarme la oportunidad de realizar mi tesis doctoral en su grupo, por confiar en mí desde el primer minuto sin conocerme, estar siempre dispuesto a enseñarme y por apoyarme y guiarme siempre que lo he necesitado. A mi co-director, Dr. Juan Martín Caballero, por confiar en mí incluso antes de saber que iba a realizar mi tesis, por saber apreciar mi potencial, por las clases magistrales de ratoncitos incluso antes de ser veterinaria y por asesorarme en decisiones importantes y momentos cruciales de mi carrera. Gracias, sin vuestra confianza nada de esto hubiera sucedido.

A Coral, el meu pilar incondicional durant tot aquest temps. No tinc paraules per agrair tot el que m'has arribat a donar dia rere dia durant 3 anys. Per les xarles interminables, hores de piscina, berenars, PCR i cues mortals, per donar-me sempre consell (dins i fora del lab), per ser una segona mare quasi quasi!! Al Dr. Jordi Farrés, el meu segon mentor a l'arribar. Com veus la teva petita padawan ha arribat lluny… jajaja gràcies, pel suport i els consells, per animar-me quan més ho he necessitat i per omplir els passadissos i el laboratori de pura alegria. A mis compis de despacho y de laboratorio, Miguel y Laura. Madre mía, no sé que hubiera hecho sin vuestros cafés, charlas filosóficas, quejas a diario por todo (lo que me habéis aguantado no tiene nombre…), horas al sol cual lagartijas comiendo… en fin, un gracias se queda corto, habéis sido los mejores labmates y compañeros de peripecias que me podía haber encontrado.

A tots els compis de feina durant tot aquest temps, en especial als de la 2a planta del IMIM, desde els meus inicis com a estudiant de màster fins a la defensa de la tesis, per crear el millor ambient de treball que mai em podria haver imaginat i per haver creat el millor equip de volley! (Game of Balls!!!). Menció especial a tots els membres de Pilar Navarro Lab per treballar plegats en moltíssimes ocasions, pel suport científic i perquè m'enduc un bon grapat d'amics d'aquella banda del passadís ☺! Un gràcies immens a Cerutti Lab…per tots els anticossos que us he arribat a robar durant aquest temps, per tot el feedback que

m'heu aportat (científic i personal) tots i cadascú de vosaltres i per estar sempre disponibles i disposats a ajudar-me en tot. Un gràcies especial al Dr. Jordi Sintes, per acceptar ser membre del comité de seguiment del meu projecte i per tots els consells vitals que m'has donat; i a la Dra. Ada Yeste, per ser la millor gympartner que es pot tenir i per ser un dels meus grans suports a la recta final. A la Dra. Erika López, por enseñarme como hacer la primera figura de mi vida jajaj por darme los mejores consejos por los pasillos y por estar siempre dispuesta a echar una mano! Eskerrik asko! A tots els companys de immuno UPF de la 3a planta, per ajudar-me en tot moment sempre que ho he necessitat, y por supuesto a la Dra. Cristina López-Rodríguez, por ser mi tutora de tesis y miembro del comité de seguimiento, por todos los ánimos que siempre me has dado y por todas tus aportaciones constructivas para ayudarme a mejorar. Agrair també al Dr. Gabriel Gil per ser també membre del meu comitè de seguiment, per tots els comentaris i ajuda dessinteresada que m'ha donat. GRÀCIES A TOTS!

A tots els tècnics i treballadors de l'estabulari, en especial a Marisol, Marta, Yoli, Roser, Pep, Tomàs, Juanillo, Bego, Mireia, Sara i Patri. Per estar sempre sempre disponibles per solucionar-me tots els contratemps que he tingut, per fer-me mil favors, per ensenyar-me durant les pràctiques de final de carrera (i per deixar-me seguir aprenent un cop començada la tesis), per tenir sempre un somriure cada cop que he baixat i per cuidarme els ratolinets com si fossin els vostres fills. Gràcies, sou els millors.

A tot l'equip de citometria de flux, a Oscar Fornàs i Eva Julià per tota l'ajuda incondicional amb qualsevol dubte i problema que he tingut. Por supuesto a mi queridísima Erika Ramírez… Sin ti aún estaría pasando tubos… por las charlas non stop durante horas contándonos la vida y por hacerme reir aún estando en la miseria con mis tinciones intracelulares y mis ciclos. Saber que estabas arriba y que me ibas a recibir con la alegría que te caracteriza hacía que fuera menos duro todo! Gràcies, per tot l'esforç i professionalitat que demostreu cada dia.

A tots i cadascun dels meus amics, els de sempre i els que m'enduc d'aquesta gran etapa. A Laura Canal, la millor veïna, amiga i companya d'experiències que puc tenir; a Maria Paredes, per estar allà CADA

DIA i quasi cada hora, per treure'm a patinar i a prendre l'aire en els moments més crítics; a Irene Pérez, per les hores infinites al telèfon, ja que la distància no ens permet veuren's tot el que ens agradaria; a Marta Rebull, Laura Marruecos i Judith Vinaixa, de les millors amistats que m'enduc del meu pas pel PRBB, per aportar pau i tranquil·litat quan més l'he necessitat i escoltar-me SEMPRE; a les dues Martetes, Bainac i Guillen, perquè malgrat estiguem desperdigades, aconseguiu estar allà passi el que passi; a tots els meus amics de Veterinària UAB i del màster de Immuno y por supuesto a todos y cada uno de vosotros, mi segunda familia: Albert, Irene, Eva, Héctor, David y Jordi, lo mejor que me podría haber cruzado, la suerte de este ultimo año. Por todo lo que me habéis demostrado en tan poco tiempo, por animarme y preguntarme siempre, por todas las cenas, comidas, salidas, paseos, risas, salidas en patines y partidas de cartas (y las que quedan…), pero sobretodo por no dejarme sola ni que me rindiera nunca.

A toda mi familia de Tarragona, desde mis queridos abuelitos, hasta mis tíos y primas. Por preocuparos y preguntarme siempre, por vuestro amor incondicional y por esa alegría con la que siempre me recibís cada vez que voy a visitaros y que me dan la fuerza para continuar trabajando en todo lo que hago. A tu, àvia, la meva guia des del cel. M'has vist començar, però estic segura que també em veus acabar i estàs orgullosa. La que més forces em dóna cada dia i la que està sempre present en mi. Finalment, als meus pares, què dir… pel suport i tot l'amor que m'heu brindat sempre durant tot aquest temps. Només vosaltres heu viscut d'aprop tot el meu camí, m'heu ajudat, escoltat i heu donat el millor de vosaltres per a que jo pogués assolir la meva meta (inclús sense entendre molt bé què feia…). Heu sigut el refugi en els meus moments més dèbils (i els que heu rebut més els meus moments de tensió) i els únics capaços de fer que treiés forces d'on fós. Al meu germà… Al que sento més a prop de tots malgrat la distància. Al meu futur post doc i al que arribarà més lluny que ningú (i que jo per suposat). Per compartir peripècies al meu lab, per ajudar-me en la escriptura, per les hores interminables de skype i per fer-me riure sempre, sempre! Sempre seràs el meu petit gran investigador ☺. Us estimo família, sense vosaltres no seria on sóc!

This work has been partially funded by the following grants:

- SAF2014-53467-R, from Spanish Ministerio de Economía y Competitividad (MINECO).

- Fundació La Marató de TV3 (20134130).

This PhD thesis has received funding from IMIM (Institut Hospital del Mar d'Investigacions Mèdiques) for its printing.

We thank The Targeted Mutagenesis and Transgenesis Department at the Mouse Clinical Institute (Institut Clinique de la Souris, MCI/ICS, Phenomin) for establishing the Parp-$2^{f/f}$ mouse mutant line.

ABSTRACT

T-cell homeostasis must be tightly regulated and maintained in order to guarantee appropriate immune responses and prevent immunopathology. This maintenance depends on MHC-TCR interaction and cytokine-mediated signals among others. However, cell intrinsic factors that modulate essential functions in T-cells must be also integrated to support genomic stability and contribute to the control of T-cell homeostasis.

The present work establishes a coordinated role of poly (ADP-ribose) polymerase-1 (PARP-1) and PARP-2 in maintaining T-lymphocyte number and function, demonstrated by the defective thymocyte maturation and diminished numbers of peripheral $CD4^+$ and $CD8^+$ T cells in mice bearing a T-cell specific deletion of PARP-2 in a PARP-1-deficient background. Moreover, this T-cell lymphopenia is associated with an increased DNA-damage and concomitant cell death, leading to highly aggressive spontaneous T-cell lymphomas in PARP-1/PARP-2 double-deficient mice.

Our findings highlight the importance of understanding the specific involvement of both proteins in key biological processes that could have an impact on the development and exploitation of PARP-inhibitors.

RESUM

L'homeòstasi de la cèl·lula T ha d'estar estrictament regulada per tal de garantir una correcta resposta immunitària i prevenir alhora qualsevol problema immunopatològic. Aquest correcte manteniment depèn, entre d'altres, de la interacció amb el complex MHC-TCR i de les senyals de diferents interleuquines. No obstant, hi ha altres factors intrínsecs que intervenen en la modulació de les funcions vitals de la cèl·lula T i que han d'estar també correctament integrats en tot el sistema per tal de garantir una correcta estabilitat genòmica i contribuir en el control de l'homeòstasi de la cèl·lula T.

El present treball estableix el paper coordinat entre els enzims poli (ADP-ribosa) polimerasa-1 (PARP-1) i PARP-2 en el manteniment del nombre i la funció dels limfòcits T, tal i com es demostra amb el defecte en maduració i el descens en el número de cèl·lules $CD4^+$ i $CD8^+$ perifèriques que tenen els ratolins amb deleció de PARP-2 en un background PARP-1 deficient. A més a més, aquesta limfopènia està associada amb un increment del dany en el ADN i una concomitant mort cel·lular, que condueix al desenvolupament espontani de limfomes T molt agressius en els ratolins dobles deficients per PARP-1 i PARP-2.

Els nostres resultats posen de manifest la importància de conèixer correctament el paper específic de les dues proteïnes en processos biològics rellevants, ja que podria tenir especial impacte en el desenvolupament i l'explotació dels inhibidors PARP.

PREFACE

The work presented in this PhD has been accomplished in the Poly (ADP-ribose) polymerases group, led by Dr. José Yélamos, from the Cancer Research Program in the Institut Hospital del Mar d'Investigacions Mèdiques (IMIM), at the Parc de Recerca Biomèdica de Barcelona (PRBB).

The main goal of the group is to improve the knowledge of the roles of poly (ADP-ribosyl)ation, catalyzed by PARP family members (specially PARP-1 and PARP-2), as a critical signalling pathway in both innate and acquired immune response.

Therefore, the core of this PhD thesis is the study of the specific involvement of PARP-1 and PARP-2 in the field of T cell development and function, through the characterization and the study of an innovative conditional mouse model, with a T cell specific deletion of PARP-2 in a PARP-1 deficient background.

Results obtained in the present work could allow then the identification of new therapeutic targets, as current PARP inhibitors used in anti-cancer therapy present inhibitory activity against different isoforms of PARP family, and lack target specificity, thus presenting off-target effects.

INDEX

ABBREVIATIONS

ABC: Avidin-Biotin Complex

ADP: Adenosine Diphosphate

AIF: Apoptosis-Inducing Factor

ALC1: Amplified in Liver Cancer 1

alt-NHEJ: alternative Non-Homologous End-Joining

AMD: Auto-Modification Domain

AMPK: AMP- activated Protein Kinase

AP-1: Activator Protein 1

AP: Apurinic or Apyrimidinic site

APC: Antigen Presenting Cell

APE1: AP Endonuclease 1

APLF: Aprataxin-Like Factor

ARH3: ADP-Ribosylarginine Hydrolase-3

ATM: Ataxia Telangiectasia Mutated

ATP: Adenosine TriPhosphate

ATR: Ataxia Telangiectasia and Rad3-related

Bcl-2: B Cell Lymphoma 2

BER: Base Excision Repair

BM: Bone Marrow

BRCA1/2: BReast CAncer susceptibility genes 1/2

BRCT: BReast Cancer Susceptibility Protein C

BrdU: 5-Bromo-2'-deoxyUridine

C-NHEJ: Clasical Non-Homologous End-Joining

Cenp: Centromere Protein

CldU: 5-Chloro-2'-deoxyuridine

cTEC: cortical Thymic Epithelial Cell

CTL: Cytotoxic T Cell

DBD: DNA-Binding Domain

DDR: DNA Damage Response

DN: Double Negative

DNA-PK: DNA-dependent Protein Kinase

DP: Double Positive

DSBR: Double Strand Break Repair

DSBs: Double Strand Breaks

EDTA: Ethylene Diamine Tetraacetic Acid

ELISA: Enzyme-Linked Immunosorbent Assay

ER: Estrogen Receptor

ES: Embryonic Stem

FACT: Facilitates Chromatin Transcription

FBS: Fetal Bovine Serum

FOXO: Forkhead Box

Foxp3: Forkhead box p3

GC: Germinal Center

H2AX: Histone H2A member X

HDL: High Density Lipoprotein

HMGP: High Mobility Group Proteins

HP: Heterochromatin Protein

HR: Homologous Recombination

HRD: Homologous Recombination Deficient

HRP: Horseradish Peroxidase

I-CAM: Intracellular Adhesion Molecule

I.P: IntraPeritoneal

ICOS: Inducible T-cell Co Stimulator

IdU: 5-Iodo-2'-deoxyuridine

IFN-γ: InterFeroN γ

IL: Interleukine

iT_{reg}: Induced T Regulatory

L-CAM: Liver Cell Adhesion Molecule

LDL: Low Density Lipoprotein

LSP: L-Selectin Positive cells

MAR: Mono (ADP-ribose)

MHC: Major Histocompatibility Complex

MMR: Mismatch Repair

MRN: MRE11-RAD50-NBS1

mTEC: medullary Thymic Epithelial Cell

mTOR: mammalian Target Of Rapamycin

NAD: Nicotinamide Adenine Dinucleotide

NER: Nucleotide Excision Repair

NFAT: Nuclear Factor of Activated T-cells

NFkappaB: Nuclear Factor of activated B cells

NHEJ: Non-Homologous End-Joining

NKAP: NFkappaB Activating Protein

NLS: Nuclear Localization Signal

NoLS: Nucleolar Localization Signal

$nT_{reg:}$ Natural T Regulatory

O.D: Optical Density

O.N: Over Night

PAR: Poly (ADP-ribose)

PARG: Poly (ADP-ribose) Glycohydrolase

PARP: Poly (ADP-ribose) Polymerase

PCR: Polymerase Chain Reaction

PD-1: Programmed Death-1

PPAR: Peroxisome Proliferator-Activated Receptor

PS: PhosphatidylSerine

R.T: Room Temperature

RAG 1/2: Recombinant-Activating Gene

RBC: Red Blood Cell

RIP: Receptor Interaction Protein

ROR: Retinoid-related Orphan Receptor

RPA: Replication Protein A

RTE: Recent Thymic Emigrants

SCID: Severe Combined ImmunoDeficient

SIRT1: Sirtuine 1

SLO: Secondary Lymphoid Organ

SP: Single Positive

Sp1: Specifiticy Protein 1

SREBP1: Sterol Regulatory Element-Binding Transcription factor 1

SSBR: Single Strand Break Repair

SSBs: Single Strand Breaks

TBX: T-box Transcription Factor

TCR: T cell receptor

T_{FH}: T Follicular Helper

Th: T Helper

TIF1β: Transcriptional Intermediary Factor 1 β

TNF: Tumour Necrosis Factor

TNP-KLH: Trinitro-Phenyl-conjugated Keyhole Limpet Hemocyanin

T_{reg}: T Regulatory

TRF2: Telomeric Repeat Binding Factor 2

V-CAM: Vascular Cell Adhesion Molecule

V(D)J: Variable Diversity and Joining

WAT: White Adipose Tissue

XRCC: X-ray Repair Cross-Complementing

INTRODUCTION

1 POLY (ADP-RIBOSE) POLYMERASES

1.1 The poly (ADP-ribose) polymerase family

Poly (ADP-ribose) polymerases (PARP) comprise a family of seventeen ADP-ribosyltransferases that transfer ADP-ribose unit of β-NAD^+ on specific target amino acids[1]. While PARP-9 and PARP-13 are enzymatically inactive[1,2], other members of the family (PARP-3, PARP-4, PARP-7, PARP-8, PARP-10, PARP-11, PARP-12, PARP-14, PARP-15, and PARP-16) present mono (ADP-ribose) (MAR) activity[1,3,4], consisting of the transfer of a single mono-ADP-ribose molecule to target proteins. The rest of the PARP family proteins (PARP-1, PARP-2, PARP-5a, PARP-5b, and PARP-6) exhibit a proper poly(ADP-ribosyl)ation activity (PARylation)[1] which involves the homopolymerisation of the ADP-ribose unit of β-NAD^+ on specific amino acids. The resulting poly(ADP-ribose) (PAR) polymers vary in size and branching, conferring diverse functional and structural effects on target proteins[1–3].

PARylation is a dynamic process with a rapid turnover, as indicated by the short half-life of the polymer, which is degraded by the action of at least two ADP-ribose-protein hydrolases: poly (ADP-ribose) glycohydrolase (PARG), which accounts for the majority of the hydrolase activity, and ADP-ribosylarginine hydrolase-3 (ARH3)[2,5,7,10–12]. Different PARG isoforms have been related with functions in the nucleus, cytosol or mitochondria[9]. These enzymes reverse the reaction

by the cleavage of the polymers into free mono or poly (ADP-ribose)[4,7–9], which can also serve as signalling molecules. PARylation of target proteins controls an extensive range of cellular processes, such as DNA repair, transcriptional regulation, mitochondrial function, RNA interference, cell division, and regulation of other protein modifications, such as ubiquitynilation[5] (**Figure 1**).

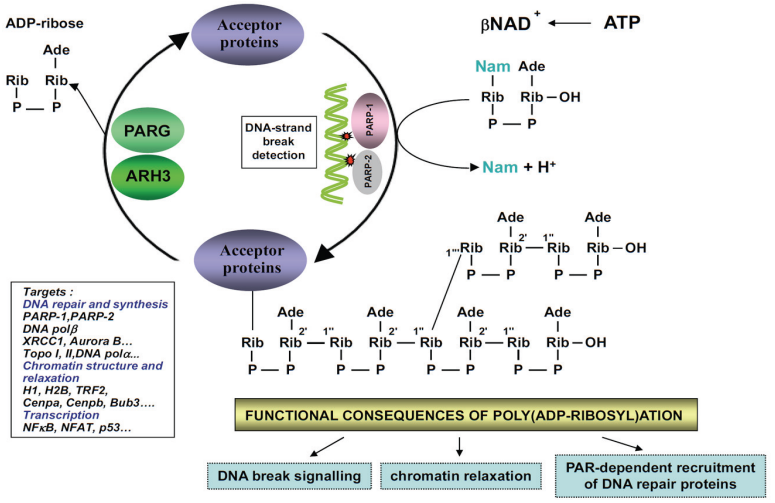

Figure 1. PARylation reaction activated by DNA strand breaks. PARP-1 and PARP-2 recognize DNA-strand breaks generated by genotoxic agents, causing their activation. Activated enzymes hydrolyze β-NAD^+ and transfer ADP-ribose moiety onto amino acid residues of acceptor proteins, which are involved in numerous biological processes. PARG and ARH3 reverse the reaction by releasing ADP-ribose units. Adapted from[4].

PARP enzymes share a conserved catalytic domain, with a PARP signature motif acting as active site[8,10]. Characterization of this domain was established based on the catalytic residue Glu988 of PARP-1, considered the founding member and the most extensively studied enzyme[1,3,5,7,8]. PARP catalytic domain is located at the C-terminus of

the protein, adjacent to some other motifs related to RNA or DNA binding, protein-protein interactions or cell signalling[8,12], such as tryptophan–tryptophan–glutamate (WWE) domains, PAR-binding zinc finger (PBZ), macroH2-like domains, and ubiquitin- or RNA-binding motifs[1,3,8] (**Figure 2**).

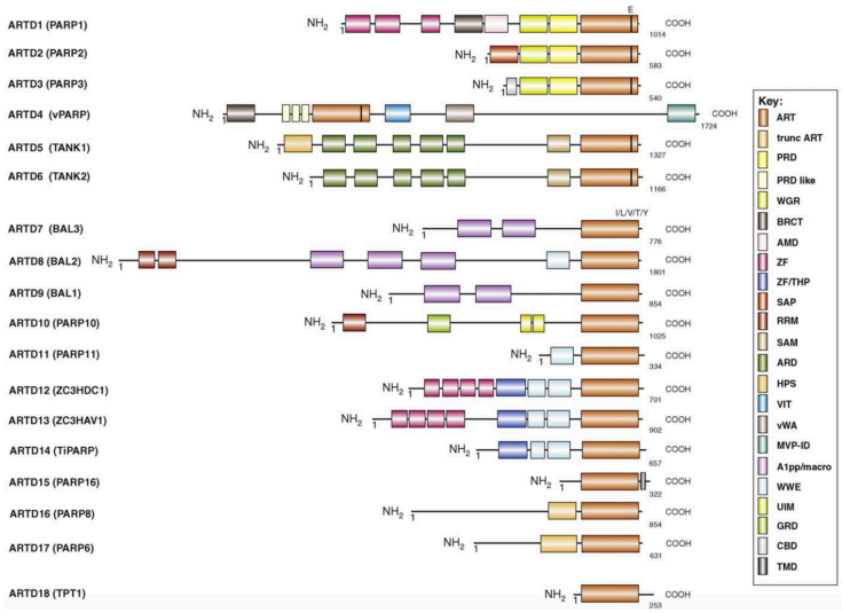

Figure 2. Schematic domain architecture of the PARP family. The most important protein domains are illustrated in color boxes. PARP domain is the region considered homologous to PARP signature (residues 859–908 of PARP-1). Other domains that are present in PARP family are WGR domain, Zn fingers, macrodomains, or WWE domain. Adapted from[3].

1.2 DNA-damage dependent PARPs

DNA-damage dependent PARPs (PARP-1, PARP-2 and PARP-3) are a subfamily of PARP proteins whose catalytic activity is initiated in response to DNA strand breaks[8,13–15]. PARP-1 (113 kD) and PARP-2 (62 kD) PARylated target proteins in order to modify their properties

and recruit DNA repair proteins, decondensate chromatin, regulate transcription factors or signal DNA breaks.

PARP-1 is a highly conserved nuclear protein in mammals, but absent in yeast, encoded by a gene located at position 1q41-42 and 1H5 in human and murine genome respectively, consisting of 23 exons spanning ~43 kb[4,16]. Its protein structure comprises three major domains: (i) DNA-binding domain (DBD), which contains two Zn fingers responsible for DNA break and protein-protein interactions[11], and a nuclear localization signal (NLS)[13,17,18]; (ii) a central auto modification domain (AMD), containing a Breast Cancer Susceptibility Protein C (BRCT) motif responsible for protein-protein interactions; and (iii) domain F, or catalytic domain, which is located at C-terminal region and contains a NAD^+-binding domain and the highly conserved 'PARP signature' motif[4,7,10,11,17,19] (**Figure 3A**). Recently, a third zinc finger motif has been identified in human PARP-1 C-domain, and it is conserved among all PARP-1 homologs. Interestingly, this new Zn finger region is not crucial for DNA binding activity, but it is involved in protein-protein interactions, contributing to PARP-1 DNA-dependent stimulation[11]. Under normal conditions, inactive PARP-1 is located in the nucleopasm[7].

PARP-2 is also a nuclear protein encoded by the *Parp-2* gene, mapping to position 14q11.2 and 14C1 in the human and murine genome respectively[18]. PARP-2 protein was discovered due to the presence of residual DNA-dependent PARP activity in embryonic PARP-$1^{-/-}$ fibroblasts[18,20]. It lacks N-terminal Zn fingers and BRCT domain

present in PARP-1 protein, but it is also composed by (i) a N-terminal region, containing a highly basic DBD, a NLS signal, and nucleolar localization signal (NoLS)[13,17,18]; (ii) a central domain E, homologous to domain E of PARP-1, which acts both as the interacting interface with different partners (e.g., DNA polymerase β, and DNA ligase III), and as an auto modification domain[4,13,21]; and (iii) a domain F, or C-terminal catalytic domain, which is the common feature among all PARP enzymes (**Figure 3B**).

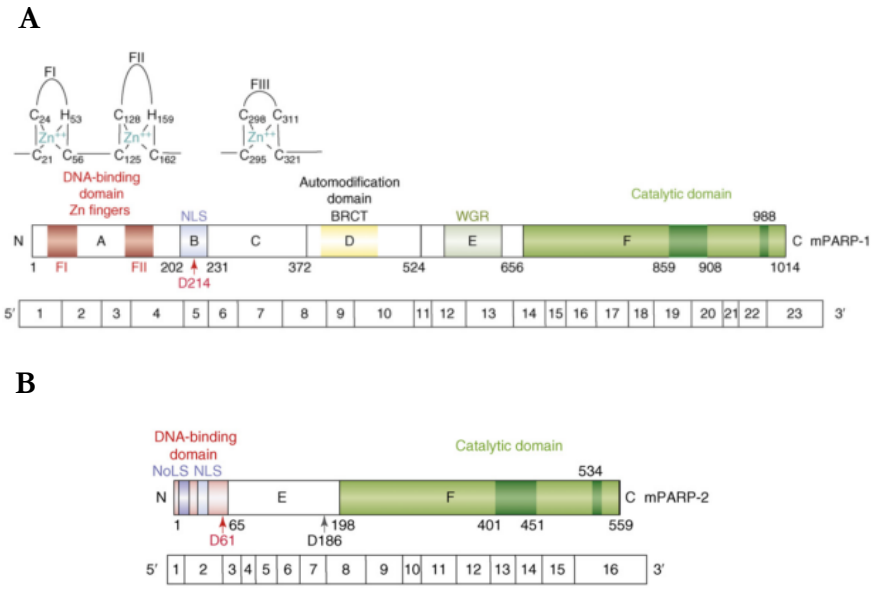

Figure 3. Schematic representation of mouse *Parp-1* and *Parp-2* genes and their protein domains. In this figure there are represented the different protein domains present in (A) PARP-1, such as DBD (with Zn fingers and NLS), AMD (with BRCT motif), and catalytic domain; and in (B) PARP-2: DBD (with NLS and NoLS), domain E (essential for DNA-dependent activity); and domain F or catalytic domain. Adapted from[13].

Although PARP-2 only represents 5% to 10% of the total PARP activity in response to DNA damage[13], its catalytic domain shows a

~69% homology with PARP-1 catalytic domain[10,12]. However, PARP-1 and PARP-2 differ in their DBD architecture, indicating different substrates specificities for these two proteins[4,7,12,18]. Although both enzymes present affinity for nicked DNA and are involved in base excision repair (BER) and single strand break (SSB) repair[22] (SSBR), PARP-1 is also a sensor of double-strand breaks (DSBs) and can bind to unrepaired DNA[23], whereas PARP-2 recognizes gaps and flaps structures[10,13,23]. Moreover, recent studies using single-molecule AFM imaging corroborate a higher specificity of PARP-2 to SSBs over DSBs and undamaged DNA[23]. Other differences are that PARP-1 preferentially PARylated the linker histone H1 and PARP-2 present a major tendency to modify a core histone[4,15].

PARP-3 (60 kD) has also been described as a DNA-dependent PARP because of its role in cellular response to DNA DSBs, facilitating the recruitment of aprataxin-like factor (APLF)[24]. It displays a 61% similarity with PARP-1, and presents a key function in genomic integrity and mitotic division[10,24]. However, as mentioned before, PARP-3 differentiates from the other DNA-dependent PARPs in being a mono (ADP-ribosyl) transferase, and in requiring partner proteins, including Ku70/Ku80, to efficiently recruit to DNA damage sites[22,24].

1.3 Physiological roles of PARP-1 and PARP-2

1.3.1 DNA repair

Cellular genome is continuously exposed to both exogenous (irradiation, drugs), and endogenous (reactive oxygen species, eroded telomeres, intermediates of immune and meiotic recombination) genotoxic agents that induce DNA damage. In order to protect their genome from the consequences of accumulation of unrepaired lesions, cells have developed a complex DNA repair network[4,14,25]. If these lesions are not properly repaired because cells are defective in DNA repair pathways, they can first block genome replication and transcription, leading to mutations or DNA aberrations, and eventually to cancer[4,13,26]. In this context, DNA damage dependent PARPs are playing a dual role in the DNA damage response, as they act as DNA damage sensors and signal transducers through their physical association with or by the PARylation of their partner proteins, including histones, topoisomerases or DNA helicases[4,8,12].

PARP-$1^{-/-}$ and PARP-$2^{-/-}$ cells present an increased spontaneous genomic instability[20,27,28], but PARP-2 null mice do not exhibit a propensity for the development of spontaneous tumours[14,28], and PARP-$1^{-/-}$ mice develop spontaneous mammary and liver tumours with long latency and at a low incidence[27,29]. However, both enzymes present a synergistic role in accelerating tumour development in p53 null mice[28,30], and PARP-$1^{-/-}$ and PARP-$2^{-/-}$ mice are both sensitive to high dose of ionizing radiation and alkylating agents[13].

Altogether, it is well established that PARP-1 and PARP-2 have key shared functions in cellular responses to DNA damage, as they both heterodimerise, have common nuclear binding proteins, and contribute to SSBR/BER processes[21,31]. In addition, mice double deficient for both proteins are not viable and die at the onset of gastrulation, suggesting a critical role for PARP-1 and PARP-2 during embryonic development[14].

1.3.1.1 PARP-1 and PARP-2 in BER

BER is a defence mechanism cells use for the repair of DNA lesions caused by oxidative base damage, various forms of alkylating damage, apurinic/apirimidinic (AP) sites, and uracil residues in DNA[31]. The reaction is initiated by the generation of AP sites by DNA glycosylases, and followed by the action of AP endonuclease 1 (APE1) and other polymerases and ligases, which complete their repair through strand incision[31,32].

The role of PARP-1 and PARP-2 proteins in BER has been well established[21], as both PARP enzymes are required simultaneously to act at the BER complex, especially for the recruitment step of X-ray repair cross-complementing I (XRCC1) at the damage sites[10,21,33]. Both proteins can interact with other BER repair factors, such as DNA polymerase β and DNA ligase III[33]. However, recruitment of XRCC1 protein is dependent on PARP-1 activity[34–36], but not on PARP-2[33], and both proteins accumulate with different kinetics. While PARP-1 accumulates fast and transiently, PARP-2 has a delayed and persistent accumulation at repair sites[33], suggesting a role of PARP-2 protein in

later steps of the BER process[21,33]. This is supported by the fact that PARP-1 has higher affinity for SSB and PARP-2 for gaps or flaps structures that correspond to more advanced repair intermediates. Therefore, PARP-1 and PARP-2 have key but distinct roles in the spatial and temporal organization of SSBR/BER processes[13].

1.3.1.2 PARP-1 and PARP-2 in nucleotide excision repair (NER) and mismatch repair (MMR).

NER pathway is a process that initiates with the detection of helix-distorting lesions, and acts as a repairer of DNA lesions caused by UV radiation, mutagenic chemicals, or chemotherapeutic drugs[32]. Although there are several studies that indicate an activation of PARP-1 in UV-induced DNA damage and a role in lesion recognition steps in NER, the exact mechanistic features of its roles remain unclear[37–39]. There is some data that points out the possibility that PARP activation at the lesion site may be induced in order to remodelate chromatin therefore facilitating NER pathway in DNA[10].

MMR pathway plays an important role in repairing small insertions/deletions acquired during DNA replication[32], and also in predisposition to cancer and response to therapy. However, the implication of PARP-1 and PARP-2 in this pathway remains largely unclear[4].

1.3.1.3 PARP-1 and PARP-2 in DNA double-strand breaks repair (DSBR)

Proper repair of DSBs is crucial for a correct genomic stability, and they can be repaired by two major mechanisms, homologous recombination (HR) or non-homologous end-joining (NHEJ), depending on the context of DNA damage[32,40,41].

HR is a multistep process that also serves as a repair mechanism of DSBs, especially in yeast and bacteria, which acts at the S or G2 phase of the cell cycle[32]. HR is initiated by SSBs that, when accumulated on S phase, result in increased collapsed fork and are converted to DSBs. This process requires various proteins, including the MRE11-RAD50-NBS1 (MRN) complex for end-processing, replication protein A (RPA), and BReast Cancer Susceptibility (BRCA) 1 and BRCA2 to finally repair DNA lesions[26,32]. PARP-1 and PARP-2 play a role in early detection of stalled or collapsed forks, in the recruitment of Mre11 for subsequent end processing, and allowing RAD51 to proceed to HR pathway[42].

NHEJ is the major repair pathway in mammalian cells, and relies basically on DNA-dependent protein kinase subunit (DNA-PKcs), which binds to the heterodimer of Ku70/Ku80 proteins, and the XRCC4-DNA ligase complex IV[43,44]. Several studies report a functional interaction between PARP-1 and other proteins of NHEJ, as it can stimulate DNA-PKcs through ADP-ribosylation, and PARP-1/Ku80 double null mice present early embryonic lethality[27,44]. Moreover, mice deficient for PARP-1 or PARP-2 and ataxia

telangiectasia mutated (ATM), a signalling kinase that initiates the transduction cascade at DSBs sites, are also not viable and die at embryonic stages[16].

Interestingly, recent data suggest that PARP-1 is involved in an alternative pathway of DSBR, named alternative NHEJ (alt-NHEJ), which cooperates when the classical NHEJ (C-NHEJ) or HR pathways are compromised[45]. It consists of another simple end joining process with similar repairing proteins already present at DSB, although ligation is mainly orchestrated by DNA ligase III or I, instead of DNA ligase IV present in the C-NHEJ process[46,47](**Figure 4**). Alt-NHEJ is present in tumour cells lacking HR or C-NHEJ pathway, thus being an interesting target for inhibition[45]. Taking all this data into account, it is suggested a role of PARP-1 in NHEJ, although the specific roles of PARP-2 in this field remain unknown.

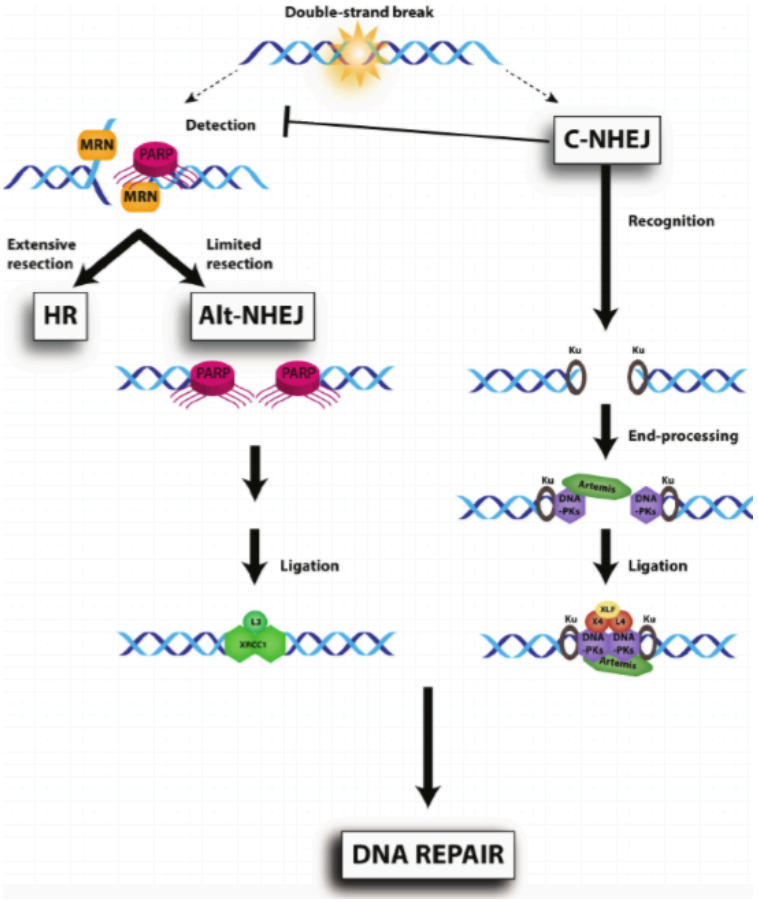

Figure 4. Schematic representation of DNA repair by HR, C-NHEJ, and alt-NHEJ. NHEJ process accounts for 75% of DSBR and it can be divided in two major sub-pathways, the classical one that depends on DNA-PKs, and the alt-NHEJ, which acts as a back-up repair pathway when C-NHEJ is compromised. In contrast to C-NHEJ, PARP-1 is the mainly promoter of this alternative process that also involves the activity of different factors, including XRCC1 and DNA-ligase III. Adapted from[48].

1.3.2 Chromatin structure, epigenetic modifications and transcription

In response to DNA damage, chromatin undergoes rapid decondensation to facilitate genome monitoring by enhancing access of proteins involved in DNA damage response (DDR)[49]. Chromatin is

organised in repeated units called nucleosomes, which at the same time contain two heterodimers of the core histones H2A and H2B, one tetramer of the core histones H3 and H4, and 146 bp of DNA[50]. Chromatin can change its functional properties by post-translational modifications of residues within histones, including phosphorylation, methylation, ubiquitination, and ADP-ribosylation[51]. Several studies establish that glutamic acid residues in histone H1 and histone H2B can be modified by PARylation[52,53]. Recently, it has been discovered that PARP-1, but not PARP-2, covalently modifies all four core histones on specific lysine residues[51]. PARylation has also been related to non-histone chromosomal proteins modifications, including High Mobility Group Proteins (HMGP) and the heterochromatin proteins HP1a and HP1b[54]. ATM/ATR/DNA-PK mediated phosphorylation of the histone H2A member X (γ-H2AX) is another form of signal to recruit DNA damage response factors, such as histone chaperone facilitates chromatin transcription (FACT) (Spt16/SSRP1), DNA-PK, and PARP-1, in order to promote DNA repair and amplify DNA signalling[55,56].

Through its role in chromatin dynamics, PARP-1 also plays a role in transcription regulation, as it can act as promoter-specific co-regulator of different transcriptional regulators, such as Nuclear Factor of activated B cells (NF-κB), Nuclear Factor of Activated T cells (NFAT), and Specificity Protein 1 (Sp1), among others[57,58]. Recently, it has been shown that PARP-1 also regulates chromatin structure and transcription through PARylation of different chromatin remodelling enzymes, including the histone demethylase KDM5B, chromatin

remodels DNMT-1 and ISWI, and more recently Amplified in Liver Cancer 1 (ALC1)[2,56,59]. It has also been described that PARP-1 dependent PARylation sets up a transient repressive chromatin structure that helps blocking DNA transcription, facilitating DNA repair[60]. Altogether, gene regulation by PARP-1 can have both positive and negative effects on transcription[2,61,62].

Regarding PARP-2, it can also act as positive or negative regulator of transcription, although it seems to be mostly a positive cofactor that regulates ~600-1000 genes[63]. It can interact with different transcription factors, such as nuclear receptors Estrogen Receptor (ER)α and Peroxisome Proliferator-Activated Receptor (PPAR)[64]. PARP-2 can also regulate gene expression by its relation with Transcriptional Intermediary Factor 1 (TIF1β) and Heterochromatin Protein (HP) 1α[65]. Moreover, Szántó et al. recently found that PARP-2 is a suppressor of Sterol Regulatory Element-Binding Transcription factor 1 (SREBP1), as demonstrated by the higher levels of cholesterol present in PARP-$2^{-/-}$ mice[66].

Both PARP-1 and PARP-2 can also interact with Sirtuin 1 (SIRT1) deacetylase, which at the same time controls a wide range of transcription factors, such as p53, Peroxisome proliferator-activated receptor-gamma co-activator 1α (PGC-1α) and Forkhead Box (FOXO) family, thus playing a role in regulating metabolic homeostasis in response to dynamic NAD^+ levels[67].

1.3.3 Replication stress

Several studies suggest a relationship between perturbations in replication fork, increased replication-dependent DNA damage and tumorigenesis[68,69]. As oncogene activation can be induced by replication stress[70], DNA replication must be perfectly regulated in order to prevent genomic instability, and therefore carcinogenesis[70–72].

Apart from the coordinated role of PARP-1 and PARP-2 in detecting and restarting stalled replication forks, via Mre11-dependent initiation of HR[42], recent work in mouse erythroblasts establish a specific role of PARP-2 in the replication stress response in erythropoiesis. Parp-2$^{-/-}$, but not Parp-1$^{-/-}$, mice display various biomarkers of replication stress in their erythroblasts, including accumulation of γ-H2AX in S-phase, micronuclei formation, and increased CHK1 and RPA phosphorylation, leading to chronic anaemia in steady-state conditions[73]. PARP-2 is also involved in other processes with high proliferation rates, similar to patterns observed in mice with ATR-hypomorphism, which display an impaired replication stress response[74]. In addition, PARP-2 has been identified in a genome-wide RNAi screen for replication stress response genes, pointing towards a specific function of this enzyme in replication stress responses[75].

1.3.3.1 Cell cycle regulation

Assembly of cell cycle progression, checkpoint controls, and other processes involved in maintenance of genomic integrity is crucial for a proper cellular proliferation. Impairments on cell cycle progression or

checkpoint dysfunctions can lead to uncontrolled proliferation and accumulation of DNA damage, producing genomic instability[76].

Several works point toward a specific involvement of PARP-2 enzyme in cell cycle progression. Erythroid progenitors from PARP-2 deficient mice present G2/M cell cycle arrest[63], and PARP-2 overexpression in Human Embryonic Kidney 293 (HEK293) cell line prevents premature G1 exit[77]. Moreover, PARP-2 represses various cell cycle-related genes, such as p21, RB, E2F1 and c-MYC, through its interaction and recruitment of histone deacetylases HDAC5 and HDAC7, and histone methyltransferase G9a[77]. p21 is an important cell cycle regulator that acts both in G1/S and G2/M transitions[78] and presents a functional interaction with PARP-2 enzyme, suggested by the new-born lethality observed in double knock out mice for both proteins[63].

1.3.4 Chromosome segregation

Centromere is a crucial structure for the correct chromosome segregation during mitosis and meiosis, and is part of the kinetochore, a complex molecular machine that serves as the interface between sister chromatids and the mitotic spindle[79,80]. The attachment of sister chromatids to kinetochores is controlled by several proteins to maintain correct genomic stability and avoid missegregation and centrosome amplification, processes that can occur in cancer cells. Post-translational modifications of centromere-associated proteins are a mechanism of regulation of the kinetochore assembly and centromere activity[79].

PARP-1 and PARP-2 can interact with centromere protein A (Cenpa), centromere protein B (Cenpb), and mitotic spindle checkpoint Bub3, allowing the decondensation of centromere and the access of DNA repair processes[79,81]. While PARP-1 is associated with centromeric/pericentromeric heterochromatin region, PARP-2 is more specific to centromeric chromatin[81]. Moreover, PARP-2$^{-/-}$ cells display DNA-damage-induced kinetochore defects that lead to missegregation in mitotic cells, which is also present in PARP-2 null male mice. These defects are related with impaired centromeric heterochromatin and/or abnormal spindle configurations[82]. Altogether, PARP-1 and PARP-2 play an important role in chromosome segregation through the maintenance of centromeric heterochromatin structure and/or mitotic spindle integrity.

1.3.5 Telomere maintenance

Telomeres are structures of heterochromatin domains, formed by repetitive DNA TTAGGG repeats, that cap the end of chromosomes in order to protect them from being recognised as DSBs. Telomere shortening occurs in each cell division and is related with ageing, as progressive loss of telomeric protection causes cell cycle arrest and/or apoptosis[83]. PARP-2 presents physical and functional association with Telomeric Repeat Binding Factor 2 (TRF2), a protein that protects telomeres by its remodelling into large duplex loops (t-loops). This interaction can be due to covalent heteromodification of the dimerization domain of TRF2, or non-covalent binding of PARP-2 to the TRF2 DNA-binding domain[84]. In both cases, TRF2 regulation modifies t-loop structures of the telomeres in order to facilitate access

to the repair machinery, suggesting an additional role of PARP-2 in telomerase integrity. The role of PARP-1 in telomerase integrity is less clear, although it has been proved that it can bind to a nonamer region closely resembling telomeric repeats[85].

1.3.6 Cell death

Persistent stress conditions force cells to activate different cell death pathways in order to kill themselves. These processes include apoptosis, autophagy, and parthanatos, depending on their regulation. Apoptosis, or Programmed Cell Death type 1, is the most well known one and consists in an energy-dependent process characterized by DNA fragmentation, protein cleavage, chromatin condensation and formation of apoptotic bodies[86,87]. The choice between activation of the apoptotic pathway or other cell death processes is dependent on Adenosine Triphosphate (ATP) intracellular levels[88].

Apoptosis is initiated by the activation of PARP activity, mainly by PARP-1, leading to NAD and ATP consumption[86], thus impacting the intracellular energetic pool. As PARP-1 acts as a critical death substrate, PARP activity has to be immediately limited by cleaving the enzyme in two inactive fragments[89,90] due to the action of the protease caspase-3[91,92]. In this way, PARP-1 cleavage is considered a hallmark of apoptosis, as it conserves ATP levels to facilitate the conversion of necrosis to apoptosis[2,86,89,90](**Figure 5**).

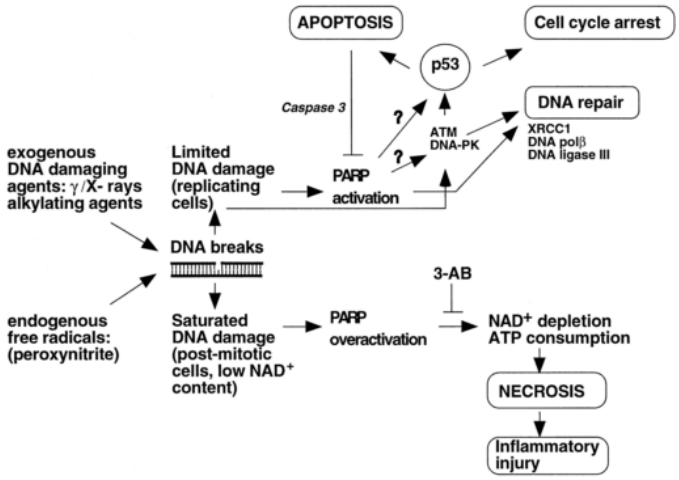

Figure 5. Role of PARP in DNA damage surveillance and inflammatory injury. PARP proteins can act as DNA surviving factor under physiological conditions, as they permit the recruitment of DNA repair machinery to undergo DNA repair pathways. Engagement of the apoptotic pathway occurs downstream of p53 activation; however, the molecular determinants to go through cell cycle arrest, apoptosis or DNA repair remain unknown. Adapted from[19].

However, it was recently described that cells lacking this cleaved molecule response normally to treatment with anti-Fas, tumour neurosis factor α, γ- irradiation, and dexamethasone, indicating that PARP is dispensable in apoptosis[93]. Regarding PARP-2, array analysis suggest that it is not a regulator of the expression of apoptotic genes, but it is involved in regulating transcription of cell cycle factors[86].

Recycling and self-degradation of cellular damage components is called autophagy, whose regulation depends on serine/threonine kinases, such as mammalian Target Of Rapamycin (mTOR), and AMP-activated Protein Kinase (AMPK) activation. Interestingly, PARP-1 supports AMPK activation, which at the same time

phosphorylates and activates it[66]. Therefore, PAR activity, mainly orchestrated by PARP-1, can modulate and enhance autophagy by up streaming mTOR-AMPK regulators[86,94].

Parthanatos is another form of caspase-independent cell death, which includes translocation of mitochondrial factors. PARP-1 overactivation has been attributed to depletion of cellular energy and release of death effector Apoptosis-Inducing Factor (AIF) from the mitochondria to the nucleus, thanks to its PAR-binding motif. This facilitates chromatin condensation and DNA fragmentation[86,95].

PARP enzymes can also be involved in necroptosis, a novel idea of programmed necrosis that involves the action of Receptor-Interacting Proteins (RIPs), which are activated upon stress, and promote cell death through the stimulation of the NF-kB pathway[86,96]. As RIP factor contains a PARP binding motif, PARP-1 can modulate necroptosis directly through its physical association with RIP, or indirectly by poly (ADP-ribosyl)ation of target necroptotic effectors[86].

1.3.7 Other functions of PARP-1 and PARP-2 proteins

PARP-1 and PARP-2 are also involved in a wide range of other cellular processes and compartments, such as immune system, inflammation, or metabolic diseases.

1.3.7.1 Immune system and inflammation

PARP-1 and PARP-2 regulate the development and maturation of immune cells and erythrocytes. PARP-2 causes shortened lifespan of erythrocytes and impaired differentiation of erythroid progenitors, leading to chronic anaemia[63]. Genetic inactivation of this enzyme in mice also results in bone marrow failure in response to low doses of γ-irradiation, suggesting a role of PARP-2 in DNA damage response in hematopoietic stem cell compartment, maintaining its homeostasis under stress conditions[73]. On the other hand, PARP-1 has been involved in the terminal differentiation of other cell types, including monocytes, dendritic cells, and natural killer cells[97].

Both PARP-1 and PARP-2 enzymes can regulate inflammation, acting as cofactors of pro-inflammatory regulators (e.g., NF-kB, NFAT, activator protein -1 (AP-1), Sp1), or due to their regulation of non-classical regulators of inflammation, such as SIRT1. Activation of these transcription factors allows the production of pro-inflammatory cytokines and chemokines (e.g., TNF-α, IL-1β, IL-16, IL-12 or IL-8), selectins, adhesion molecules (e.g., I-CAM, V-CAM, or L-CAM), and other inflammatory factors[97]. Diverse inflammatory pathologies are PARP mediated, and they involve the central nerve system, bones, gastro intestinal tract (e.g., colitis), skin, kidneys, muscle, cardiovascular system (e.g., atherosclerosis), or the respiratory system (e.g., asthma) among others[2].

The two enzymes seem to be playing a role in autoimmune diseases (e.g., autoimmune encephalomyelitis or autoimmune nephritis), and

recently PARP-1 inhibition has been described as a target for autoantibodies in autoimmune pathologies[98].

1.3.7.2 Regulation of cell differentiation processes

PARP-2 is described to be crucial for meiosis I and haploid gamete differentiation, as PARP-$2^{-/-}$ male mice exhibit hypo fertility associated with an impaired spermatogenesis characterized by a delayed nuclear elongation[82]. This enzyme is involved in other cellular differentiation processes, such as adipocyte differentiation or thymic development. PARP-2 null mice present lipodystrophy, comprising adipodegeneration, reduced weight of white adipose tissue (WAT)[99], and an impaired number of double positive (DP) thymocytes, due to compromised survival of these cells undergoing TCRα recombination. Thus, PARP-2 in T-cell prevents the activation of DNA damage-dependent apoptotic pathway during rearrangement of TCRα in positive selection, suggesting a critical role of this enzyme in T-cell survival during thymopoiesis[28]. It has also been established that in some myeloid leukaemia cell lines PARP inhibition can facilitate differentiation toward monocyte/macrophage or neutrophil granulocyte linage, suggesting a role of PARP enzymes in bone-marrow-derived cells differentiation[100].

On the other hand, several studies point out that PARP-1 is involved in B and T-cell differentiation and functions. Knocking PARP-1 out, defective Variable Diversity and Joining (V(D)J) recombination in Severe Combined Immuno Deficient (SCID) mice can be partially rescued, indicating that these enzyme can act as anti-recombinogenic

factor during T and B cell maturation[101]. Interestingly, PARP-1 is also important in terminal osteogenic differentiation, as PAR polymer is released from dead osteoblasts to become part of the extracellular matrix[102].

1.3.7.3 Metabolic regulation and disease

PARP-1 and PARP-2 seem to be determinant in fat and glucose metabolism. Their deletion or pharmacological inhibition protects from aging and high-fat feeding-induced obesity, as PARP-1 and PARP-2 knock out mice present higher catabolism in brown adipose tissue and liver respectively[103]. Furthermore, PARP-$2^{-/-}$ mice display reduced serum levels of High Density Lipoprotein (HDL), detailing an impaired cholesterol transport[66]. Although the role of PARP-1 in cholesterol homeostasis is unclear, its inhibition normalises pathological Low Density Lipoprotein (LDL)/HDL ratios, suggesting a connection of this enzyme with fat homeostasis[104].

Regarding glucose metabolism, several data suggest that PARP-1 deletion improves insulin sensitivity, enhancing mitochondrial biogenesis in skeletal muscle. On the other hand, PARP-2 plays a role in β cell proliferation in the pancreas, as PARP-$2^{-/-}$ mice present smaller islets, reduced insulin content, and do not respond properly after a glucose load[103]. Type I diabetes, type II diabetes, and metabolic syndrome are pathologies related with an impaired insulin sensibility or impaired glucose/lipid metabolism, processes that are PARP dependent[103].

2 PARP PROTEINS AS THERAPEUTIC TARGET IN CANCER

Genomic instability is a hallmark of cancer that has served for its treatment by radiotherapy and DNA-damaging chemotherapy[105]. In this context, PARP inhibitors have emerged as anticancer drugs, as single agents or in combination with other DNA damaging compounds[106–108] or monoclonal antibodies[109]. When using them as chemo/radipotentiators, PARP inhibitors can enhance genomic dysfunction by compromising tumour DNA damage repair mechanisms. However, current drugs only target the catalytic site of PARP enzymes, which is very similar among all PARP family members, and there are not available specific PARP inhibitors[100,107,110].

Published data in 2005 identify that PARP inhibitors can induce cell death in BRCA-deficient cell lines, through the concept of 'synthetic lethality': two non-lethal mutations do not have any effect when occurring individually, but, when in combination, they lead to cell death[105,111]. Cancer cells that lack BRCA-1 and BRCA-2 function have an impaired HR pathway. PARP inhibition in these defective cells leads to an accumulation of SSBs that can be converted into DSBs, but cannot be repaired by HR in the absence of BRCA proteins, therefore resulting in mitotic failure and cell death[106,111] (**Figure 6**).

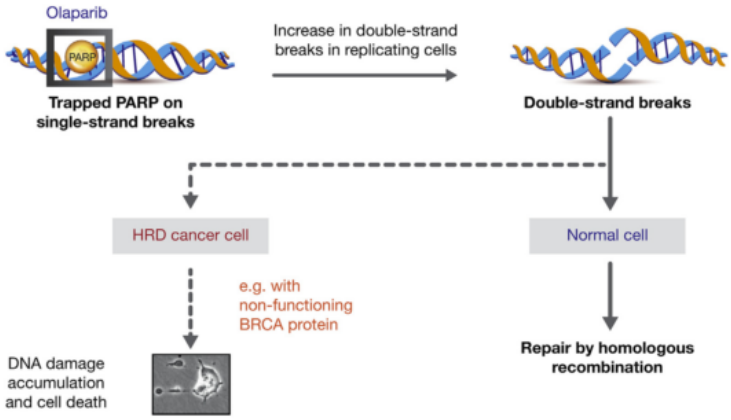

Figure 6. Synthetic lethality in homologous recombination deficient (HRD) cells. SSBs can be repaired in normal conditions by PARP proteins. PARP inhibitors, as olaparib, trap inactivated PARP onto SSBs, leading to DSBs accumulation during replication. In tumor cells harboring HRD, such as BRCA-1/2 mutation, this leads to DNA accumulation and cell death. Adapted from[105].

Synthetic lethality concept seems to be a promising approach in cancer treatment; in fact, early clinical trials have demonstrated significant activity of single-agent PARP inhibitors (e.g., olaparib) in BRCA-deficient breast and ovarian cancer[111,112] (**Table 1**). Apart from BRCA-mutant, there are several other sporadic cancers that present different mechanisms of BRCA deficiency and/or other HR repair components, a phenomenon called 'BRCAness'[106,107,113]. It has been described that tumour cells exhibiting this phenotype can be also sensitive to PARP inhibition[96,114,115]. In this line, defects in XRCC2 and XRCC3, or disruption of critical components of HR pathway, such as RAD51, RAD54, DSS1, RPA1, NSB1, ATM, ATR, CHK1, or CHK2, have been described to cause hypersensitivity to PARP inhibition[108,115,116]. A major challenge is now to identify patients with

different HR repair deficiencies than BRCA-1 or BRCA-2, which can respond to PARP inhibition treatment. Accordingly, there are some genetic approaches using siRNA to silence genes related with DNA repair and testing sensibility of transfected cells to PARP inhibition[117].

Table 1. Current PARP inhibitor compounds in clinical development. Adapted from[118].

Drug name	Pharmaceutical company	Current investigational phase in breast cancer
Olaparib (AZD2281)	AstraZeneca	Phase 3 studies in adjuvant and advanced settings in germline BRCAm breast cancer
Veliparib (ABT-888)	Abbvie	Phase 3 study in neoadjuvant setting in combination with carboplatin and standard therapy in triple-negative breast cancer
		Phase 2/3 studies in advanced setting as combination therapy in germline BRCAm breast cancer
Niraparib (formerly MK-4827)	Tesaro	Phase 3 study in advanced setting in germline BRCAm breast cancer
Talazoparib (BMN-673)	BioMarin Pharmaceuticals	Phase 3 study in advanced setting in germline BRCAm breast cancer
		Phase 2 studies in advanced setting in BRCAm breast cancer
		Phase 2 study in advanced setting in germline BRCA intact breast cancer
		Phase 2 study in neoadjuvant setting in BRCAm breast cancer
Rucaparib (formerly AG-14699)	Clovis Oncology	Phase 2 study in advanced setting in patients with known germline BRCAm solid tumors
		Phase 2 study in adjuvant setting in triple-negative breast cancer or germline BRCAm breast cancer
CEP-9722	Teva Pharmaceutical Industries	Phase 2 study in advanced setting in solid tumors

BRCAm, *BRCA1/2* mutation-associated

As PARP inhibitors are actually therapeutic drugs in cancer, it is important to develop isoform-specific PARP inhibitors, to design new therapeutic approaches and to identify new target molecules[4]. Therefore, there are some issues that need to be addressed: (i) to elucidate the specific roles of PARP-1 and PARP-2 in DDR and monitoring, (ii) to study long-term effects of PARP inhibitors, as both enzymes are involved in tumour suppression[28], and (iii) to explore the specific details of DDR pathways to overcome resistances caused by BRCA-1/2 reactivation[119].

3 T CELL DEVELOPMENT AND FUNCTION

3.1 T-cell development in the thymus

T cell development is initiated in the thymus, when bone marrow-derived lymphocytes precursors migrate to the cortical region of the organ through blood vessels, and undergo different maturation stages to become functional T-lymphocytes, which exit the thymus, and colonize the peripheral lymphoid tissues[120,121].

Development of T cells in the thymus is a complex process that includes four different maturation stages based on the expression of the co-receptors CD4 and CD8[120]: double negative (DN, $CD4^-CD8^-$), double positive (DP, $CD4^+CD8^+$), single positive CD4 (SPCD4, $CD4^+CD8^-$), and single positive CD8 (SPCD8, $CD4^-CD8^+$). The DN subset is a heterogeneous subpopulation that can be divided in four groups based on the expression of additional markers CD25 and CD44. DN1 ($CD25^-CD44^+$)[122–124] acquire expression of CD25 and become DN2 thymoctyes ($CD25^+CD44^+$), which migrate from premedullary to inner cortex of the thymus to proliferate and become DN3a cells ($CD25^+CD44^{lo}$), when they start to down-regulate the expression of CD25 to become DN3b ($CD25^{lo}CD44^{lo}$) thymocytes[125]. At DN3b stage, thymocytes acquire T lineage commitment and start to express the heterodimeric T-cell receptor (TCR) pair, designated as α/β or γ/δ in some cases[126,127]. Therefore, cells start to rearrange TCR β, γ, or δ gene loci through recombination of variable (V), diversity

(D), and joining (J) segments, a process called V(D)J recombination[128], which requires the up regulation of Recombination-Activating Gene (RAG) 1 and RAG2. Survival of DN2, DN3 and DN4 subsets depends on IL-7 signals and the up regulation of B-cell lymphoma 2 (Bcl-2) pro-survival molecule, as demonstrated by the 100-fold reduction of these subpopulations in IL-7 or IL-7R knock out mice[125,129]. A successful TCRβ rearrangement, and its intracellular expression, is crucial for the assembly with pre-Tα chain and CD3 molecules. This produces pre-TCR complex that leads to DN4 differentiation ($CD25^{-}CD44^{lo}$), before undertaking a strong proliferation to generate αβ lineage DP thymoctyes, the most abundant population in the thymus[125, 128,130–132].

Once DP thymocytes have survived to previous β-selection, they initiate TCRα locus rearrangement by using 3′ gene segments, encoding the α-chain variable region (Vα), and 5′ gene segments, encoding the α-chain joining region (Jα)[125,131]. To final rearrange Vα to Jα segments, RAG1 and RAG2 are re-expressed again, in order to detect and cleave recombination sequences located adjacent to the coding V and J segments[125,128,131,133]. After primary rearrangement, cells that are not positively selected can undergo multiple cycles of TCRα chain recombination, providing several opportunities for being positively selected, and maximising the chances of forming a functional αβ TCR complex[96,125,131]. During rearrangement of TCR chains, RAG activity introduces DSBs lesions between V, D, or J coding sequences, and flanking recombination signal sequences[133,134]

that must be properly repaired by different enzymes such as XRCC4, ligase IV, and DNA-PKc complex (catalytic subunit, Ku80 and Ku86), among others[135].

Cortical thymic epithelial cells (cTEC) express high density of major histocompatibility complex (MHC) class I and class II molecules associated with self-peptide, and interact with αβ-$TCR^+CD4^+CD8^+$ DP thymocytes in order to determine their fate[136]. First, TCR with low affinity for self-antigens leads to cell dead by neglect/apoptosis, and only thymocytes with intermediate levels of TCR signalling undergo positive selection. MHC class specificity determines the lineage fate, as recognition with MHC I signals initiates $CD8^+$ differentiation, whereas contact with MHC class II induces $CD4^+$ lineage commitment[137]. Selected DP-committed cells go through negative selection in the thymic medulla, which consists of acute apoptosis of cells that express TCR with excessive avidity for self-ligands[137–139], and it is critical for the acquisition of central and peripheral T-cell tolerance[140]. As cells undergo maturation, they decrease CD69 and CD24 expression, while CD62L expression is upregulated[141,142]. Lastly, CD4SP and CD8SP cells are exported from the thymic medulla to the periphery lymphoid tissues, where they are named recent thymic emigrants (RTE), to continue their maturation in order to gain functional competency and enter the long-lived naive peripheral T cell pool[143] (**Figure 7**).

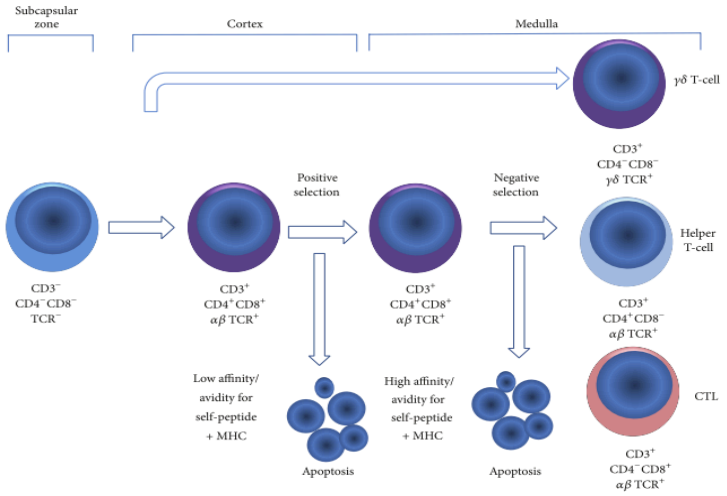

Figure 7. T-cell progenitor differentiation and maturation within the thymus. Rearrangement and assembly of β and α chain of TCR, and up regulation of CD4 and CD8 markers give rise to DP thymocytes. This subset goes through positive selection when entering in contact to self-antigens presented by cTECs. Cells that present low affinity for self-MHC die by apoptosis, while positively DP cells migrate to the medulla, where they bind to restricted antigens presented by medullary thymic epithelial cells (mTECs). Excessive affinity for self-peptides leads to cell death by negative selection. Single positive $CD4^+$ and $CD8^+$ thymocytes are then exported to periphery to continue their maturation, and give raise to $CD4^+$helper T-cells or $CD8^+$ cytotoxic T lymphocytes (CTL). Adapted from[138].

3.2 Peripheral T cell development

RTE are the most recent population exported from the thymus present in peripheral lymphoid tissues that matures phenotypically and functionally within secondary lymphoid organs (SLO) to become naïve T cells. There, they contact with other cell types, such as dendritic cells, and cytokines (e.g., IL-7), to gradually down regulate CD24 expression and up-regulate Qa2, CD28, CD45RB, and IL-7Rα cell surface markers[144]. Recent data indicates that NF-kB Activating Protein (NKAP) transcriptional repressor is crucial to complete T cell

maturation, as demonstrated by the complete block of RTE further maturation when NKAP is missing[143].

Peripheral naïve T cell pool must be constantly maintained in a limited space, balancing the loss and the replacement of cells through the continuous output from the thymus. Homeostasis of naïve compartment must also preserve the diversity and policlonality in order to detect and destroy an extent number pathogens[145,146]. IL-7 produced by stromal tissues is critical in controlling survival of both peripheral CD4 and CD8 naïve T cells[147–150], as demonstrated by the impaired naïve T cell survival when injecting mice with monoclonal IL-7 specific blocking antibodies[147].

When naïve CD4 and CD8 subsets present in SLO enter in contact with an antigen, they progress through memory T cells, which can be differentiated based on phenotypic and functional criteria[138,151]. In the case of murine cells, naïve pool does not express CD44, but express CD62L, being the last one a critical player in their migration into peripheral lymphoid tissues. On the other hand, memory population express higher levels of CD44[151], and it can be divided in central memory ($CD62L^{+}CD44^{hi}$) and effector memory T cells ($CD62L^{-}CD44^{hi}$)[138]. In addition, memory population present other functional differences compared to naïve compartment: (i) they are more efficient in responding to an infection, (ii) they are less dependent on co-stimulation for an optimal response, and (iii) they secrete several cytokines, such as IL-4 and interferon γ (IFN-γ), whereas naïve cells mainly produce IL-2[151].

Upon interaction with cognate antigens presented by antigen-presenting cells (APCs), naïve $CD4^+$ cells can also acquire effector function and differentiate into T helper 1 (Th_1), Th_2, Th_{17}, T follicular helper (T_{FH}), and T regulatory (T_{reg}) cells, depending on co-stimulatory molecules and cytokine signals present in the microenvironment[138,152–157]. IFN-γ and IL-12 signals promote Th_1 polarization, a subset of effector cells characterized by the production of IFN-γ, IL-18, IL-2, and Tumor Necrosis Factor β (TNF-β), and their involvement in responses against intracellular microorganisms[138]. On the other hand, Th_2 cells are induced by the presence of IL-4 from dendritic cells and activated macrophages, and they are capable to secrete IL-4, IL-5, and IL-13, necessary for humoral immunity to control helminths, as well as other extracellular pathogens. Regarding Th_{17} population, they differentiate from naïve $CD4^+$ cells in response to TCR signalling in the presence of IL-6 and Transforming Growth Factor β (TGF-β), but not IL-23[158]. Accordingly, they secrete IL-17 and IL-22, and they play a role in battle extracellular bacteria and fungi[153].

T_{FH} are a subset of effector cells that express high levels of surface markers Inducible T-cell Co-stimulator (ICOS), CD40L, Programmed Death-1 (PD-1), and CD84 among others[138]. They are specialized cells that provide help to B cells and are crucial for a correct germinal centre (GC) formation, affinity maturation, and the development of antibodies from memory B cells[159]. T_{FH} secrete IL-21, an important cytokine involved in GC B-cell responses, which at the same time promotes T_{FH} phenotype, creating a positive feedback loop[154]. T_{reg} cells are mainly produced by the normal thymus and have an essential role

in maintaining immune homeostasis, controlling and preventing pathological T cell immune responses[153,156,160]. Their differentiation and function depends on Forkhead box p3 (Foxp3) expression and they can develop from $CD4^+CD25^+$ cells in the thymus (also named natural T or nT_{reg}) or from $Foxp3^-$ naïve cells in the periphery, through TGF-β induction (induced or iT_{reg})[161,162] (**Figure 8**).

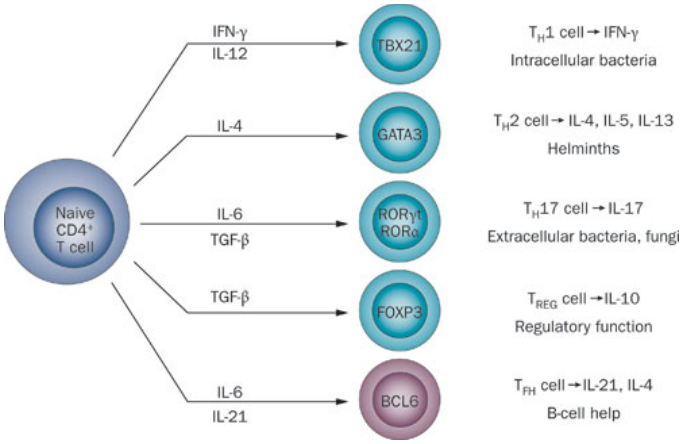

Figure 8. $CD4^+$ naïve T cell differentiation into different T-cell subsets. Depending on cytokine signals present in the microenvironment, $CD4^+$ naïve T cells can up regulate the expression of different transcription factors, which determine their fate and the cytokines they will produce. Abbreviations: BCL6, B-cell lymphoma 6; GATA3, GATA-binding factor 3; RORα, retinoid-related orphan receptor-α; RORγt, retinoid-related orphan receptor-γt; TBX21, T-box transcription factor TBX21. Adapted from[163].

APCs also interact with naïve $CD8^+$ cells in order to differentiate them into CTL, which control virus infections and intracellular bacteria[164]. $CD8^+$ cells acquire effector functions and start to proliferate when receiving co-stimulatory signals, such as CD28, in combination with prolonged exposure to both antigen and IL-12[164,165]. Recently, IL-6 has also been suggested as a contributor to $CD8^+$ cell development

through the induction of inflammation, although its role in this field has not been fully established[166]. Once cytotoxic $CD8^+$ cells have been differentiated and activated, they secrete anti-infectious cytokines, such as TNF and IFN-γ, as well as death-inducing molecules (e.g., granzyme B) or perforin that are crucial for the elimination of infected cells[167].

4 ROLE OF PARP PROTEINS IN T CELLS

The role of PARP-1 and PARP-2 in T cell development and function has just been started to elucidate. It is known that both proteins are expressed in the thymus, especially in cortex and sub-capsular areas where immature lymphocytes proliferate[97]. PARP-2 has also been described as an important player in T cell survival during thymopoiesis, as demonstrated by the reduction in DP lifespan in *Parp-2*, but not *Parp-1,* knock out thymocytes. These *Parp-2*$^{-/-}$ DP cells present a defective TCRα repertoire toward the 5'Jα segments, leading to DP death when initiating multiple rounds of TCRα rearrangements[168]. Thymocytes of *Parp-2* deficient mice exhibit an increased apoptosis, associated with DSBs accumulation, but their survival and development can be restored in a p53$^{-/-}$ background although leading to thymoma development[28].

On the other hand, PARP-1 plays a role in peripheral T cells, as PARP-1 deficient T cells display a defective proliferation in the absence of APCs and upon activation with anti-CD3 plus anti-CD28 antibodies[169]. PARP-1$^{-/-}$ cells decreased proliferation is associated with an increased number of CD4^{+}CD25^{+}Foxp3^{+} T cells[170–172] but normal suppressor function, suggesting that this enzyme might be playing a role in T_{reg} differentiation and development[171]. Thus, the excessive suppressive role of T_{reg} in PARP-1 deficient mice results in an impaired CD4^{+} cell proliferation and IL-2 production[172]. On the other hand, interaction of PARP-1 with NFAT leads to a positive regulation

of NFAT-dependent cytokine transcription, including IL-2 and IL-4[173].

As mentioned before, regarding T cell activation, PARP-1 is involved in the regulation of NFAT, which is critical for T lymphocyte functionality. Concretely, NFATc1 and NFATc2 can be physically associated or poly (ADP-ribosyl)ated by PARP-1 enzyme, delaying NFAT nuclear export[174]. PARP-1 also regulates, positively or negatively, other genes encoding for various chemokines and cytokines, this way contributing through Th_1/Th_2 balance[169]. This was demonstrated by the increased production of cytokine IFN-γ and chemokines Xcl1, Ccl4 and Ccl9[173], and the reduction of IL-4, IL-5 and IL-13 production in PARP-$1^{-/-}$ T cells, suggesting a role of this enzyme in Th_2 differentiation[97,175]. Newest data demonstrate that PARP inhibitors completely protect $CD8^+$ T cells from radical-induced apoptosis and restored their cytotoxic function, suggesting that PARP-1 activation is crucial in protecting CD8 T cells from apoptosis upon oxidative stress[176].

More findings described a role of PARP-1 in adaptive immune responses by both modulating ability of dendritic cells to stimulate T cells or directly affecting T and B cell function[177,178]. Although PARP-1 deficient mice present normal T independent responses, reduced levels of immunoglobulin IgG2a and increased levels of IgA and IgG2b were observed in these animals[177].

HYPOTHESIS AND OBJECTIVES

PARP-1 and PARP-2 belong to a family of enzymes that play a role in the DDR, due to their physical association with and/or PARylation of target proteins, causing chromatin decondensation around the lesion, recruitment of DNA repair machinery and accelerated DNA repair[11,14]. Although the deletion of one of these PARPs does not lead to any major physiological failure, highlighting the redundancy in DNA damage repair pathways, simultaneous deficiency of PARP-1 and PARP-2 leads to embryonic lethality[14]. Moreover, these two enzymes have been described to be involved in T-cell biology[97], PARP-1 in biasing Th1 phenotype[169], and PARP-2 affecting DP survival and T cell development[168]. However, the effect of PARP-1 and PARP-2 double deficiency in T cells remains unknown.

The aim of the present thesis is to study the functional interaction between the two most important DNA damage dependent PARP's, PARP-1 and PARP-2, in T cell development, homeostasis and function. To achieve this general objective, we proposed the following goals:

1. To generate and characterize a mouse model with a PARP-2 specific deletion in CD4 expressing cells, in a PARP-1 deficient background.
2. To explore the specific and redundant roles of PARP-1 and PARP-2 in T cell development.
3. To determine the specific and redundant roles of PARP-1 and PARP-2 in T cell function.

MATHERIAL AND METHODS

1 MOUSE MODEL

1.1 Mice

Parp-1$^{-/-}$ and transgenic mice for cre-recombinase driven by Cd4 promoter (Cd4-cre) have been previously described[25,179]. The *Parp-2*$^{flox/flox}$ (*Parp-2*$^{f/f}$) mice were established at the MCI/ICS (Institut Clinique de la Souris-ICS-MCI, Phenomin, Illkirch, France). For the construction of the targeting vector, a 0.34 kb fragment encompassing exon 8 was amplified by PCR (from 129S2/SvPas ES cells genomic DNA) and subcloned in an MCI proprietary vector. This MCI vector contains a LoxP site as well as a floxed and flipped Neomycin resistance cassette. A 3 kb fragment (corresponding to the 5' homology arm) and a 2.87 kb (corresponding to the 3' homology arms) were amplified by PCR and subcloned in step1 plasmid to generate the final targeting construct.

The linearized construct was electroporated in 129S2/SvPas mouse embryonic stem (ES) cells.. After selection, targeted clones were identified by PCR using external primers and further confirmed by Southern blot with 5' and 3' external probes. Two positive ES clones were injected into C57BL/6J blastocysts and male chimeras derived gave germline transmission.

Parp-2$^{f/f}$ mice were crossed with Cd4-cre-transgenic mice producing heterozygous offspring, which were then crossed with *Parp-1*$^{-/-}$ mice.

The resulting *Cd4-cre; Parp-2$^{f/-}$; Parp-1$^{+/-}$* animals were subsequently backcrossed to generate all the possible cohorts.
B6.SJL-PtprcaPepcb/BoyCrl strain (Charles River Laboratories, Wilmington, MA) was used as congenic CD45.1 mice. These animals were crossed with wild-type C57BL/6J mice (CD45.2) in order to generate heterozygous CD45.1/2 cohorts (B6SJL) for using them as recipient in bone marrow competitive-reconstitution transplant experiment.

All mice were in a B6 genetic background and kept under specific pathogen-free conditions at the Barcelona Biomedical Research Park (PRBB). Colony management was carried out by the use of the PRBB Animal House informatics platform. The PRBB Animal Care Committees approved all studies.

1.2 Mouse genotyping

1.2.1 Tail biopsy

We used a tail biopsy (between 0.5 and 1.5 cm) obtained during mice weaning to genotipically characterize the mice. After that, all littermates were marked on their ears for future recognition. Tail tissues were kept at -20ºC in an eppendorf tube duly identified before the DNA genomic extraction.

1.2.2 Genomic DNA extraction

Extraction of genomic DNA was obtained from the tail biopsy by using an isopropanol precipitation protocol, showed in **box 1.**

Box 1

DNA extraction

1. Add 400µl of lysis buffer (100mM TrisHCl pH8.5 + 5mM EDTA + 200mM NaCl + 1% SDS) and 12 µl of proteinase K (stock at 20 mg/ml).
2. Vortex.
3. Over-night incubation at 55ºC.
4. Vortex and spin down at 17000xg for 8 minutes.
5. Transfer the supernatant into a new tube and add 350µl of isopropanol (mix thoroughly until see precipitated DNA).
6. Spin down at 17000xg for 5 minutes and remove the supernatant.
7. Add 350µl 70% ethanol.
8. Spin down at 17000xg for 3 minutes and remove the supernatant.
9. Let pellet dry and resuspend it in 500µl of TE buffer (1M TrisHCl pH8.0 + 0.5M EDTA).
10. Keep samples at R.T until their use.

1.2.3 PCR

PCRs were performed at any of two thermo cyclers (MyCycler Thermalcycler; BioRad®, Hercules, CA and MJ Mini™ Personal Thermal Cycler; BioRad®, Hercules, CA). Primers (Sigma-Aldrich®, St.Louis, MO) were stored at 10µM. The other reagents we used came from Roche® (Basel, Switzerland) and were stored at -20ºC. **Table 2** shows primer sequences and **Table 3** PCR conditions for each gene.

Table 2. Primers sequences used for mice genotyping.

Gene	Primer 1 (5'-3')	Primer 2 (5'-3')	Primer 3 (5'-3')	WT size	KO modified gene size
Parp-1	ggccagatgcgcctgtccaagaag	ggcgaggatctcgtcgtgacccatg	cttgatggccgggagctgcttcttc	200 bp	700bp

Gene	Forward sequence (5'-3')	Reverse sequence (5'-3')	WT size	KO modified gene size
Cd4-Cre	tcgatgcaacgagtgatgaggttcg	acagcattgctgtcacttggtcgtg	0 bp	300 bp
Parp-2 $^{flox/flox}$	ccccaaaccagagtcccatcc	ctcgagtgtttcactgtgagggag	497 bp	657 bp

Table 3. PCR conditions used for each gene.

Gene	Mix composition per sample	PCR conditions
Parp-1	10,2 µl H_2O 2µl Buffer 10x (without Mg) 1,2µl Mg_2Cl 50mM 0,3µl dNTPs 25mM 1µl Primer 1, 10µM 1µl Primer 2, 10µM 2µl Primer 3, 10µM 0,3µl Taq Polymerase 2µl DNA	94º – 3 min **35 cycles** (94º – 30 sec; 66º-30 sec; 72º 1 min) 72º – 5 min Keep at 4º
Parp-2$^{flox/flox}$	11,05µl H_2O 2µl Buffer 10x (without Mg) 0,6µl Mg2Cl 50mM 0,15µl dNTPs 25mM 2µl Primer forward, 10µM 2µl Primer reverse, 10µM 0,2µl Taq Polymerase 2µl DNA	94º – 3 min 35 cycles (94º – 30 sec; 62º-30 sec; 72º 1 min) 72º – 5 min Keep at 4º
Cd4-Cre	12,88µl H_2O 2µl Buffer 10x (without Mg) 1,2µl Mg_2Cl 50mM 0,16µl dNTPs 25mM 0,8µl Primer forward, 10µM 0,8µl Primer reverse, 10µM 0,16µl Taq Polymerase 2µl DNA	94º – 5 min **35 cycles** (94º – 30 sec; 56º-30 sec; 72º 30 sec) 72º – 5 min Keep at 4º

2 CELL EXTRACTION PROTOCOLS

For all cell preparations, mice were previously sacrificed by CO_2 asphyxia.

2.1 Thymus cell preparation

Thymocytes were obtained from the thymus, which is anatomically located in the anterior superior mediastinum (under the ribs, attached above the heart in the midline). After its removal, thymus was dispersed through a 100μm Nylon filter (BD Falcon) into a 50ml tube, with the help of a 2ml syringe plunger (B. Braun Melsungen AG, Germany). Cells were resuspended in 20 ml of cold PBS.

2.2 Spleen cell preparation

Splenocytes were obtained from the spleen, an organ of predominantly lympho-erythropoietic function, which is situated inside the abdomen at the left superior abdominal quadrant. After its removal, the spleen was also dispersed through a 100μm Nylon filter (BD Falcon) into a 50ml tube with the help of a 2ml syringe plunger (B. Braun Melsungen AG, Germany). Because splenocytes have higher tendency to form aggregates they were resuspended in 10 ml PBS containing 2mM EDTA and 5% Fetal Bovine Serum (FBS).

2.3 Bone marrow cell preparation

Bone marrow (BM) cells were obtained directly from the femur (and tibia when necessary) that was separated from the mouse muscle with the help of scissors and scalpel. Then, the two femur's head were cut and cold PBS was forced through with help of a 0,5x16mm insulin 100UI syringe (KD Medical GmbH Hospital Products, Berlin,

Germany) until the bone was left totally white, meaning that all BM cells were collect. Finally, these cells were passed through a 100μm Nylon filter (BD Falcon, Franklin Lakes, NJ) with the help of a 2ml syringe plunger. Cells were resuspended in 10 ml PBS.

2.4 Cell count

After all cell preparations total number of cells was counted.

For thymocytes, an aliquot of cells was resuspended at 1:20 dilution in cold PBS. In contrast, for splenocytes, an aliquot of cells was separated and treated following protocol detailed in **box 2**.

Box 2

Spleen cell count protocol

1. Resuspend cells with ACK lysis buffer (BioWithaker, Walkersville, MD) at 1:3 dilution, in order to lyse red blood cells (RBC).
2. Incubate for 4 minutes at room temperature (R.T).
3. Recover osmolarity by adding PBS to obtain a 1:5 cell dilution.
4. Separate an aliquot of this cell dilution and resuspend it 1:1 in PBS.
5. Separate another aliquot of this 1:10 solution and resuspendit it 1:1 in a TURK solution (1% acetic acid + 1/2500 Blue Giemsa in H_2O) to finally lyse the remaining RBC and contrast live cells (final dilution 1:20).

BM cells were first resuspended in cold PBS at 1:10 dilution and after in 1:1 TURK dilution, to finally obtain a 1:20 dilution before its count.

In all cases, thymocytes, splenocytes and BM cells were counted with a Bürke chamber (Brand Scientific GMBH, Wertheim, Germany).

3 FLOW CYTOMETRY

3.1 Cell surface staining

Cell suspensions were first washed with 1ml of cold PBS, resuspended in PBS containing 5% of FBS (staining buffer) and incubated with appropriate antibodies at 4ºC covered from light. RBCs were lysed using ACK lysis buffer and dead cells were excluded using DAPI staining, following protocol detailed in **box 3**. All antibodies used are indicated in **Table 4. Table 5** indicates the combinations used for the identification of each population.

Box 3

Cell surface staining protocol

1. Pippette the necessary number of cells into a new eppendorf and centrifuge at 300xg for 5 minutes.
2. Discard the supernatant and resuspend the pellet in staining buffer containing the appropriated antibodies (1µl antibody per 10^6 cells in 100µl of staining buffer).
3. Incubate for 20 min at 4°C protected from the light.
4. Wash with 1ml PBS 1X and centrifuge at 300xg for 5 minutes.
5. Resuspend in 150 µl ACK lysing buffer and incubate for 4 min at RT.
6. Wash with 1 ml PBS 1X and centrifuge at 300xg for 5 minutes.
7. Resuspend cells in 300µl of PBS 1X and DAPI (dilution 1:100, final concentration 2 µg/ml).

Table 4. Primary antibodies used in flow cytometry.

Antigen	Fluorochrome	Clone	Isotype	Dilution	Company	Reference
CD4	PE	GK1.5	Rat (LEW) IgG2b, κ	1/100	BD Pharmingen™	553730
	PE-Cy7		Rat IgG2b, κ		BioLegend ®	100422
CD8	APC	53-6.7	Rat IgG2a, κ	1/100	BioLegend ®	100712
	FitC					100706
	PE	H35-17.2	Rat IgG2b, κ		BD Pharmingen™	550798
CD62L	PE	MEL-14	Rat IgG2a, κ	1/100	eBioscience	12-0621-81
	APC			1/100		17-0621-81
CD44	PerCP/Cy5.5	IM7	Rat IgG2b, κ	1/100	BD Pharmingen™	560570
	FitC					553133
TCRβ	PE	H57-597	Armenian Hamster IgG2, λ1	1/100	BD Pharmingen™	553172
	PerCP/Cy5.5		Armenian Hamster IgG	1/100	BioLegend ®	109228
CD45R (B220)	PerCP	RA3-6B2	Rat IgG2a, κ	1/100	BD Pharmingen™	553093
CD24	FitC	M1/69	Rat (DA) IgG2b, κ	1/100	BD Pharmingen™	553261
	PE	30-F1	IgG2c, κ	1/100	eBioscience	12-0241-81
CD127	APC	A7R34	Rat IgG2b, κ	1/100	BioLegend ®	135011
CD69	PerCP	H1.2F3	Hamster IgG	1/100	BioLegend ®	104520
CD3	APC-Cy7	17A2	Rat (SD) IgG2b, κ	1/100	BD Pharmingen™	560590
CXCR5	FitC	2G8	Rat IgG2a, κ	1/100	BD Pharmingen™	561989
CD278 (ICOS)	PE	7E.17G9	Rat IgG2b, κ	1/100	BioLegend ®	117405
CD279 (PD-1)	APC	J43	Armenian Hamster IgG2, κ	1/100	BD Pharmingen™	562671
GL7	FitC	GL7	Rat (LOU) IgM, κ	1/100	BD Pharmingen™	562080
CD45.1	PE	A20	Mouse A.SW IgG2a, κ	1/100	BD Pharmingen™	553776
	APC-Cy7					560579
CD45.2	FitC	104	Mouse SJL IgG2a, κ	1/100	BD Pharmingen™	553772
IgD	PE-Cy7	11-26c.2a	Rat IgG2a, κ	1/100	BioLegend ®	405719
BrdU	APC	3D4	Mouse IgG1, κ	1/50	BD Pharmingen™	51-23619L
Active caspase 3	FitC	C92-605	Rabbit IgG	1/5	BD Pharmingen™	51-68654X
Annexin V	FitC	-	-	1/25	BD Pharmingen™	51-65874X
γH2AX (Ser139)	FitC	JBW301	Mouse IgG1	1/10	Millipore	17-344

Table 5. Cell surface phenotype defining each population.

	Population name	Cell surface phenotype
Thymus	Double positive (DP)	$CD4^+$ $CD8^+$
	Double negative (DN)	$CD4^-$ $CD8^-$
	Single positive CD4 (CD4SP)	$CD4^+$ $CD8^-$
	Single positive CD8 (CD8SP)	$CD4^-$ $CD8^+$
	Single positive mature CD4	$TCR\beta^{hi}$ $CD24^{lo}$ $CD4^+$ $CD8^-$
	Single positive mature CD8	$TCR\beta^{hi}$ $CD24^{lo}$ $CD4^-$ $CD8^+$
Spleen	Naïve CD4 cell	$CD4^+$ $CD62L^+$ $CD44^{lo}$
	Naïve CD8 cell	$CD8^+$ $CD62L^+$ $CD44^{lo}$
	Central memory CD4 cell	$CD4^+$ $CD62L^{hi}$ $CD44^{hi}$
	Central memory CD8 cell	$CD8^+$ $CD62L^{hi}$ $CD44^{hi}$
	Effector memory CD4 cell	$CD4^+$ $CD62L^-$ $CD44^{hi}$
	Effector memory CD8 cell	CD8+ $CD62L^-$ $CD44^{hi}$
	T follicular helper cell	$CD3^+CD4^+CXCR5^+PD1^+ICOS^+$

3.2 Intracellular staining

For intracellular staining, cells were first stained for cell surface markers (if necessary), fix and made permeable by using BD Cytofix/Cytoperm (BD Bioscience), and finally stained for specific intracellular antigens. During all protocol cells were kept with wash buffer for an efficient binding and washing (**box 4**).

Box 4

Intracellular staining protocol

1. Stain for cell surface markers (if necessary).
2. Fix and permeabilize cells.
   a. Resuspend the cells in 100 µl of BD Cytofix/Cytoperm Buffer.
   b. Incubate for 15-30 min at 4°C protected from the light.
   c. Wash with 1ml of Perm Wash Buffer 1X and centrifuge at 300xg for 5min.
   d. Resuspend in 300 µl of PBS+5%FBS and leave the samples over night (O.N) at 4°C or continue to step 3.
3. Incubate with intracellular antigens for 30 min at R.T, protected from the light.
4. Wash two times with 1ml of Wash Buffer 1X and centrifuge at 300xg for 5 min.
5. Wash with 1ml of PBS 1X and centrifuge at 300xg for 5 min.
6. Resuspend cells in 300µl of PBS 1X.

3.3 FACS Acquisition and Analysis

All samples were acquired with either FACS LSRII or FACS Fortessa cytometers (BD Bioscience), and data analysed using FACS DIVA (BD Bioscience) and FlowJo (TreeStar, Inc., Aslhand, OR) softwares. Doublets were excluded using FSC-H/FSC-W and SSC-H/SSC-W before the analysis.

3.4 Cell sorting

Cells were surface stained with appropriate antibodies and then sorted using FACS AriaIISORP (BD Bioscience).

4 T CELL ISOLATION AND CULTURE

Total thymocytes and splenocytes were resuspended in DMEM media supplemented with 10% FBS and seeded in 96-well plate ($2x10^5$ cells/well). When indicated, cells were treated with 10ng/ml recombinant mouse IL-7 (Prepotech).

T cells were isolated from spleen suspension of 8-12 weeks old mice by magnetic depletion of non-T cells following the instructions of the MACS mouse Pan T cell isolation kit (Milteny Biotec, Bergisch Gladbach, Germany). Non-T cells are indirectly magnetically labeled with a cocktail of biotin-conjugated monoclonal antibodies (CD11b, CD11c, CD19, CD45R (B220), CD49b (DX5), CD105, anti-MHC class II and Ter-119) as primary labeling reagent; and anti-biotin monoclonal antibodies conjugated to MicroBeads as secondary labeling reagent. The magnetically labeled non-T cells are depleted by retaining them on a MACS® LS Column in the magnetic field of a MACS Separator, while the unlabeled T cells pass through the column.

Untouched purified T cells were resuspended in DMEM media suplemented with 10% FBS + 1% non-essential amino acids + 5% Penicilin-Streptavidin + 50 μM β-mercaptoethanol, seeded in 24 or 48-well plates ($1x10^6$ cells/well), stimulated with anti-CD3 (5 μg/ml) and anti-CD28 (5 μg/ml), and collected at different time points after stimulation.

5 CELL CYCLE ANALYSIS

5-bromo-2'-deoxyuridine (BrdU) is a non-radioactive analog of the DNA precursor thymidine that is incorporated into newly synthesized DNA by cells entering and progressing through the S phase (DNA synthesis) of cell cycle. Combination with a DNA staining (DAPI) permits the characterization of cell cycle stages (G_0/G_1, S, G_2/M).

For in vivo BrdU labeling experiments, mice received two intraperitoneal injection of BrdU (BD Bioscience; 1mg/6g of mouse weight) at 24h and 12h before sacrificed. Cells were first surface stained, fixed, permeabilized and intracellularly stained using BrdU Flow Kit (BD Bioscience), following manufacturer's instructions. Samples were acquired using FACS Fortessa and analysed using FACS Diva software.

6 SURVIVAL ANALYSIS

6.1 Annexin V staining

Binding of Annexin V to phosphatidylserine (PS) is a non-quantitative technique to detect cells that have exposed this phospholipid on the cell surface, an event found in apoptosis as well as other forms of cell death. The assay combines Annexin V staining of PS with the staining of DNA in the cell nucleus (DAPI), in order to differentiate viable cells from the apoptotic and necrotic ones.

Cells were first cell surface stained when necessary, before proceeding to Annexin V detection following manufacturer's instructions (BD Bioscience). Samples were kept during all process with Binding Buffer 1X (no washing required) because binding of Annexin V to PS is Ca^{2+} dependent.

6.2 Active-caspase-3 staining

Active-caspase-3 staining was also used as a marker of apoptosis. Cells were cell surface stained (**box 3**) for the necessary antibodies, before proceed to intracellular staining for active-caspase-3, following protocol detailed in **box 4**.

Samples were acquired using FACS Fortessa and analysed using FACS DIVA software.

7 WESTERN BLOT

Cells were counted, lysed using 50 μl of homemade lysing buffer (Tris-HCl 67mM pH6.8 + 2% SDS) per $1x10^6$ cells, and adjusted with homemade Laemmli Buffer 4X (Tris-HCl 62,5mM pH6,8 + 5% β-mercaptoethanol + 2% SDS + 40% glicerol + 0,05% bromophenol blue). Protocol followed is detailed in **box 5** and antibodies used are indicated in **table 6**.

Immunobloting with tubulin or β-actin (Sigma-Aldrich), depending on the protein molecular weight, was done to determine protein loading in each lane.

Box 5

Western Blot

1. Mix samples with Laemmli Buffer 4X (dilution 1:1) and heat them for 5 min at 95°C.
2. Load onto a 10% or 15% SDS-PAGE gel (depending on molecular weight of targeted protein) and run samples until protein of interest is in the center of the gel.
3. Transfer onto a PVDF membrane at 360 mA for 1h or 90 minutes, depending on the thickness of SDS-PAGE gel.
4. Block membrane with 5% milk in TBS (TrisHCl 50mM pH7,4 + 150mM NaCl) for 1h at R.T.
5. Incubate with primary antibody O.N at 4°C.
6. Wash 3 times for 5 min with TBST in agitation.
7. Incubate with secondary antibody for 1h at R.T.
8. Wash 3 times for 5 min with TBST in agitation.
9. Enhace chemiluminescence treatment of membranes with ECL reactives (GE Healthcare Europe GmbH, Barcelona, Spain) and/or ECL prime for 1 to 5 min and subsequent exposure to a medical X-ray film (Agfa-Gevaert N.V., Mortsel, Belgium).

Table 6. Antibodies used for western blot.

Antigen	Clone	Molecular weight	Incubation	Origin	Dilution	Company
Parp-1	A6.4.12	110 kDa	O.N	mouse	1/20 (in TBST + 5% milk)	Homemade
Parp-2	175	64 kDa	O.N	rabbit	1/1000 (in TBST + 5% BSA)	Homemade
Tubuline	dm1a	52 kDa	1h	mouse	1/8000 (in TBST + 5% milk)	Sigma-Aldrich
β -actine	AC-15	42kDa	1h	mouse	1/5000 (in TBST + 5% milk)	Sigma-Aldrich
IgGs rabbit (HRP)	-	-	1h	-	1/2000 (in TBST)	Dako
IgGs mouse (HRP)	-	-	1h	rabbit	1/2500 (in TBST + 5% milk)	Dako

8 PARP ENZYMATIC ACTIVITY ASSAY

T cells were isolated from spleen, cultured 14 hours in the presence of anti-CD3 (5 μg/ml) plus anti-CD28 (5 μg/ml), lysed as indicated[180], and PARP activity determined in protein extracts using *HT Universal Colorimetric PARP Assay Kit* (Trevigen) following manufacturer's instructions.

9 MIXED BONE MARROW CHIMERAS

For competitive-repopulation BM experiment, $1x10^6$ competitor BM cells from wild-type B6.SJL mice expressing CD45.1$^+$ leukocyte cell surface marker were mixed at 1:1 ratio with donor BM cells ($1x10^6$) from either *Cd4-cre;Parp-2$^{f/f}$;Parp-1$^{-/-}$*, *Cd4-cre;Parp-2$^{+/+}$;Parp-1$^{-/-}$*, *Cd4-cre;Parp-2$^{f/f}$;Parp-1$^{+/+}$*, or control mice (*Cd4-cre;Parp$^{+/+}$;Parp-1$^{+/+}$*) expressing CD45.2$^+$ marker. This mixture was intravenously injected (in retro-orbital venous sinus) into sub-lethally irradiated (9,5 Gy for females and 9 Gy for males) B6 x B6.SJL F1 (CD45.1$^+$/CD45.2$^+$) recipient mice.

B and T cell reconstitution was analysed 10 weeks later by flow cytometry. For that, splenocytes samples were stained for B220, CD4, CD8, CD62L and CD44 cell surface markers, and CD45.1 and CD45.2 expression was studied in each subpopulation (**box 3**).

10 T-DEPENDENT ANTIBODY RESPONSE

To test T-cell dependent responses, 8–12-week old animals were immunized intraperitoneally with 100 μg/mouse of trinitro-phenyl-conjugated keyhole limpet hemocyanin (TNP-KLH) (Biosearch Technologies, Novato, CA) in Sigma Adjuvant System (Sigma-Aldrich). Serum was collected from tail vein at 14 days after immunization. An Enzyme-Linked Immunosorbent Assay (ELISA) was applied for quantification of TNP-specific immunoglobulins in the sera, as indicated in **box 6.** IgM (clone R6-60.02), IgG1 (clone A85-1), IgG2a (clone R19-15), IgG2b (clone R12-3), and IgG3 (clone R40-82) antibodies (BD Bioscience) were used in this protocol.

Box 6

ELISA

1. Coat 96-well-plate with TNP-BSA (5 μg/ml) in Tris-HCl 0,1M pH8 O.N at 4°C.
2. Remove coat without washing
3. Block with PBS+5% milk for 1h at 37 °C or O.N at 4°C.
4. Remove blocking without washing.
5. Incubate sera at different concentrations in PBS+5% milk for 1h at 37°C.
6. Wash 5 times with PBS-T.
7. Incubate with appropriate biotinilated antibody in PBS+5% milk for 1h at 37°C.
8. Wash 5 times with PBS-T.
9. Incubate with streptavidine-horseradish peroxidase conjugate (*HRP*) (Dako) in PBS-5% milk for 1h at R.T.
10. Wash 5 times with PBS-T.
11. Incubate with 3,3',5,5'-Tetramethylbenzidine (*HRP substrate*) for 15-20 min protected from the light, until color appears.
12. Read at 630nm.

11 COMET ASSAY

Alkaline comet assay was performed on sorted $CD4^+$ and $CD8^+$ cells by using a commercial kit (Trevigen) in accordance with the manufacturer's instructions. Samples were analysed under an Olympus BX61 fluorescent microscope with fluorescein filter. The number of cells with the presence of tail was the parameter used for the data analysis.

12 HISTOLOGY

Tissue samples from liver, spleen, lung, thymus, kidney, stomach and intestine were fixed in 4% buffered-formalin for 36h, processed and paraffin-embedded. Then, 3 μm thick sections were obtained for subsequent histopathological examination and staining with a standard hematoxylin/eosin protocol. For immunohistopathologic characterization of T cell lymphoid tumours, an indirect Avidin-Biotin Complex (ABC) immunohistochemical procedure was performed using a polyclonal rabbit anti-CD3 antigen (Dako) (1:500 dilution, O.N). As secondary antibody, an EnVision Flex anti-rabbit was used (36ºC incubation for 20 min). Carlos Martínez from Universidad de Murcia performed all immunohistochemistry stainings.

13 DNA COMBING

T cells were seeded in 24 or 6 well-plate ($1x10^6$ cells/well) and stimulated with anti-CD3 (5μg/ml) and anti-CD28 (5μg/ml). After activation during 40h and prior to any protocol, cells were pulsed with 5-Iodo-2'-deoxyuridine (IdU) (Sigma) 50 μM (stock at 120 mM) during 15 minutes, and follow by a second pulse with 5-Chloro-2'-deoxyuridine (CldU) (Sigma) 50 μM (stock at 120 mM) for additional 15 minutes.

DNA combing was performed following protocols detailed in **box 7** and **8**, while antibodies used are shown in **table 7**.

Box 7

BrdU and DNA revelation

1. (Protocol for $2x10^6$ cells). Collet cells (in 15 ml tubes) after IdU and CldU pulse, and spin down for 10 min at 400xg.
2. Resuspend in 1 ml of *pepsine solution* (0,5 mg/ml pepsine + 30mM HCl + H_2O), pippete and then add 0,5 ml of pepsine (1,5 ml final volume).
3. Incubate cells for 20 min at 37°C (vortex every 5 minutes).
4. Spin down cells for 10 min at 400xg.
5. Resuspend in 1 ml of HCl 2N, pipette and add 0,5 ml more (1,5 ml final volume). Let cells at R.T for 20 min.
6. Add a maximum of PBS 1X and spin down cells for 10 min at 400xg.
7. Wash once in PBS 1X (up to 15 ml) and spin down cells for 10 min at 400xg.
8. Resuspend cells in 250 µl of *Bu buffer* (0,5% FBS + 0,5% Tween 20 + Hepes 1M + PBS 1X) with 50 µl of mouse Anti-BrdU and incubate 1h at R.T
9. Transfer samples in a 1,5 ml Eppendorf.
10. Add up to 1,5 ml of PBS 1X and spin down cells for 10 min at 600xg.
11. Resuspend in 200 µl of *Bu buffer* with 4 µl rabbit anti-mouse secondary antibody. Incubate 1h at R.T.
12. Add up to 1,5 ml of PBS 1X and spin down cells for 10 min at 600xg.
13. Resuspend in 200 µl Bu buffer with 4 µl donkey anti-rabbit secondary antibody. Incubate 1h at R.T.
14. Add up to 1,5 ml of PBS 1X and spin down cells for 10 min at 600xg.
15. Resuspend cells in 300 µl of PBS and DAPI (dilution 1:100, final concentration 2 µg/ml).

Box 8

DNA combed fibres

1. Collet cells (in 15 ml tubes) after IdU and CldU pulse and spin down for 10 min at 400xg.
2. For DNA spreading, resuspend cells at $1x10^6$ cells/ml in cold PBS 1X.
3. Put 3 µl of cells onto microscope slide and wait approximately 5 min, or until drop appears to be drying slightly at edges.
4. Add 7 µl of *spreading buffer* (0,5% SDS in 200mM Tris-HCl, pH5,5, 50mM EDTA) by gravity to allow forming a nice drop.
5. Wait 3-4 minutes, then angle to allow drop to run down slide (~ 45°). *If it does not move, go even at 90°, making sure not going too fast.*
6. Fix for 10 min in 3:1 methanol:acetic acid. At this point, slides can stay in the fridge for at least a month/year at -20°C.
7. For DNA denaturation, put the slide into 2,5M ultrapure HCl for 45min at R.T.
8. Transfer the slide into 70% EtOH (1 min), 90% EtOH (1 min) and 100 % EtOH (1 min).
9. Dry and subsequently wash 3 times in PBS 1X (cold is better), 5 min each.

For blocking and immunostaining, we added 100 µl of antibody solution per slide and cover each one with a 22x64mm coverslip.

10. Blocking O.N at 4°C with blocking solution (blocking reagent (Roche)+ 0,05% Tween-20 + NaOH ph7-7,5) or 30 min at R.T.
11. Incubate with rat anti-BrdU (AbD serotec) for 45 min at R.T
12. Wash 15 min with 10mM Tris-HCl pH 7,4 + 400mM NaCl + 0,2% Tween-20 (*helps removing potential cross-reaction).*
13. Wash x3 for 5 min with PBS 1X
14. Incubate with chicken anti-rat Alexa Fluor 488 for 20 min at R.T
15. Wash x3 for 3 min with PBS 1X.
16. Incubate with goat anti-chicken Alexa Fluor 488 for 20 min at R.T
17. Wash x3 for 3 min in PBS 1X.
18. Incubate with mouse anti-BrdU for 45 min at R.T
19. Incubate with 0,5 M NaCl + 20mM Tris-HCl + 0,05% Tween for 5 min.
20. Wash once with PBS + Tween 0,05% for 5 min and once with PBS 1X for 5 min.
21. Incubate with rabbit anti-mouse Alexa Fluor 350 for 20 min at R.T
22. Wash x3 for 3 min with PBS 1X.

After incubations, wash x3 with PBS 1X for 3 min.

23. Incubate with donkey anti-rabbit Alexa Fluor 350 for 20 min at R.T.
24. Incubate with mouse anti-DNA for 45 min at R.T
25. Incubate with rabbit anti-mouse Alexa Fluor 594 for 20 min at R.T
26. Incubate with donkey anti-rabbit Alexa Fluor 594 for 20 min at R.T
27. Mount with 20 µl of 10% PBS 1X and 90% glycerol.
28. Cover with coverslip and seal the slides with a nail polish.
29. Keep at -20°C.

Table 7. Antibodies used in DNA combing.

Antigen	Fluorochrome	Clone	Host	Dilution
BrdU	Unconjugate	BU1/75 (ICR1)	Rat	1/750
		B44	Mouse	1/5
DNA (Single Stranded)		16-19	Mouse	1/50
Igs-rat	Alexa Fluor 488	-	Chicken	1/300
Igs-chicken			Goat	1/250
Igs-mouse	Alexa Fluor 350	-	Rabbit	1/50
	Alexa Fluor 594	Polyclonal		1/50
Igs-rabbit	Alexa Fluor 350	Polyclonal	Donkey	1/50
	Alexa Fluor 594	Polyclonal		1/50

Slides were examined with an inverted-fluorescence microscopy (Olympus BX61 microscope). Confocal images (Confocal microscope Leica TCS SPE) were acquired with Leica Application Suite Advance Fluorescence software (Leica Microsystems CMS GmbH).

14 STATISTICAL ANALYSIS

Results are presented as mean values ± SEM. The log-rank test was used to determine the statistical of animal survival. An unpaired two-tailed Mann-Whitney was used to analyse all the experiments. P values of less than 0.05 were considered to indicate statistical significance.

RESULTS

1 GENERATION OF MICE WITH A T-CELL SPECIFIC DELETION OF PARP-2 IN A PARP-1 DEFICIENT BACKGROUND

Mice that are simultaneously deficient for the expression of PARP-1 and PARP-2 are not viable and they die at stage E8.5 of the embryonic development[14], suggesting a functional interaction between the two proteins. In order to study the roles of both enzymes in T cells, we have generated embryonic stem (ES) cells with a *Parp-2* gene containing loxP sites that flank exon 8 (*Parp-2*$^{f/f}$) (**Figure 9A**). Two ES clones with an appropriately floxed locus were used to generate chimeras, which were bred with C57BL/6J mice to obtain germline transmission of the floxed allele.

Mice homozygous for floxed *Parp-2* (*Parp-2*$^{f/f}$) were crossed with *Cd4-cre* mice to induce a T-cell-specific recombination. The resulting *Cd4-cre;Parp-2*$^{f/+}$ mice were crossed with *Parp-1*$^{-/-}$ mice to generate heterozygous animals, which were then intercrossed to give all possible combinations of *Parp-2*, *Parp-1* and *Cd4-cre* targeted alleles (**Figure 9B**).

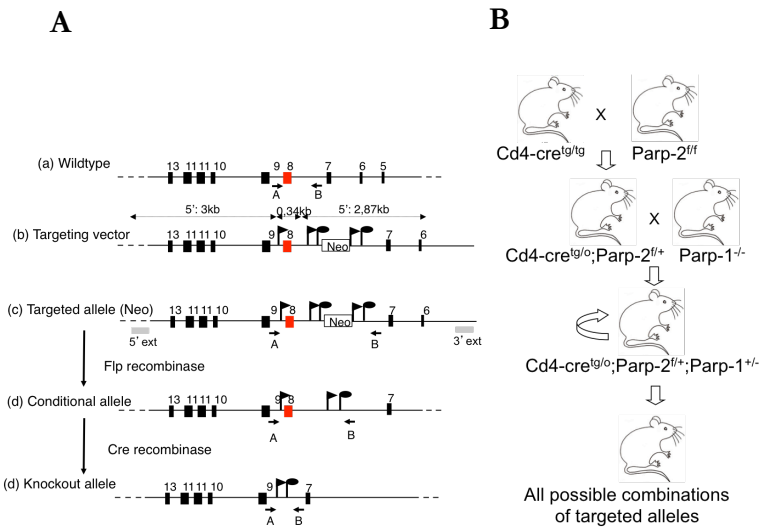

Figure 9. Generation of the conditional mouse model. (A) Construct for the generation of *Parp-2*$^{flox/flox}$ allele. (B) Backcrossing strategy for the generation of mice with all possible combinations of targeted alleles.

To check the deletion efficiency of *Parp-2* by cre-recombinase in CD4 expressing cells, thymocyte populations of all genotypes were sorted and the presence of the floxed allele was analysed by PCR. A complete loss of the floxed allele (266 bp band) was observed in $CD4^+CD8^+$(DP), $CD4^+CD8^-$(CD4SP) and $CD4^-CD8^+$(CD8SP) thymocytes of *Cd4-cre;Parp-2*$^{f/f}$ mice. However, as expected, in these animals the floxed allele was present in $CD4^-CD8^-$ (DN) cells (657 bp band), because this population is not affected by the recombinase, as it does not express the CD4 molecule. *Cd4-cre;Parp-2*$^{+/+}$*;Parp-1*$^{-/-}$ and *Cd4-cre;Parp-2*$^{+/+}$*;Parp-1*$^{+/+}$ control mice only exhibit the 497 bp wyld-type band, as these animals do not have any genetic modification in the *Parp-2* gene (**Figure 10A**).

To confirm *Parp-2* specific deletion at protein level, western blot using proteins from DP thymocytes was performed in all genotypes. As predictable from the pattern of gene deletion, the expression of PARP-2 protein was abolished in *Cd4-cre;Parp-2$^{f/f}$* DP cells (**Figure 10B**), but it was present in control and *Cd4-cre;Parp-2$^{+/+}$;Parp-1$^{-/-}$* DP cells. Accordingly, PARP-1 expression in DP subset was abolished in *Cd4-cre;Parp-2^{++};Parp-1$^{-/-}$* and *Cd4-cre;Parp-2$^{f/f}$;Parp-1$^{-/-}$* thymocytes.

To finally corroborate that the deletion of PARP-2 is specific from CD4 expressing cells, PARP-1 and PARP-2 protein expression was also analysed by western blot in sorted B-cells, CD4$^+$ T-cells and CD8$^+$ T-cells from spleen. Verifying our previous results regarding PARP expression, our data pointed out a complete and selective loss of PARP-2 in *Cd4-cre; Parp-2$^{f/f}$* T-cell compartment, but not in the B cell subset (**Figure 10C**). As expected, PARP-1 expression was also eliminated in T and B cell compartment from *Cd4-cre; Parp-2^{++};Parp-1$^{-/-}$* and *Cd4-cre; Parp-2$^{f/f}$;Parp-1$^{-/-}$* mice.

In addition, PARP activity was assessed in T cells upon *in vitro* activation with anti-CD3 plus anti-CD28. Although this activity was not affected in T-cells singly deficient for PARP-2 compared to control, our data showed a similar strong reduction in PARP-1 deficient T cells, in both *Cd4-cre;Parp-2^{++};Parp-1$^{-/-}$* and *Cd4-cre;Parp-2$^{f/f}$;Parp-1$^{-/-}$* genotypes, supporting previous results showing that global PARP activity is mainly dependent on PARP-1[168] (**Figure 10D**).

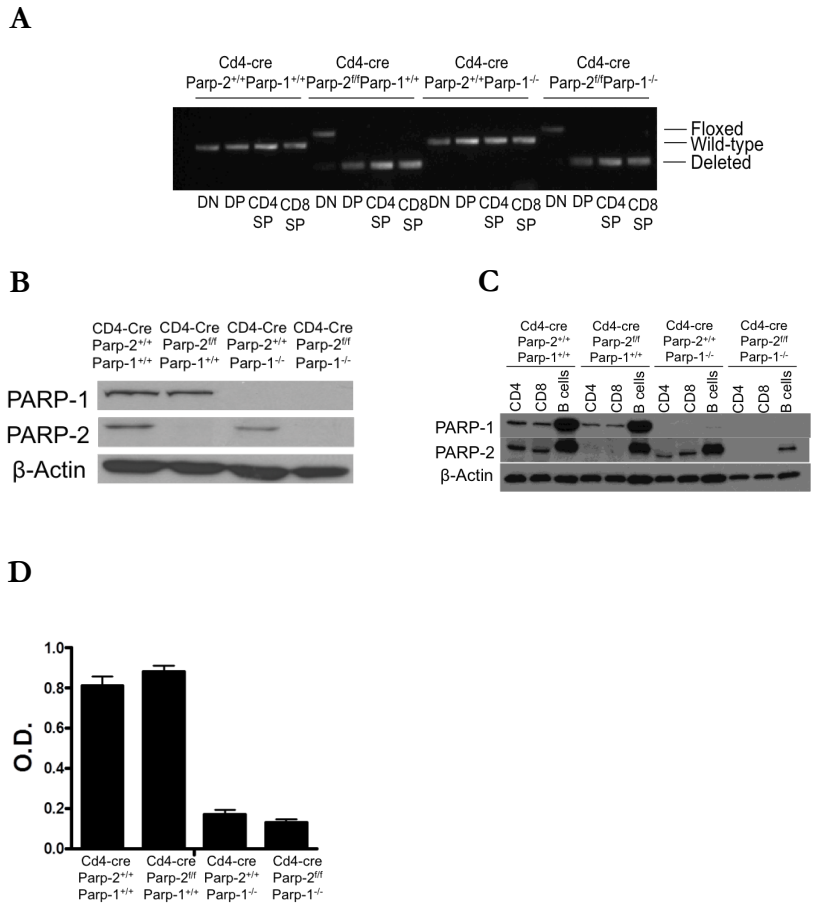

Figure 10. Efficiency of Parp-2 deletion in T cells from *Cd4-cre;Parp-2$^{f/f}$* mice. (A) PCR analysis of Parp-2 floxed allele from genomic DNA in thymic DN, DP, CD4SP, and CD8SP subsets from *Cd4-cre;Parp-2$^{+/+}$;Parp-1$^{+/+}$, Cd4-cre;Parp-2$^{f/f}$;Parp-1$^{+/+}$, Cd4-cre;Parp-2$^{+/+}$;Parp-1$^{-/-}$* and *Cd4-cre;Parp-2$^{f/f}$;Parp-1$^{-/-}$* mice. Western-blot analysis of PARP-1 and PARP-2 expression in (B) sorted DP thymocytes and (C) sorted CD4^{+}, CD8^{+} and B cells from spleen. (D) PARP activity in protein extracts from spleen T cells upon *in vitro* activation with anti-CD3 plus anti-CD28. Graph results represent the mean ± SEM of a representative experiment from two independent experiments carried out in triplicate.

2 CHARACTERIZATION OF THE EFFECTS OF PARP-1/PARP-2 DOUBLY DEFICIENCY IN T-CELL HOMEOSTASIS

Previous data from the group showed that the deletion of PARP-2, but not PARP-1, in mice lead to a smaller thymus, associated with a reduction in DP thymocyte number due to a decreased lifespan, without affecting peripheral T-cell number[168]. To investigate whether PARP-1-deficiency could modify the effect of PARP-2-deficiency on T cell development in thymus, we first counted total number of thymocytes from PARP-1-single-mutant (*Cd4-cre;Parp-2*$^{+/+}$*;Parp-1*$^{-/-}$), PARP-2-single-mutant (*Cd4-cre;Parp-2*$^{f/f}$*;Parp-1*$^{+/+}$), PARP-1/PARP-2-double-mutant (*Cd4-cre;Parp-2*$^{f/f}$*;Parp-1*$^{-/-}$) and control (*Cd4-cre;Parp-2*$^{+/+}$*;Parp-1*$^{+/+}$) mice, and flow cytometry was also performed to characterize different thymoctyes subsets (**Figures 11A and 11B**).

Cell counting revealed that PARP-2-single-mutant and PARP-1/PARP-2 double mutant mice presented a decreased number of total and DP thymocytes, compared to age-matched PARP-1-single-mutant and control mice, while no differences were found in DN compartment. These results are in agreement with previous data suggesting that PARP-1 is dispensable during thymocyte development[168]. However, further analysis of thymocytes concluded that only PARP-1/PARP-2 doubly-deficient mice showed a reduced number of CD4SP and CD8SP thymocytes, compared with PARP-1 and PARP-2 single-mutant and control animals, suggesting that both

enzymes are necessary for advanced steps of T cell development in thymus (**Figure 11B**).

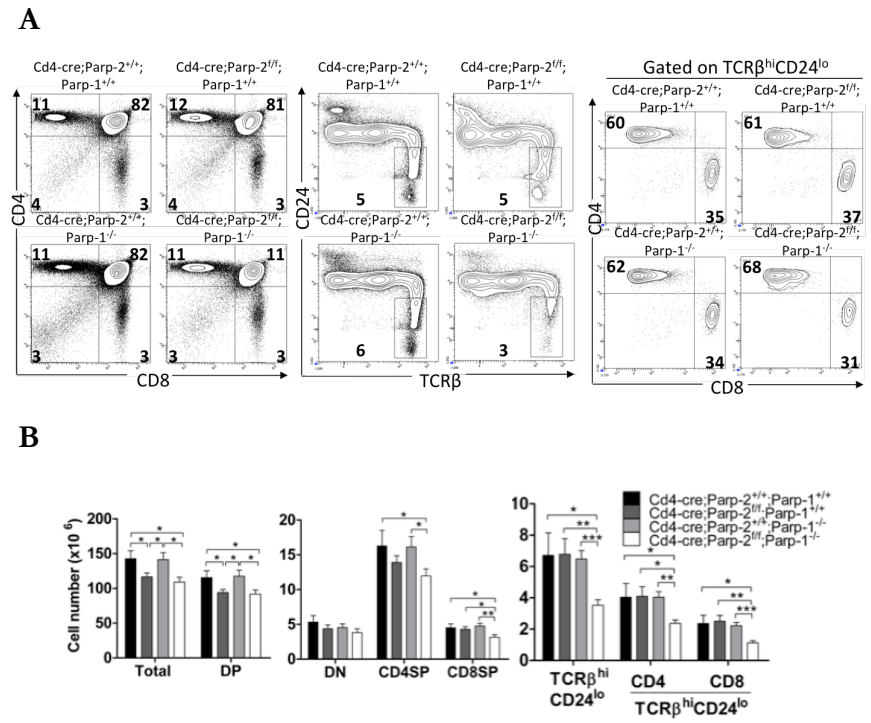

Figure 11. T-cell specific deletion of PARP-2 in a PARP-1-deficient background impairs thymocyte development and maturation. (A) Representative dot-plots of CD4, CD8, TCRβ and CD24 expression in thymocytes from 8 to 10-weeks old mice of the indicated genotypes. Percentage of cells in the individual subpopulations is indicated in each quadrant. (B) Graphs showing the absolute number of thymocytes in each subpopulation. Values represent the mean ± SEM from at least 8 mice of each genotype. *, statistically significant differences $P< 0.05$; **, $P< 0.01$; ***, $P< 0.001$

Flow cytometry was also performed to analyse mature thymocyte subpopulation, defined as TCRβ^{hi} CD24^{lo}. Our results pointed out that only PARP-1/PARP-2-double mutant mice had a significant reduction in SP mature population, in CD4 and CD8 lineages, compared to control, PARP-1 single-mutant and PARP-2 single-mutant mice,

pointing out that both proteins are required for a correct thymocyte maturation (**Figures 11A and 11B**).

To study whether this defect in thymocyte development and maturation had an impact on peripheral T cell compartment, cell count and flow cytometry of splenocytes were also performed. Consistent with a reduction in mature CD4SP and CD8SP thymocytes, T-cell-specific deletion of PARP-2, in a PARP-1 deficient background, also resulted in a significant decrease in both the proportion and absolute number of T cells in the spleen. However, as expected, there were no differences in the B-cell compartment (**Figures 12A and 12B**). Although both $CD4^+$ and $CD8^+$ T-cell number was decreased in the absence of PARP-1 and PARP-2, $CD8^+$ T-cell population was affected most, as indicated by the CD4/CD8 ratio. This parameter was 2-fold higher in double deficient mice (ratio of 3,4) compared with single-mutants (ratio of 1,9) and control animals (ratio of 1,7).

We took advantage of cell surface markers CD62L and CD44 to analyse by flow cytometry the naïve ($CD62L^+CD44^{low}$), central memory ($CD62L^+CD44^{high}$) and effector memory ($CD62L^-CD44^{high}$) peripheral T cell compartments[181], both in $CD4^+$ and $CD8^+$ lineages (**Figure 12A**). Our data indicated that the overall decreased peripheral T-cell number not only impacted the number of $CD4^+$ and $CD8^+$ naïve cells, but also a specific deficiency in central and effector memory T cells was very markedly observed in mice with double-deficiency for PARP-1 and PARP-2. The imbalance ratio of splenic

naïve/memory T cells of PARP-1/PARP-2 double mutant mice points towards an impaired generation and/or survival of memory T cells (**Figure 12B**). Altogether, our data indicates a compensatory or redundant function of PARP-1 and PARP-2 in T cell homeostasis, as single deficiency for one of the proteins has no impact on the peripheral T cell compartments, but when both proteins are missing there is a profound and selective alteration on T cell subsets.

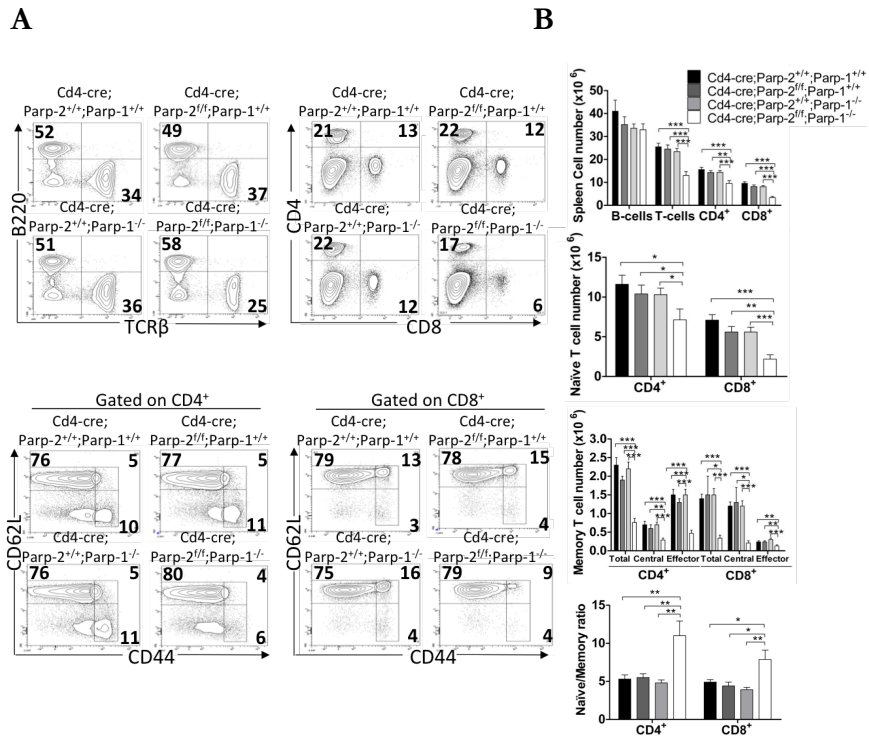

Figure 12. T-cell specific deletion of PARP-2 in a PARP-1-deficient background impairs T-cell homeostasis. (A) Representative dot-plots of TCRβ, B220, CD4, CD8, CD62L and CD44 expression in splenocytes of the indicated genotypes. Percentage of cells in the individual subpopulations is indicated in each quadrant. (B) Graphs showing the total number of splenocytes, absolute number of cells in each subpopulation, and naïve/memory ratio in $CD4^+$ and $CD8^+$ lineages. Values represent the mean ± SEM from at least 8 mice of each genotype. *, statistically significant differences $P< 0.05$; **, $P< 0.01$; ***, $P< 0.001$.

3 IL-7 SURVIVAL RESPONSE IS NOT ALTERED IN PARP-1/PARP-2 DOUBLE-DEFICIENT THYMOCYTES AND PERIPHERAL NAÏVE T LYMPHOCYTES

IL-7 has been described as a survival factor both in mature thymocytes and peripheral naïve T cells, by increasing the expression of antiapoptotic molecule Bcl-2[182,183]. IL-7 signalling is needed to prevent DN4 atrophy and maintain their proliferation and differentiation to DP thymocytes[125]. Moreover, this interleukin is also required to expand naïve T cell subset through phosphorylation signalling pathways[146] .

Accordingly, to study if the decreased number of thymocytes and peripheral T cells was due to a deficient IL-7Rα cell surface expression, its levels were analysed by flow cytometry on resting mature thymocytes and peripheral T-cells. Although there were no differences on IL-7Rα expression between the four genotypes in CD4SP and CD8SP thymocytes (**Figure 13A**), when analysing PARP-1/PARP-2 doubly deficient naïve $CD4^+$ and $CD8^+$ T cells of the spleen, they expressed lower levels of IL7-Rα, compared to control and single-deficient naïve $CD4^+$ and $CD8^+$ T cells (**Figure 13B**).

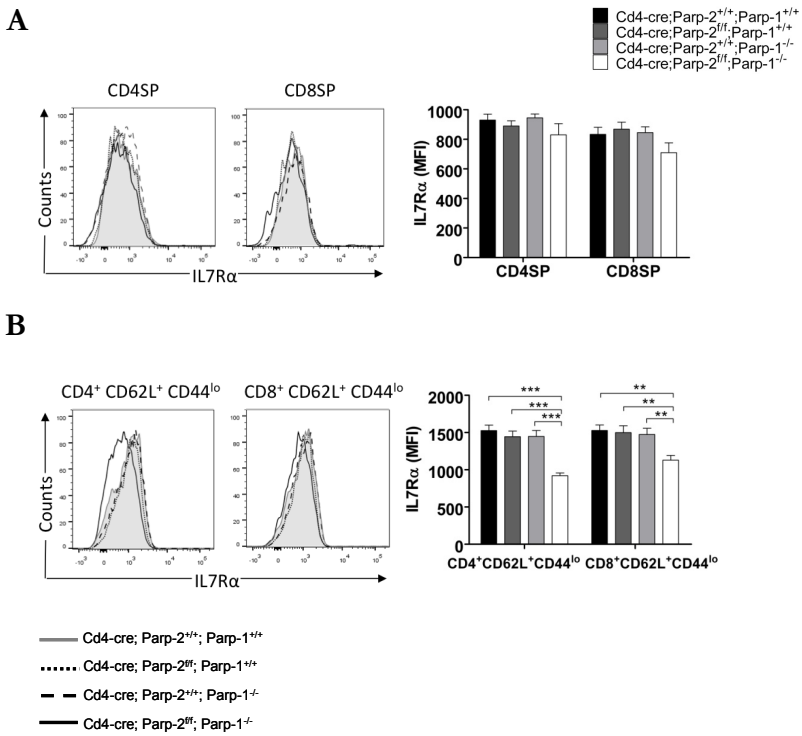

Figure 13. IL-7Rα cell surface levels. Representative histograms and quantification of IL-7Rα expression by flow cytometry in (A) CD4SP and CD8SP thymocytes and in (B) $CD4^+CD62L^+CD44^{lo}$ and $CD8^+CD62L^+CD44^{lo}$ splenocytes derived from *Cd4-cre;Parp-*$2^{+/+}$*;Parp-*$1^{+/+}$*, Cd4-cre;Parp-*$2^{f/f}$*;Parp-*$1^{+/+}$*, Cd4-cre;Parp-*$2^{+/+}$*;Parp-*$1^{-/-}$ *and Cd4-cre;Parp-*$2^{f/f}$*;Parp-*$1^{-/-}$ mice. MFI, mean fluorescent intensity. *, statistically significant differences $P< 0.05$; **, $P< 0.01$; ***, $P< 0.001$.

To further study if this slightly decrease in IL-7Rα expression has functional consequences, the capacity of mature thymocytes and peripheral naïve T cells to respond to IL-7 were examined. Hence, we analysed whether the addition of recombinant IL-7 (rIL-7) was able to support survival of T cells *in vitro* by culturing thymocytes and peripheral T cells in the presence or absence of this interleukin.

Our results concluded that in the absence of rIL-7, survival of $CD4^+$ and $CD8^+$ thymocytes and peripheral T-cells was similar in all genotypes. Moreover, when added rIL-7, a related enhanced survival was observed in the four groups, both in $CD4^+$ and $CD8^+$ T-cell subsets (**Figures 14A and 14B**), suggesting that IL-7 survival response is not affected in PARP-1/PARP-2 double deficient T cells. Our results are in agreement with previous data showing that small differences in IL-7Rα expression have no biological consequences[143]. In fact, IL-7Rα heterozygous mice do not present any peripheral T-cell defect[184,185].

A

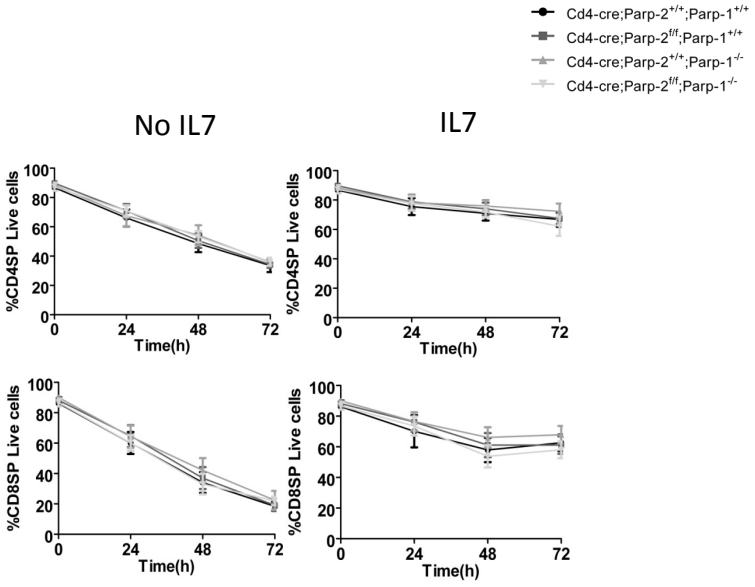

B

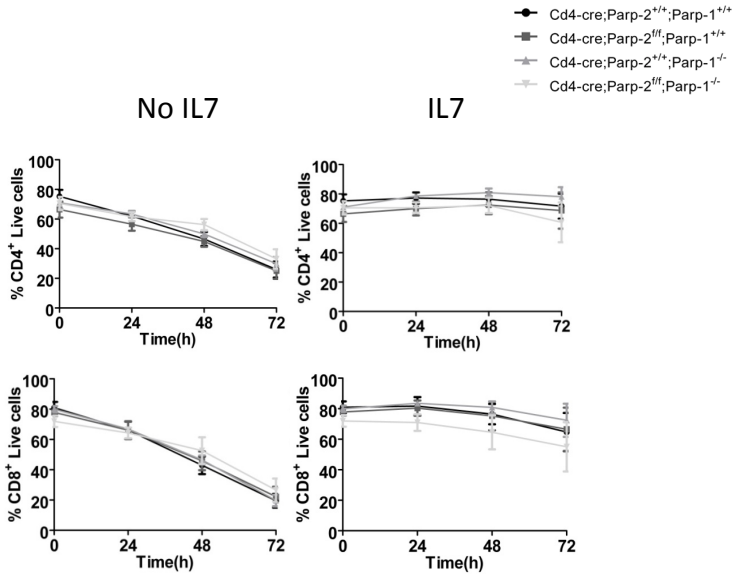

Figure 14. IL-7 respond is not responsible for T-cell defect on PARP-1/PARP-2 double deficient T cells. Survival analysis in (A) CD4SP and CD8SP thymocytes and (B) $CD4^+$ and $CD8^+$ splenocytes from control, PARP-1 and PARP-2 single-deficient and PARP-1/PARP-2 double-deficient mice. Cells were cultured in medium with or without 10 ng/ml recombinant IL-7 (rIL-7) and the proportion of live (Annexin V^-DAPI^-) cells was assessed by flow cytometry at different time points. *, statistically significant difference $P< 0.05$, ** $P< 0.01$, *** $P< 0.001$.

4 IMPAIRED T CELLS RECONSTITUTION CAPACITY OF PARP-1/PARP-2 DOUBLE DEFICIENT BONE MARROW PROGENITORS

To further elucidate whether the defect in PARP-1/PARP-2 doubly deficient T cells is due to intrinsic causes, mixed bone marrow chimeric mice were generated. For that, sub-lethally irradiated B6xB6.SJL F1 recipient mice (CD45.1/CD45.2) were reconstituted with an intravenous injection of 1:1 mixture of CD45.1 competitor wild-type cells and CD45.2 control, *Cd4-cre;Parp-2$^{f/f}$;Parp-1$^{+/+}$*, *Cd4-cre;Parp-2$^{+/+}$;Parp-1$^{-/-}$*, and *Cd4-cre;Parp-2$^{f/f}$;Parp-1$^{-/-}$* donor bone marrow cells (**Figure 15**). Contribution of CD45.2 to peripheral naïve and memory T cell subsets, from both $CD4^+$ and $CD8^+$ lineages from the four groups was analysed 10 weeks later by flow cytometry (**Figure 16)**.

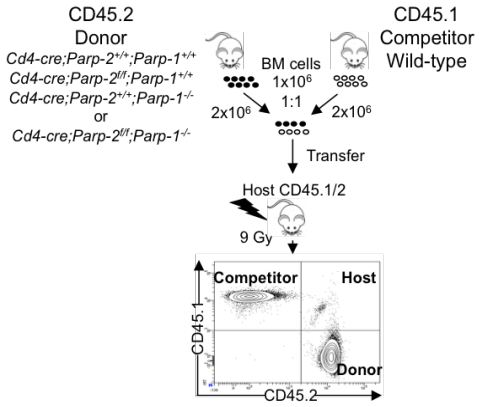

Figure 15. Strategy for the generation of mixed bone marrow chimeras. Sub-lethally irradiated (9,5Gy for females and 9Gy for males) B6xB6.SJL F1 (CD45.1/CD45.2) recipient mice were reconstituted with a 1:1 mixture of CD45.1 competitor wild-type bone marrow cells and CD45.2 control, PARP-1-single-deficient, PARP-2-single-deficient or PARP-1/PARP-2-double-deficient bone marrow donor cells.

Single-deficiency for PARP-1 and PARP-2 already compromised CD45.2 reconstitution in $CD4^+$ and $CD8^+$ memory T cell subset. However, an accumulative effect was observed in CD45.2 PARP-1/PARP-2 double-deficient T cells, as their capacity of reconstitution was severely affected in $CD4^+$ and $CD8^+$ memory compartment, compared to control, PARP-1 single-deficient and PARP-2 single deficient donor cells (**Figures 17**).

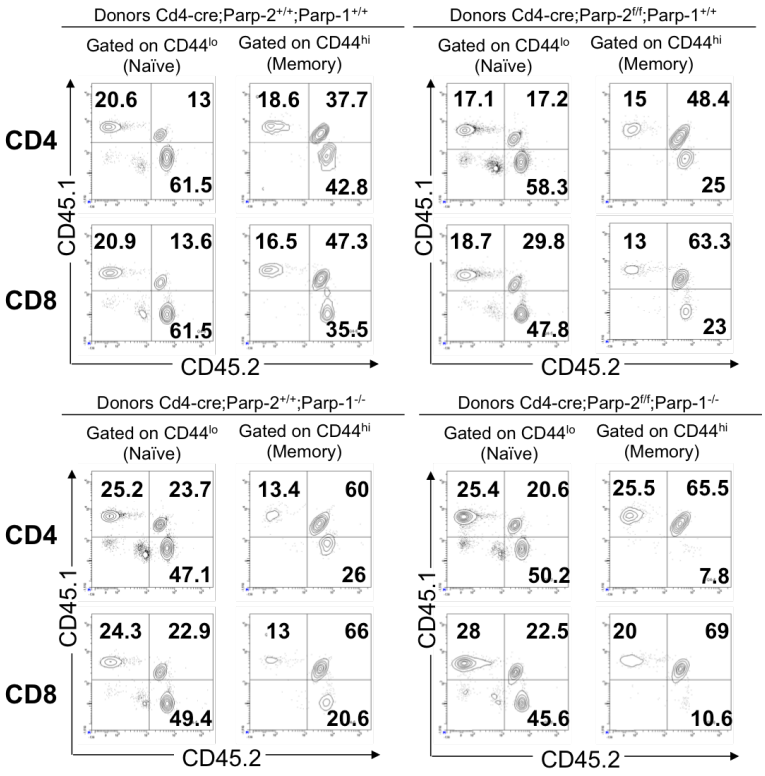

Figure 16. Analysis of CD45.2 contribution in bone marrow chimeras. Representative dot-plots of CD45.1 and CD45.2 expression in $CD4^+$ and $CD8^+$ naïve and memory T-cell population by flow cytometry. Percentage of cells in the individual subset is indicated in each quadrant.

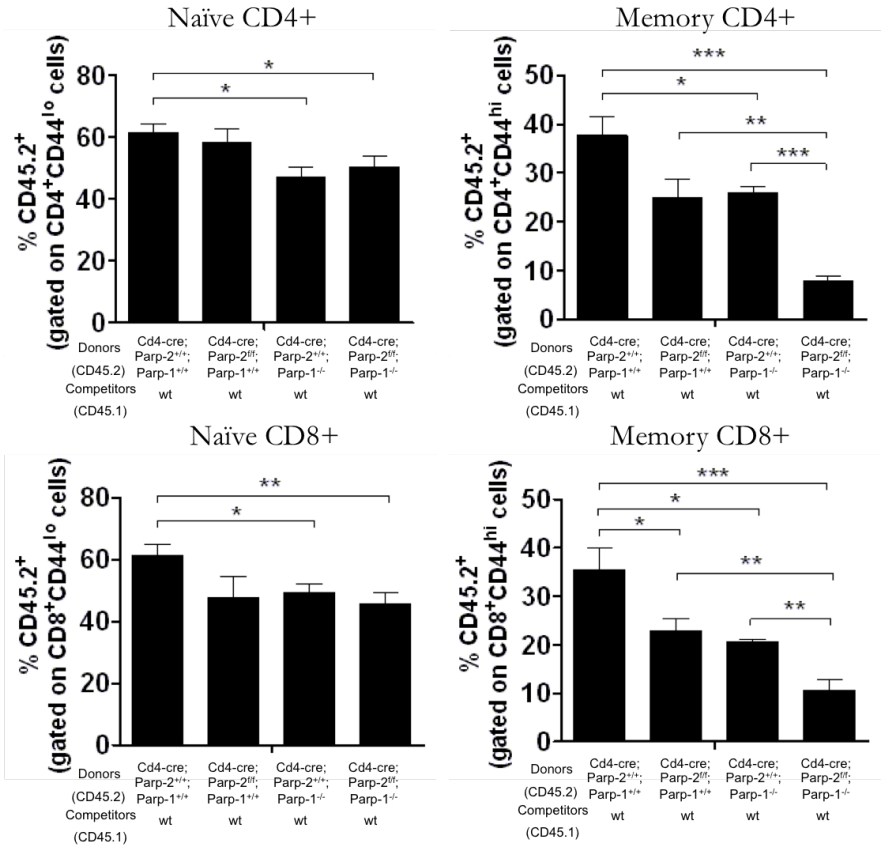

Figure 17. PARP-1/PARP-2 double deficient T cells present an intrinsic defect. Graphs showing the percentage of CD45.2$^+$ cells from the indicated bone marrow donor cells in naïve (CD44^{lo}) and memory (CD44^{hi}) CD4$^+$ and CD8$^+$ T-cell subsets. Values represent the mean ± SEM from at least 4 mice of each genotype. *, statistically significant difference $P< 0.05$, ** $P< 0.01$, *** $P< 0.001$.

5 ANALYSIS OF T-CELL PROLIFERATION IN MICE DOUBLY-DEFICIENT FOR PARP-1 AND PARP-2

To evaluate whether the reduced T cell number in mice carrying a specific deletion of PARP-2 in a PARP-1 deficient background was secondary to proliferation defects, BrdU was intraperitoneally injected and its incorporation was measured over a period of 24h *in vivo*. The proportion of cells that entered to S phase was analysed by flow cytometry in resting conditions and after a challenge with a T-dependent antigen (TNP-KLH) at seven days post immunization.

Interestingly, the percentage of $BrdU^+$ cells was significantly increased in $CD4^+$ and $CD8^+$ resting memory T cells from mice doubly deficient for PARP-1 and PARP-2, compared to control and either PARP-1 or PARP-2-single-mutant T cells. However, when analysing the naïve T cell subset, which present a lower proliferation rate compared to memory T cells and B cell population, there were a similar percentage of BrdU incorporation in the four genotypes (**Figure 18A**).

A similar increase in BrdU incorporation was also observed in memory T cells from PARP-1/PARP-2 doubly-deficient mice at day seven post-immunization with TNP-KLH T cell dependent antigen, compared to control and PARP-1 or PARP-2 single deficient animals, while no significant differences were found in naïve $CD4^+$ and $CD8^+$ and B cell compartment (**Figure 18B**). Despite an increased percentage of BrdU incorporation in PARP-1/PARP-2 double mutant

mice challenged with T-dependent antigen, these animals presented a significant reduced number of total $CD4^+$ and $CD8^+$ T cells, and also an impaired naïve, central and effector memory cell number compared to control and PARP-1 and PARP-2 single-deficient animals (**Figure 19**).

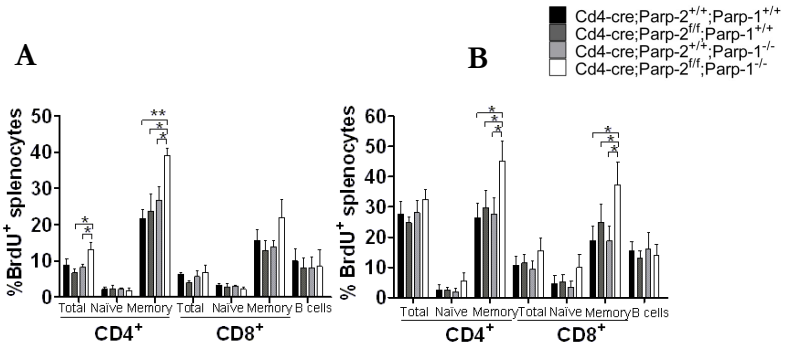

Figure 18. Effect of PARP-1/PARP-2-double deficiency in T cell proliferation. In vivo proliferation of T cell subsets was determined in 10-12 week-old mice by two intraperitoneal (i.p) injections of BrdU (1mg/6 g mouse weight) at -24h and at -12h before sacrificed in (A) resting conditions or (B) 7 days after immunization with the TNP-KLH T-dependent antigen. Bars represent mean ± SEM values of percentage of $BrdU^+$ cells. Data was obtained from at least 6 mice per genotype from two independent experiments. *, statistically significant differences $P<0.05$, **, $P<0.01$; ***, $P<0.001$.

Our results are consistent with no defects on PARP-1/PARP-2-double-deficient T cells in initiating DNA synthesis in response to proliferation stimulus. In fact, these cells divided even more rapidly compared to PARP-1 and PARP-2 single mutant or control mice, to replenish the partially void memory T-cell niche. The reduced number of cells in this subpopulation could be then the result of an increased cell death, as consequence of elevated DNA-strand breaks, rather than a compromised homeostatic proliferation.

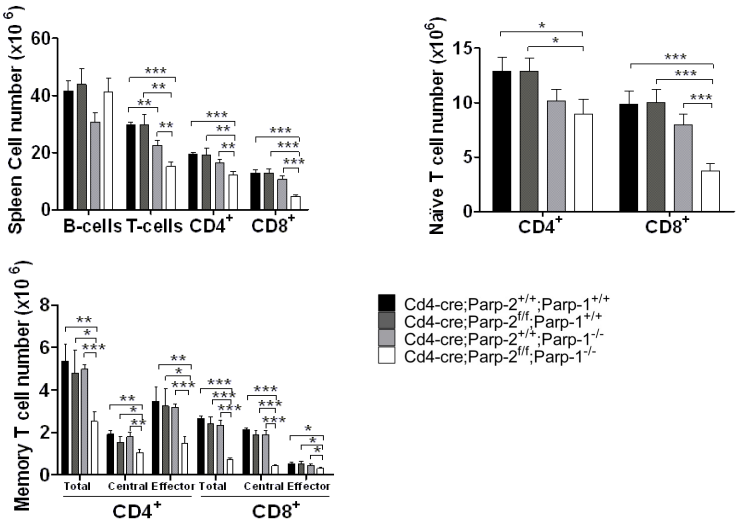

Figure 19. Analysis of spleen subpopulations at day seven post-immunization. Graph showing the absolute number of splenocytes in each population. Naïve, $CD62L^{+}CD44^{lo}$; central memory, $CD62L^{+}CD44^{hi}$; effector memory, $CD62L^{-}CD44^{hi}$. Data was obtained from at least 6 mice per genotype from two independent experiments. *, statistically significant differences $P<0.05$, **, $P<0.01$; ***, $P<0.001$.

DNA replication was also measured by DNA combed fibres technique, in T cells activated with anti-CD3 plus anti-CD28 during 40h. Cultured T cells were exposed to IdU and CldU pulses (15 minutes each), and replication fork velocity was evaluated in each genotype (**Figure 20A**). Our data showed that PARP-1/PARP-2 double-deficient T cells do not exhibit any defect in the fork replication velocity compared with control, PARP-1, and PARP-2 single deficient T cells (**Figure 20B**).

A

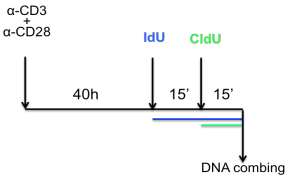

Replication fork speed =

Length of the second pulse (**CldU track**) (kb)

Duration of the second pulse (min)

B

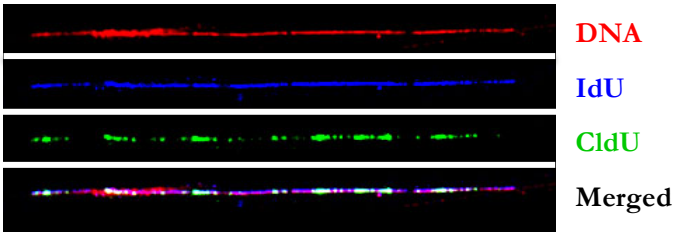

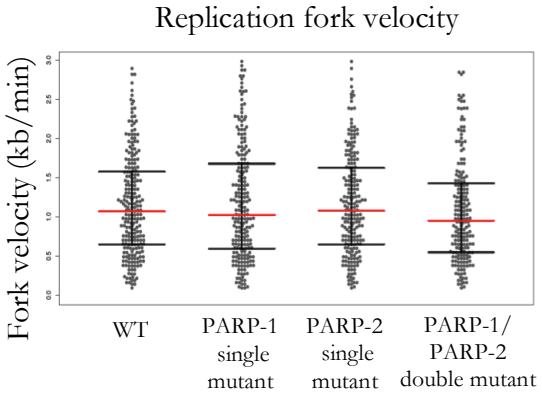

Figure 20. Single molecule analysis of the replication fork velocity in activated T cells using DNA molecular combing. (A) Diagram representing the different treatments approached: T cells were activated with anti-CD3 plus anti-CD8 for 40h and then labelled by two successive pulses of IdU and CldU, for 15 minutes each. Replication fork speed was calculated by dividing the length of the second pulse (CldU size) with the duration of the second CldU pulse. (B) Representative DNA fibre visualized using specific primary antibodies and fluorescently-labelled secondary antibodies (DNA is shown in red, IdU-labelled DNA in blue, and CldU-labelled DNA in green); and graphic showing replication fork velocity (kb/min) in T cells from the indicated genotypes.

6 T-CELL SPECIFIC DISRUPTION OF PARP-2 IN A PARP-1-DEFICIENT BACKGROUND LEADS TO DNA-DAMAGE AND T-CELL DEATH

In order to study if the reduced T cell niche in PARP-1/PARP-2-double-deficient mice is consequence of higher rates of endogenous cellular DNA-damage that is not properly repaired, flow cytometry was performed to analyse the phosphorylation status of histone H2AX (γ-H2AX) in resting T cells, a sensitive marker of DNA injury[186] and the first step in recruiting and localizing DNA repair proteins[187].

Our results showed an increased percentage of γ-H2AX-positive cells in PARP-1/PARP-2 double-deficient memory T cells, both in $CD4^+$ and $CD8^+$ lineages, while no differences were observed in the naïve T cell compartment (**Figure 21A**). To further evaluate induction and repair of DNA breaks, independently from their signalling and processing markers, T cells were exposed to an alkaline comet assay. An increased ratio of cells exhibiting comet shape was observed in PARP-1/PARP-2 double-deficient T cells, both $CD4^+$ and $CD8^+$ subpopulations, compared to control, PARP-1, and PARP-2 single mutant T cells (**Figure 21B and 21C**).

Flow cytometry was also performed to study cleaved-caspase-3 levels in resting T cells, an active form of the protease which is present in the apoptotic cell, and it is activated both by extrinsic and intrinsic pathways[188]. In agreement with higher levels of DNA damage, PARP-1/PARP-2-double-deficient memory T cells exhibited a significantly

higher number of apoptotic cells, in $CD4^+$ and $CD8^+$ compartments, compared with control, PARP-1 and PARP-2-single-deficient T cells (**Figure 21D**).

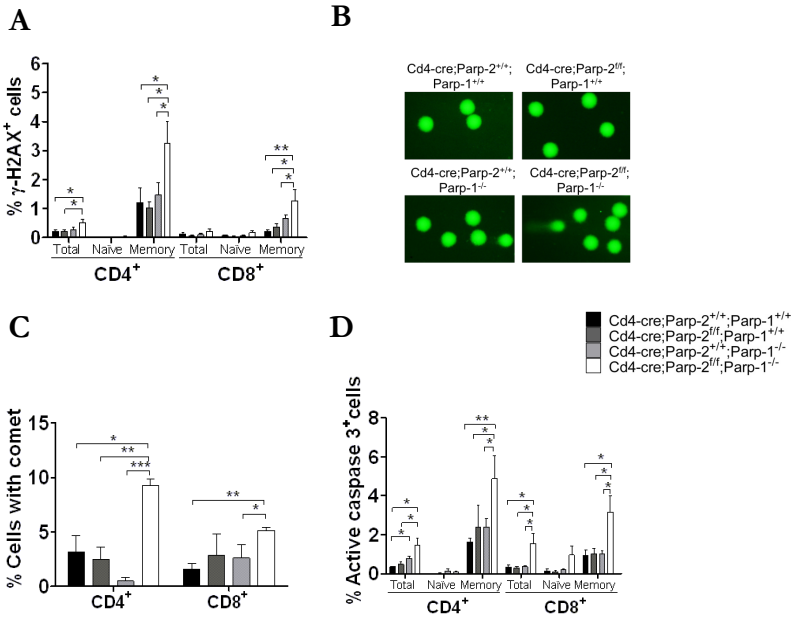

Figure 21. Effect of PARP-1/PARP-2 double deficiency on DNA damage and T-cell apoptosis. (A) DNA damage accumulation in PARP-1/PARP-2 double deficient T cells represented by percentage of γ-H_2AX^+ cells in each T cell subset, determined by flow cytometry. (B) Representative image showing DNA-damage in splenic T cells derived from mice of the indicated genotypes, visualized by alkaline comet assay. An average of 100 cells was scored from each mouse. (C) Graph showing the percentage of T cells with comet in $CD4^+$ and $CD8^+$ T cells. (D) Graph showing the percentage of active-caspase-3^+ cells in each genotype. Bars represent the mean±SEM values obtained from at least 6 mice per genotype from two independent experiments. *, statistically significant differences $P<0.05$, **, $P<0.01$; ***, $P<0.001$.

7 DEFECTIVE T-DEPENDENT ANTIBODY RESPONSE IN MICE DOUBLY DEFICIENT FOR PARP-1 AND PARP-2 IN T-CELLS

Antigen-specific T-cells provide soluble and cognate support to B cells for producing high affinity antibodies during T cell-dependent humoral immune responses. To further determine whether PARP-1 and/or PARP-2-deficiency in T cells compromised *in vivo* responsiveness to specific T-dependent antigenic challenge, *Cd4-cre;Parp-2*$^{+/+}$*;Parp-1*$^{+/+}$*, Cd4-cre;Parp-2*$^{f/f}$*;Parp-1*$^{+/+}$*, Cd4-cre;Parp-2*$^{+/+}$*;Parp-1*$^{-/-}$, and *Cd4-cre;Parp-2*$^{f/f}$*;Parp-1*$^{-/-}$ mice were immunized with a T-dependent antigen (TNP-KLH). Fourteen days post immunization sera was collected, and spleen cell subsets were analysed by flow cytometry.

Similarly to the unimmunized ones, mice that bear a double deficiency of PARP-1 and PARP-2 in their T cells presented a significant decreased number of $CD4^+$ T cells, compared to control and PARP-1 and PARP-2 single mutant mice. Moreover, these $CD4^+$ doubly deficient T cells also presented an additional defect in activation, as demonstrated by the diminished expression of the activation markers CD69 and CD44, determined by flow cytometry (**Figure 22**).

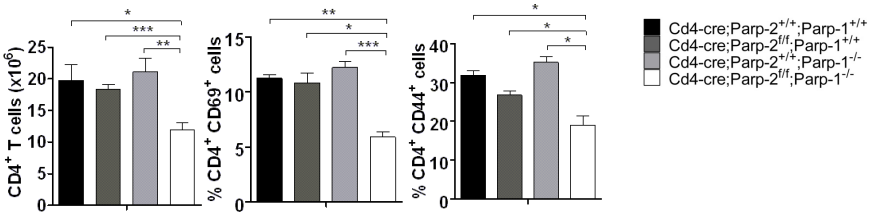

Figure 22. CD4⁺ response to T-dependent antigen in PARP-1/PARP-2 double-deficient mice. Graphs showing total number of CD4⁺ T-cells, and percentage of CD44 and CD69 activation markers in CD4⁺ T-cells. 12-weeks old *Cd4-cre;Parp-2$^{+/+}$;Parp-1$^{+/+}$, Cd4-cre;Parp-2$^{f/f}$;Parp-1$^{+/+}$, Cd4-cre;Parp-2$^{+/+}$;Parp-1$^{-/-}$,* and *Cd4-cre;Parp-2$^{f/f}$;Parp-1$^{-/-}$* mice were i.p. injected with the T-dependent antigen TNP-KLH and sigma-system adjuvant. Fourteen days after immunization, spleen samples were collected and cells were counted and stained for flow cytometry. Bars represent the mean ± SEM values from at least 7 mice of each genotype. *, statistically significant differences $P<0.05$, **, $P<0.01$; ***, $P<0.001$.

T follicular helper cells (T_{FH}) are described as a subset of non-polarized CD4$^+$ T cells that express higher levels of CXCR5, PD-1 and ICOS, among other molecules. These specialized cells are considered the true B cell helpers[189]. To study whether PARP-1 and/or PARP-2 deficiency could also impact T_{FH} population, flow cytometry was performed taking advantage of cell surface markers CD3, CD4, CXCR5, ICOS and PD-1 (**Figure 23A**). Interestingly, our results showed that both the percentage and total number of T_{FH}, defined as CD3$^+$CD4$^+$CXCR5$^+$ICOS$^+$PD-1$^+$, were reduced in mice doubly-deficient for PARP-1 and PARP-2 in T cells compared with control and single deficient PARP-1 or PARP-2 animals (**Figure 23B**).

A

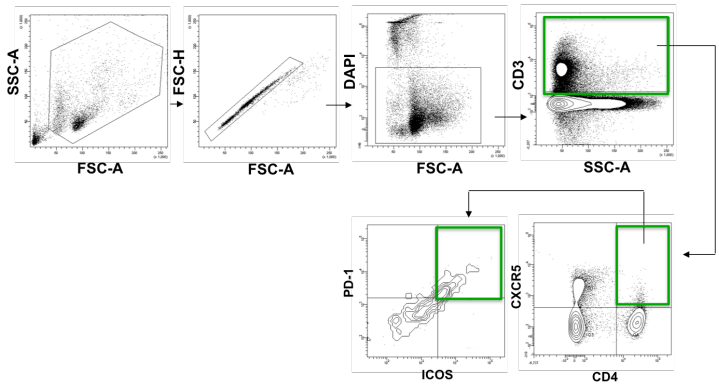

B

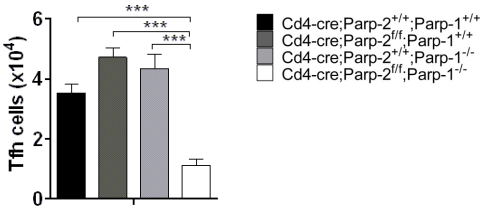

Figure 23. Defective specific response to T-dependent antigen in PARP-1/PARP-2 double-deficient mice. (A) Flow cytometry gating strategy used to analyse T_{FH} cells ($CD3^+CD4^+CXCR5^+PD\text{-}1^+ICOS^+$) from mouse spleen. (B) Graph representing total number of T_{FH} cells from all genotypes. Bars represent the mean ± SEM values from at least 7 mice of each genotype. *, statistically significant differences $P<0.05$, **, $P<0.01$; ***, $P<0.001$.

Further analysis of sera from immunized mice revealed that TNP-specific IgM, IgG1, IgG2a, IgG2b, and IgG3 levels at day 14 post-immunization were significantly reduced in PARP-1/PARP-2 double deficient animals, compared with control and mice with PARP-1 or PARP-2 single deletion (**Figure 24**).

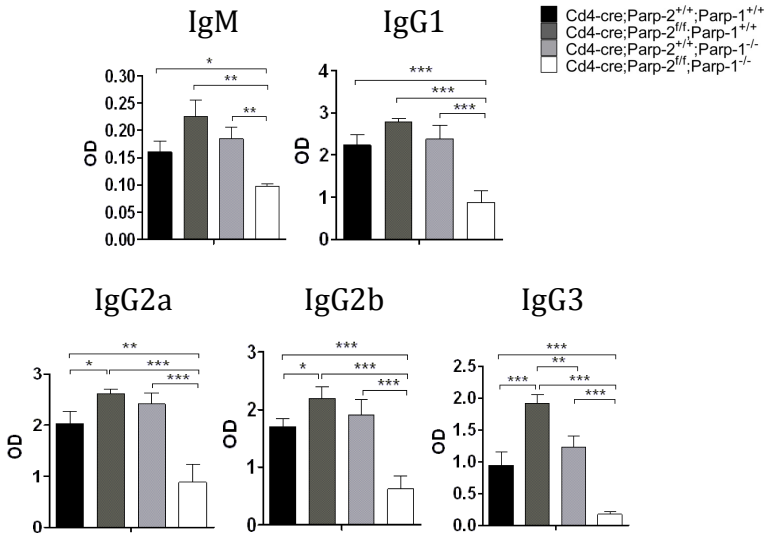

Figure 24. Impaired antibody response in PARP-1/PARP-2 double mutant mice. TNP-specific IgM, IgG1, IgG2a, IgG2b, and IgG3 levels assayed in the sera of mice by ELISA. Bars represent the mean ± SEM values from at least 7 mice of each genotype. *, statistically significant differences $P<0.05$, **, $P<0.01$; ***, $P<0.001$.

8 PARP-1/PARP-2 DOUBLE DEFICIENCY IN T CELLS LEADS TO SPONTANEOUS T-CELL LYMPHOMAS

Mice carrying a double-deletion of *Parp-1* and *Parp-2* in T-cells started to die spontaneously at the age of 10 months, and about 80% of them had died by 16 months. However, no mortality was observed in single mutant or control animals (**Figure 25**).

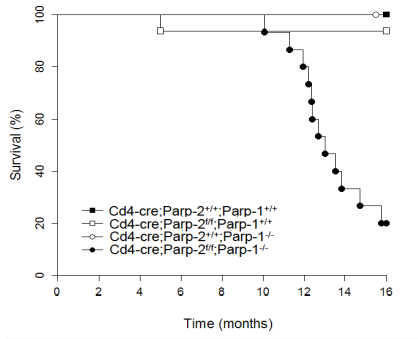

Figure 25. Increased spontaneous death in mice with T-cell specific deletion of PARP-2 in a PARP-1 deficient background. Kaplan-Meier survival curves for *Cd4-cre;Parp-2$^{+/+}$;Parp-1$^{+/+}$* (n=9), *Cd4-cre;Parp-2$^{f/f}$;Parp-1$^{+/+}$* (n=16), *Cd4-cre;Parp-2$^{+/+}$;Parp-1$^{-/-}$* (n=8), and *Cd4-cre;Parp-2$^{f/f}$;Parp-1$^{-/-}$* (n=15) mice. Percent survival is plotted as a function of time in months. Difference in survival between *Cd4-cre;Parp-2$^{f/f}$;Parp-1$^{-/-}$* and the other three genotypes was highly significant (P<0.001) by log-rank test.

The major pathologic feature identified in these animals was the presence of a highly invasive cellular population with round and euchromatic nuclei with well-developed nucleoli; and a basophilic cytoplasm, with a high mitotic index (>10 mitoses/high powerful field). When analysing the lesions by immunohistochemistry, it was

determined that the neoplastic lesions belonged to T-cell lymphoma, as they were positive for CD3 marker (**Figure 26**).

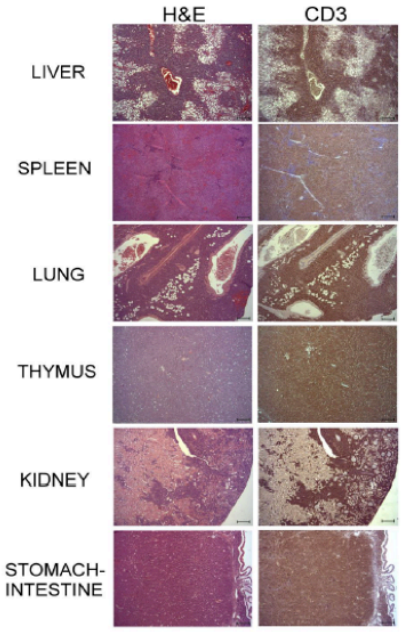

Figure 26. T-cell lymphomas as a cause of mortality in PARP-1/PARP-2 double mutant mice. Hematoxylin and eosin (left panel) and anti-CD3 (right panel) staining of fixed tissue sections reveal that mortality of *Cd4-cre;Parp-2$^{f/f}$;Parp-1$^{-/-}$* mice is due to T-cell lymphomas.

In order to establish a relationship between the neoplastic progression and the death of the mice, histopathological analysis of the affected organs was performed. Liver, kidney, thymus, spleen, lungs, heart and intestinal tract were the main affected organs (**Table 8**). Neoplastic lymphoblasts infiltrating the lungs led to a sever engrossment of the alveolar septa, with a complete obliteration of the alveolar space. In the heart, atrial septum and atrial valves were the most affected by the neoplastic infiltration and proliferation, which also induced atrophy of myocardiocytes. Regarding the liver, perivascular cuffing of neoplastic

cells were mainly located at periportal areas. Lymphoid infiltration caused severe degenerative changes in hepatocytes with pan-lobular distribution, like vacuolar and macrovesicular degeneration, atrophy, and necrosis. In kidney, perivascular infiltration affected basically the renal cortex, and induced tubular and nephron atrophy. In the digestive tract, neoplastic proliferation induced a complete loss of parenchymal architecture, with severe atrophy of intestinal vily and intestinal glands. Additionaly, neoplastic proliferation also provoked a parenchymal architecture loss in thymus and spleen, where the progression of the neoplasia induced atrophy of the red pulp.

On the basis of the severe damage that affected several vital organs, mainly the liver, the progression of the neoplasia in such organs could be correlated with the death of these animals.

Table 8. Summary of organs with highly invasive T-cell lymphomas.

Organ	Cases	%
Liver	11/11	100
Spleen	10/11	90.9
Lung	6/11	54.5
Thymus	4/11	36.4
Kidney	4/11	36.4
Stomach/Intestine	3/11	27.3

DISCUSSION

Preservation of T cell number during homeostasis, and upon antigen challenge, must be perfectly regulated to provide appropriate immune responses and prevent immunopathology. Therefore, cell division and programmed cell death must be accurately controlled to guarantee maintenance of T-cell homeostasis throughout life[190]. In addition to MHC-TCR interaction and cytokine-mediated signals, cells intrinsic factors that regulate essential functions of T cells, such as TCR rearrangements, cell cycle progression or apoptosis, are critical to preserve genomic stability and contribute to the normal T cell development[191].

Previously, we have demonstrated a role for the DNA damage response-associated protein PARP-2, but not PARP-1, in thymocyte development, without affecting peripheral T-cell homeostasis[18, 19]. In the present work we have analysed the functional interaction between PARP-1 and PARP-2, in order to deep understand their specific and redundant roles in the T cell compartment. For this purpose, we have generated PARP-1-deficient mice with a *Cd4*-promoter-driven conditional deletion of PARP-2 in T-cells, in order to overcome early lethality present in PARP-1/PARP-2 doubly deficient embryos[14].

Our results indicate that double deficiency of PARP-1/PARP-2 impacts all T-cell compartments. In addition to the reduction of DP thymocytes associated with the loss of PARP-2[18], double deficiency of PARP-1/PARP-2 in T-cells affects CD4SP and CD8SP T-cell maturation in the thymus, and leads to a strong reduction of both naïve and memory T-cells in the periphery.

The imbalance ratio of splenic naïve/memory T cells in these animals points towards an impaired generation and/or survival of memory T cells.

IL-7 is the major T cell survival cytokine for mature thymocytes, naïve, and memory T cells[123,144–146,177,178]. One hypothesis for the paucity of peripheral T cell compartment in PARP-1/PARP-2 double deficient mice is that their T cells may present an impaired IL-7 signalling pathway. However, despite slightly diminished cell surface levels of IL-7 receptor (IL-7Rα) observed in PARP-1/PARP-2 double-deficient T cells, our results indicated no defects on IL-7 response neither thymocytes nor peripheral double-mutant T cells, as the addition of recombinant IL-7 enhanced survival of cells from all genotypes to similar levels. Our findings are in agreement with previous work of Hsu *et al.,* showing that small differences in IL-7Rα expression are not necessarily biologically significant[143]. Indeed, IL-7Rα heterozygous mice do not exhibit any peripheral T cell defect[184,192].

Altogether, our data suggested a compensatory or redundant function of PARP-1 and PARP-2 in T cell homeostasis, as single deficiency for either PARP-1 or PARP-2 does not lead to any remarkable peripheral T cell deficiencies, but when both proteins are missing there is a severely and selective alteration on T cell subsets.

T cell lymphopenia can be explained by a shift in the balance between

survival and proliferation during T-cell homeostatic expansion to replenish the niche[145]. Interestingly, our *in vivo* data revealed no defect on peripheral T cells from PARP-1/PARP-2-doubly-deficiency mice in entering the S-phase after proliferation stimulus, but rather increased cell death. A remarkable impairment in acquiring memory cells is observed in IKK mutant mice, probably reflecting a survival defect during the proliferative burst associated with homeostatic expansion[193]. Moreover, DNA combing experiments revealed a similar replication fork velocity among all genotypes, suggesting a proper replication rate in T cells doubly-deficient for PARP-1 and PARP-2.

The reduced cell number in the memory T cell compartment can be explained due to higher rates of DNA-strand breaks and concomitant cell death, as indicated by the higher number of positive γH2AX and active-caspase-3 cells present in PARP-1/PARP-2 double-mutant mice. In agreement with previous data establishing a role of PARP-1 and PARP-2 in maintaining genomic instability[4], we provide evidence that both proteins function in a redundant manner in proliferating T-cells to prevent accumulation of toxic levels of unrepaired DNA-damage, that results in cell death upon homeostatic proliferation or in response to antigen, while survival is not affected in resting conditions.

The presence of T-cell lymphomas later in life in many organs of mice with double-deficiency for PARP-1 and PARP-2 suggests that T lymphocytes with DNA damage, that is not properly repaired, occasionally survive and lead to accumulation of genetic abnormalities.

Indeed, impairments in the DNA damage response in T cells have been associated with the development of peripheral T-cell lymphomas[194–197]. Overall, our data suggest a redundant role of PARP-1 and PARP-2 proteins in T-cell effector function.

Interestingly, the stronger effect was observed on the $CD8^+$ T-cell population compared to the $CD4^+$ subset in PARP-1/PARP-2 doubly-deficient mice, probably due to higher susceptibility of MHC-class-I-restricted thymocytes to apoptosis[198], and to faster proliferation of $CD8^+$ T cells than the $CD4^+$ lineage[136,199].

We also investigated whether PARP-1/PARP-2-doubly-deficient T-cells had an intrinsic defect, by generating and reconstituting bone-marrow chimeras, and analyzing the contribution of CD45.2 donor cells from all genotypes. Transplantation experiments revealed a dramatic defect on the contribution of double-deficient PARP-1 and PARP-2 donor T-cells to memory T-cell compartment, whose generation requires proliferation of naïve T-cells[200]. This redundant role for PARP-1 and PARP-2 in preserving T-cell homeostasis beyond the DP stage contrasts with other biological processes associated with a high proliferative cell rate, such as spermatogenesis[82], stress induce hematopoiesis[73] or erythropoiesis[63], in which only PARP-2 appears to be specifically involved.

To further elucidate whereas peripheral T lymphopenia in PARP-1/PARP-2 doubly-deficient mice results in functional impairment, mice from all genotypes were immunized with a T dependent antigen

(TNP-KLH), and analysed at day fourteen post-immunization. Similarly to unimmunized mice, our results revealed a decreased number of $CD4^+$ cells, which present an additional defect in activation, as demonstrated by the diminished expression of the activation markers CD69 and CD44. Moreover, PARP-1/PARP-2 double-deficient mice exhibit a defective humoral response to TNP-KLH antigen challenge, proved by the strikingly descend in the production of TNP-specific immunoglobulins IgG1, IgG2a, IgG2b, IgG3, and IgM. Impairment in antibody production can be accounted for the impaired number of T_{FH} cells[159] observed in *Cd4-cre;Parp-2$^{f/f}$;Parp-1$^{-/-}$* mice.

Our study is consistent with a model (**Figure 27**) whereby double-deficiency of PARP-1 and PARP-2 in T cells leads to DNA-damage accumulation in cells intending to proliferate to replenish the memory niche during homeostasis, and when proliferating in response to activation by antigen challenge. The presence of either PARP-1 or PARP-2 is sufficient to maintain genome integrity and prevent DNA damage accumulation and apoptosis. However, these two processes are altered in PARP-1/PARP-2 double-deficient proliferating lymphocytes, leading to lymphopenia and impaired immune responses. In addition, doubly deficient T-lymphocytes with an aberrant DNA-damage response occasionally survive with accumulated genetic abnormalities, resulting in T-cell lymphomas later in life.

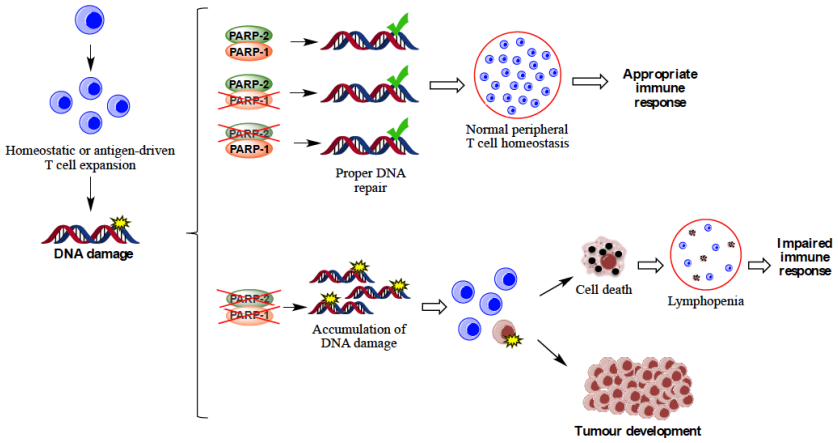

Figure 27. PARP-1/PARP-2 double-deficiency model. T-cell lymphopenia, impaired immune response and development of T-cell lymphoma in mice harboring a double deficiency of PARP-1 and PARP-2 in T cells.

Currently, there is considerable enthusiasm about the prospect of anti-cancer compounds that act through targeting PARP proteins, particularly in combination with defects in DNA-damage signalling[201–204]. However, while non-isoform-selective PARP inhibitors are available, the current compounds lack the desired selectivity and may result in differential off target effects[205–207]. Our study demonstrates a redundant role of PARP-1 and PARP-2 in T-cell immune responses and tumour suppression in T-cells, thus having implications in the design and use of non-selective PARP inhibitor drugs. Therefore, our data highlight the importance for understanding the specific role and involvement of PARP-1, PARP-2, and other PARP family members in DNA damage response and other key biological processes, in order to provide a basis for the development and rational exploitation of PARP inhibitor compounds.

CONCLUSIONS

The present work points toward a redundant role for PARP-1 and PARP-2 in T-cell homeostasis, immune responses and tumour suppression in T-cells, highlighting the importance of understanding the specific involvement of both proteins in key biological processes. This data will provide a new scenario for the development and exploitation of PARP-inhibitors, which nowadays lack isoform selectivity. Altogether, the conclusions of this thesis are:

1. PARP-2, but not PARP-1, is crucial for T-cell development in thymus.
2. Simultaneous deficiency of PARP-1 and PARP-2 in T cells results in an impaired thymocyte maturation.
3. Simultaneous deficiency of PARP-1 and PARP-2 in T cells resulted in a significant decreased in peripheral T cells.
4. Bone marrow transplantation experiments revealed a dramatic defect on the contribution of double-deficient PARP-1 and PARP-2 T-cells to the T-cell memory compartment.
5. Reduced T cell number in mice harboring PARP-1/PARP-2 double deficiency is due to an accumulation of endogenous unrepaired DNA-damage and concomitant cell death.
6. Mice with T-cell-specific ablation of PARP-2 in a PARP-1-deficient background exhibit faulty T-dependent antibody response.
7. Double deficiency of PARP-1 and PARP-2 in T cells leads to spontaneous T-cell lymphomas.

PUBLICATIONS

- Farrés, J. et al. PARP-2 sustains erythropoiesis in mice by limiting replicative stress in erythroid progenitors. *Cell Death Differ.* **22,** 1144–1157 (2014).

- Galindo, M. *et al.* Enhancing tumor-targeting monoclonal antibodies therapy by PARP inhibitors. *Oncoimmunology* **5,** 1–9 (2016).

- Navarro, J. *et al.* PARP-1/PARP-2 double deficiency in mouse T-cells results in faulty immune responses and T lymphomas (under revision in *Scientific reports*).

BIBLIOGRAPHY

1. Hottiger, M. O. Nuclear ADP-ribosylation and its role in chromatin plasticity, cell differentiation, and epigenetics. *Annu. Rev. Biochem.* **84,** 227–63 (2015).
2. Bai, P. Biology of poly(ADP-Ribose) polymerases: The factotums of cell maintenance. *Mol. Cell* **58,** 947–958 (2015).
3. Hottiger, M. O., Hassa, P. O., Lüscher, B., Schüler, H. & Koch-Nolte, F. Toward a unified nomenclature for mammalian ADP-ribosyltransferases. *Trends Biochem. Sci.* **35,** 208–219 (2010).
4. Yélamos, J., Farrés, J., Llacuna, L., Ampurdanés, C. & Martín-Caballero, J. PARP-1 and PARP-2: New players in tumor development. *Am. J. Cancer Res.* **1,** 328–346 (2011).
5. Gibson, B. A. & Kraus, W. L. New insights into the molecular and cellular functions of poly(ADP-ribose) and PARPs. *Nat. Rev. Mol. Cell Biol.* **13,** 411–424 (2012).
6. Davidovic, L., Vodenicharov, M., Affar, E. B. & Poirier, G. G. Importance of poly(ADP-ribose) glycohydrolase in the control of poly(ADP-ribose) metabolism. *Exp. Cell Res.* **268,** 7–13 (2001).
7. Smith, S. The world according to PARP. *Trends Biochem. Sci.* **26,** 174–179 (2001).
8. Schreiber, V., Dantzer, F., Ame, J.-C. & de Murcia, G. Poly(ADP-ribose): Novel functions for an old molecule. *Nat. Rev. Mol. Cell Biol.* **7,** 517–28 (2006).
9. Hottiger, M. O. *et al.* Progress in the function and regulation of ADP-ribosylation. *Sci. Signal.* **4** (2011).
10. Amé, J. C., Spenlehauer, C. & De Murcia, G. The PARP superfamily. *BioEssays* **26,** 882–893 (2004).
11. Langelier, M. F., Servent, K. M., Rogers, E. E. & Pascal, J. M. A third zinc-binding domain of human poly(ADP-ribose) polymerase-1 coordinates DNA-dependent enzyme activation. *J. Biol. Chem.* **283,** 4105–4114 (2008).
12. Nguewa, P. A., Fuertes, M. A., Valladares, B., Alonso, C. & Pérez, J. M. Poly(ADP-ribose) polymerases: Homology, structural domains and functions. Novel therapeutical applications. *Prog. Biophys. Mol. Biol.* **88,** 143–172 (2005).
13. Yélamos, J., Schreiber, V. & Dantzer, F. Toward specific functions of poly(ADP-ribose) polymerase-2. *Trends Mol. Med.* **14,** 169–178 (2008).
14. Ménissier de Murcia, J. *et al.* Functional interaction between PARP-1 and PARP-2 in chromosome stability and embryonic development in mouse. *EMBO J.* **22,** 2255–2263 (2003).
15. Oliver, A. W. *et al.* Crystal structure of the catalytic fragment of murine poly(ADP-ribose) polymerase-2. *Nucleic Acids Res.* **32,** 456–464 (2004).
16. Huber, A., Bai, P., Murcia, J. M. De & Murcia, G. De. PARP-1, PARP-2 and ATM in the DNA damage response: Functional synergy in mouse development. *DNA Repair (Amst).* **3,** 1103–1108 (2004).
17. Pion, E., Ullmann, G. M., Ame, J., Ge, D. & Murcia, G. De. DNA-induced dimerization of poly (ADP-ribose) polymerase-1 triggers its activation. *Biochemistry* **44,**14670–14681 (2005).
18. Ame, J. *et al.* PARP-2, a novel mammalian DNA damage-dependent poly (ADP-ribose) polymerase. *J. Biol. Chem.* **274,** 17860–17868 (1999).

19. Shall, S. & De Murcia, G. Poly(ADP-ribose) polymerase-1: What have we learned from the deficient mouse model? *Mutat. Res. - DNA Repair* **460,** 1–15 (2000).
20. Trucco, C., Oliver, F. J., De Murcia, G. & Ménissier-De Murcia, J. DNA repair defect in poly(ADP-ribose) polymerase-deficient cell lines. *Nucleic Acids Res.* **26,** 2644–2649 (1998).
21. Schreiber, V. *et al.* Poly(ADP-ribose) polymerase-2 (PARP-2) is required for efficient base excision DNA repair in association with PARP-1 and XRCC1. *J. Biol. Chem.* **277,** 23028–23036 (2002).
22. Langelier, M. F., Riccio, A. A. & Pascal, J. M. PARP-2 and PARP-3 are selectively activated by 5' phosphorylated DNA breaks through an allosteric regulatory mechanism shared with PARP-1. *Nucleic Acids Res.* **42,** 7762–7775 (2014).
23. Sukhanova, M. V. *et al.* Single molecule detection of PARP1 and PARP2 interaction with DNA strand breaks and their poly(ADP-ribosyl)ation using high-resolution AFM imaging. *Nucleic Acids Res.* **44,** 1–12 (2015).
24. Boehler, C. & Dantzer, F. PARP-3, a DNA-dependent PARP with emerging roles in double-strand break repair and mitotic progression. *Cell Cycle* **10,** 1023–1024 (2011).
25. de Murcia, J. M. *et al.* Requirement of poly(ADP-ribose) polymerase in recovery from DNA damage in mice and in cells. *Proc. Natl. Acad. Sci. U. S. A.* **94,** 7303–7 (1997).
26. Jackson, S. P. & Bartek, J. The DNA-damage response in human biology and disease. *Nature* **461,** 1071–1078 (2010).
27. Tong, W. M. *et al.* Synergistic role of Ku80 and poly(ADP-ribose) polymerase in suppressing chromosomal aberrations and liver cancer formation. *Cancer Res.* **62,** 6990–6996 (2002).
28. Nicolás, L. *et al.* Loss of poly(ADP-ribose) polymerase-2 leads to rapid development of spontaneous T1. Nicolás, L. et al. Loss of poly(ADP-ribose) polymerase-2 leads to rapid development of spontaneous T-cell lymphomas in p53-deficient mice. Oncogene 29, 2877–83 (2010).-cel. *Oncogene* **29,** 2877–83 (2010).
29. Tong, W. M. *et al.* Poly(ADP-ribose) polymerase-1 plays a role in suppressing mammary tumourigenesis in mice. *Oncogene* **26,** 3857–3867 (2007).
30. Tong, W. M., Hande, M. P., Lansdorp, P. M. & Wang, Z. Q. DNA strand break-sensing molecule poly(ADP-Ribose) polymerase cooperates with p53 in telomere function, chromosome stability, and tumor suppression. *Mol. Cell. Biol.* **21,** 4046–54 (2001).
31. Dantzer, F. *et al.* Base excision repair is impaired in mammalian cells lacking Poly (ADP-ribose) polymerase-1. *Biochemistry* **39,** 7559–7569 (2000).
32. Hakem, R. DNA-damage repair; the good, the bad, and the ugly. *EMBO J.* **27,** 589–605 (2008).
33. Mortusewicz, O., Amé, J. C., Schreiber, V. & Leonhardt, H. Feedback-regulated poly(ADP-ribosyl)ation by PARP-1 is required for rapid response to DNA damage in living cells. *Nucleic Acids Res.* **35,** 7665–7675 (2007).
34. El-Khamisy, S. F., Masutani, M., Suzuki, H. & Caldecott, K. W. A requirement for PARP-1 for the assembly or stability of XRCC1 nuclear foci at sites of oxidative DNA damage. *Nucleic Acids Res.* **31,** 5526–5533 (2003).

35. Lan, L. *et al.* In situ analysis of repair processes for oxidative DNA damage in mammalian cells. *Proc. Natl. Acad. Sci. U. S. A.* **101,** 13738–13743 (2004).
36. Okano, S., Lan, L., Caldecott, K. W., Mori, T. & Yasui, A. Spatial and temporal cellular responses to single-strand breaks in human cells. *Mol. Cell. Biol.* **23,** 3974–3981 (2003).
37. Ghodgaonkar, M. M., Zacal, N., Kassam, S., Rainbow, A. J. & Shah, G. M. Depletion of poly(ADP-ribose) polymerase-1 reduces host cell reactivation of a UV-damaged adenovirus-encoded reporter gene in human dermal fibroblasts. *DNA Repair (Amst).* **7,** 617–632 (2008).
38. Vodenicharov, M. D., Ghodgaonkar, M. M., Halappanavar, S. S., Shah, R. G. & Shah, G. M. Mechanism of early biphasic activation of poly(ADP-ribose) polymerase-1 in response to ultraviolet B radiation. *J. Cell Sci.* **118,** 589–599 (2005).
39. Tao, G.-H. *et al.* Effect of PARP-1 deficiency on DNA damage and repair in human bronchial epithelial cells exposed to Benzo(a)pyrene. *Mol. Biol. Rep.* **36,** 2413–2422 (2009).
40. Pardo, B., Gómez-González, B. & Aguilera, A. DNA double-strand break repair: How to fix a broken relationship. *Cell. Mol. Life Sci.* **66,** 1039–1056 (2009).
41. Yang, Y.-G., Cortes, U., Patnaik, S., Jasin, M. & Wang, Z.-Q. Ablation of PARP-1 does not interfere with the repair of DNA double-strand breaks, but compromises the reactivation of stalled replication forks. *Oncogene* **23,** 3872–3882 (2004).
42. Bryant, H. E. *et al.* PARP is activated at stalled forks to mediate Mre11-dependent replication restart and recombination. *EMBO J.* **28,** 2601–2615 (2009).
43. Audebert, M., Salles, B. & Calsou, P. Involvement of poly(ADP-ribose) polymerase-1 and XRCC1/DNA ligase III in an alternative route for DNA double-strand breaks rejoining. *J. Biol. Chem.* **279,** 55117–55126 (2004).
44. Henrie, M. S. *et al.* Lethality in PARP-1/Ku80 double mutant mice reveals physiological synergy during early embryogenesis. *DNA Repair (Amst).* **2,** 151–158 (2003).
45. Jekimovs, C. *et al.* Chemotherapeutic compounds targeting the DNA double-strand break repair pathways: The good, the bad, and the promising. *Front. Oncol.* **4,** 1–18 (2014).
46. Wang, H. *et al.* DNA Ligase III as a candidate component of backup pathways of nonhomologous end joining. *Cancer Res.* **65,** 4020–4030 (2005).
47. Mladenov, E., Magin, S., Soni, A. & Iliakis, G. DNA double-strand break repair as determinant of cellular radiosensitivity to killing and target in radiation therapy. *Front. Oncol.* **3,** 1–18 (2013).
48. Velic, D. *et al.* DNA damage signalling and repair inhibitors: The long-sought-after achilles' heel of cancer. *Biomolecules* **5,** 3204-3259(2016).
49. Soutoglou, M. T. & E. The emerging role of nuclear architecture in DNA repair and genome maintenance. *Nat. Rev. Mol. Cell Biol.* **10,** 243–254 (2012).
50. Richmond, R. K., Sargent, D. F., Richmond, T. J., Luger, K. & Ma, A. W. Crystal structure of the nucleosome core particle at 2.8 A. resolution. *Nature* **7,** 251–260 (1997).
51. Messner, S. *et al.* PARP1 ADP-ribosylates lysine residues of the core histone tails. *Nucleic Acids Res.* **38,** 6350–6362 (2010).

52. Ueda, S. K. ADP-ribosylation of histone H1. *J. Biol. Chem.* **255,** 7616–7620 (1980).
53. Poirier, G. G., de Murcia, G., Jongstra-Bilen, J., Niedergang, C. & Mandel, P. Poly(ADP-ribosyl)ation of polynucleosomes causes relaxation of chromatin structure. *Proc. Natl. Acad. Sci. U. S. A.* **79,** 3423–3427 (1982).
54. Bustin, M. High mobility group proteins. *Biochim. Biophys. Acta - Gene Regul. Mech.* **1799,** 1–2 (2010).
55. Huen, M. The DNA damage response pathways: At the crossroad of protein modifications. *Cell Res.* **18,** 8–16 (2008).
56. Ahel, D. *et al.* Europe PMC Funders group poly (ADP-ribose)-dependent regulation of DNA repair by the chromatin remodelling enzyme ALC1. *Science* **325,** 1240–1243 (2012).
57. Kraus, W.L Transcriptional control by PARP-1: Chromatin modulation, enhancer-binding, coregulation, and insulation. *Curr. Opin. Cell Biol.* **20,** 294–302 (2011).
58. Kraus, W. L. & Lis, J. T. PARP goes transcription. *Cell* **113,** 677–683 (2003).
59. Gottschalk, A. J. *et al.* Poly(ADP-ribosyl)ation directs recruitment and activation of an ATP-dependent chromatin remodeler. *Proc. Natl. Acad. Sci. U. S. A.* **106,** 13770–13774 (2009).
60. Chou, D. M. *et al.* A chromatin localization screen reveals poly (ADP ribose)-regulated recruitment of the repressive polycomb and NuRD complexes to sites of DNA damage. *Proc. Natl. Acad. Sci. U. S. A.* **107,** 18475–18480 (2010).
61. Frizzell, K. M. *et al.* Global analysis of transcriptional regulation by poly(ADP-ribose) polymerase-1 and poly(ADP-ribose) glycohydrolase in MCF-7 human breast cancer cells. *J. Biol. Chem.* **284,** 33926–33938 (2009).
62. Kraus, W. L. & Hottiger, M. O. PARP-1 and gene regulation: Progress and puzzles. *Mol. Aspects Med.* **34,** 1109–1123 (2013).
63. Farrés, J. *et al.* PARP-2 sustains erythropoiesis in mice by limiting replicative stress in erythroid progenitors. **22,** *Cell Death Differ.* 1–14 (2014).
64. Szántó, M. *et al.* Poly(ADP-ribose) polymerase-2: Emerging transcriptional roles of a DNA-repair protein. *Cell. Mol. Life Sci.* **69,** 4079–4092 (2012).
65. Quenet, D. *et al.* The histone subcode: poly(ADP-ribose) polymerase-1 (Parp-1) and Parp-2 control cell differentiation by regulating the transcriptional intermediary factor TIF1beta and the heterochromatin protein HP1alpha. *FASEB J. Off. Publ. Fed. Am. Soc. Exp. Biol.* **22,** 3853–3865 (2008).
66. Szántó, M. *et al.* Deletion of PARP-2 induces hepatic cholesterol accumulation and decrease in HDL levels. *Biochim. Biophys. Acta - Mol. Basis Dis.* **1842,** 594–602 (2014).
67. Houtkooper, R. H., Cantó, C., Wanders, R. J. & Auwerx, J. The secret life of NAD(+): An old metabolite controlling new metabolic signaling pathways. *Endocr. Rev.* **31,** 194–223 (2010).
68. Di Micco, R. *et al.* Oncogene-induced senescence is a DNA damage response triggered by DNA hyper-replication. *Nature* **444,** 638–642 (2006).
69. Bartkova, J. *et al.* Oncogene-induced senescence is part of the tumorigenesis barrier imposed by DNA damage checkpoints. *Nature* **444,** 633–637 (2006).
70. Gaillard, H., Garcia-Muse, T. & Aguilera, A. Replication stress and cancer. *Nat. Rev. Cancer* **15,** 276–289 (2015).

71. Mazouzi, A., Velimezi, G. & Loizou, J. I. DNA replication stress: Causes, resolution and disease. *Exp. Cell Res.* **329,** 85-93 (2014).
72. Macheret, M. & Halazonetis, T. D. DNA replication stress as a hallmark of cancer. *Annu. Rev. Pathol. Mech. Dis.* **10,** 425–448 (2015).
73. Farrés, J. *et al.* Parp-2 is required to maintain hematopoiesis following sublethal γ-irradiation in mice. *Blood* **122,** 44–54 (2013).
74. Murga, M. *et al.* A mouse model of the ATR-seckel syndrome reveals that replicative stress during embryogenesis limits mammalian lifespan. *Nat. Genet.* **41,** 891–898 (2010).
75. Kavanaugh, G. *et al.* A whole genome RNAi screen identifies replication stress response genes. *DNA Repair (Amst).* **35,** 55–62 (2015).
76. Diaz-Moralli, S., Tarrado-Castellarnau, M., Miranda, A. & Cascante, M. Targeting cell cycle regulation in cancer therapy. *Pharmacol. Ther.* **138,** 255–271 (2013).
77. Liang, Y. C., Hsu, C. Y., Yao, Y. L. & Yang, W. M. PARP-2 regulates cell cycle-related genes through histone deacetylation and methylation independently of poly(ADP-ribosyl)ation. *Biochem. Biophys. Res. Commun.* **431,** 58–64 (2013).
78. Iii, A. B. N. *et al.* Effects of p21 (Cip1/Waf1) at both the G1/S and the G2/M cell cycle transitions: pRb is a critical determinant in blocking DNA replication and in preventing endoreduplication. *Mol. Cell Biol.* **18,** 629–643 (1998).
79. Saxena, A., Saffery, R., Wong, L. H., Kalitsis, P. & Choo, K. H. A. Centromere proteins Cenpa, Cenpb, and Bub3 interact with poly(ADP-ribose) polymerase-1 protein and are poly(ADP-ribosyl)ated. *J. Biol. Chem.* **277,** 26921–26926 (2002).
80. Earle, E. *et al.* Poly(ADP-ribose) polymerase at active centromeres and neocentromeres at metaphase. *Hum. Mol. Genet.* **9,** 187–194 (2000).
81. Saxena, A. *et al.* Poly(ADP-ribose) polymerase 2 localizes to mammalian active centromeres and interacts with PARP-1, Cenpa, Cenpb and Bub3, but not Cenpc. *Hum. Mol. Genet.* **11,** 2319–2329 (2002).
82. Dantzer, F. *et al.* Poly(ADP-ribose) polymerase-2 contributes to the fidelity of male meiosis I and spermiogenesis. *Proc. Natl. Acad. Sci. U. S. A.* **103,** 14854–14859 (2006).
83. Donate, L. E. & Blasco, M. A. Telomeres in cancer and ageing. *Philos. Trans. R. Soc. Lond. B. Biol. Sci.* **366,** 76–84 (2011).
84. Dantzer, F. *et al.* Functional interaction between and TRF2: PARP activity negatively regulates TRF2. *Mol. Cell Biol.* **2,** 1595–1607 (2004).
85. Deng, Z. *et al.* Telomeric proteins regulate episomal maintenance of epstein-barr virus origin of plasmid replication. *Mol. Cell* **9,** 493–503 (2002).
86. Aredia, F. & Scovassi, A. I. Poly(ADP-ribose): A signaling molecule in different paradigms of cell death. *Biochem. Pharmacol.* **92,** 157–163 (2014).
87. Wyllie, A. H., Kerr, J. F. R. & Currie, A. R. Cell death: The significance of apoptosis. *Int. Rev. Cytol.* **68,** 251–306 (1980).
88. Leist, B. M., Single, B., Castoldi, A. F. & Kühnle, S. Intracellular adenosine triphosphate (ATP) concentration: A switch in the decision between apoptosis and necrosis. *J. Exp. Med.* **185,** 1481–1486 (1997).
89. Ivana Scovassi, A. & Diederich, M. Modulation of poly(ADP-ribosylation) in apoptotic cells. *Biochem. Pharmacol.* **68,** 1041–1047 (2004).

90. Soldani, C. & Scovassi, A. I. Poly(ADP-ribose) polymerase-1 cleavage during apoptosis: An update. *Apoptosis* **7,** 321–328 (2002).
91. Nicholson, D. W. *et al.* Identification and inhibition of the ICE/CED-3 protease necessary for mammalian apoptosis. *Nature* **376,** 37–43 (1995).
92. Tewari, M. *et al.* Yama/CPP32β, a mammalian homolog of CED-3, is a CrmA-inhibitable protease that cleaves the death substrate poly(ADP-ribose) polymerase. *Cell* **81,** 801–809 (1995).
93. Wang, Z. Q. *et al.* PARP is important for genomic stability but dispensable in apoptosis. *Genes Dev.* **11,** 2347–2358 (1997).
94. Zhou, J. *et al.* AMPK mediates a pro-survival autophagy downstream of PARP-1 activation in response to DNA alkylating agents. *FEBS Lett.* **587,** 170–177 (2013).
95. David, K.K., Andrabi, S.A., Dawson, T.D. & Dawson, V.L. Parthanatos, a messenger of death. *Front. Biosci.* **14,** 1116-1128 (2015).
96. Christofferson, D.E. & Yuan, J. Necroptosis as an alternative form of programmed cell death. *Curr. Opin. Cell Biol.* **48,** 1–6 (2010).
97. Rosado, M. M., Bennici, E., Novelli, F. & Pioli, C. Beyond DNA repair, the immunological role of PARP-1 and its siblings. *Immunology* **139,** 428–437 (2013).
98. Jeoung, D. *et al.* Identification of autoantibody against poly (ADP-ribose) polymerase (PARP) fragment as a serological marker in systemic lupus erythematosus. *J. Autoimmun.* **22,** 87–94 (2004).
99. Bai, P. *et al.* Peroxisome proliferator-activated receptor (PPAR)-2 controls adipocyte differentiation and adipose tissue function through the regulation of the activity of the retinoid X receptor/PPARγ heterodimer. *J. Biol. Chem.* **282,** 37738–37746 (2007).
100. László, V. & Szabó, C. The therapeutic potential of poly (ADP-ribose) polymerase inhibitors. *Pharmacol.* **54,** 375–429 (2002).
101. Brown, M. L., Franco, D., Burkle, A. & Chang, Y. Role of poly(ADP-ribosyl)ation in DNA-PKcs- independent V(D)J recombination. *Proc. Natl. Acad. Sci. U. S. A.* **99,** 4532–4537 (2002).
102. Hoekstra, H. E., Delaney, N. F., Depristo, M. A. & Hartl, D. L. NMR spectroscopy of native and in vitro tissues implicates polyADP ribose in biomineralization. *Science* **344,** 742–746 (2014).
103. Bai, P. & Cantó, C. The role of PARP-1 and PARP-2 enzymes in metabolic regulation and disease. *Cell Metab.* **16,** 290–295 (2012).
104. Hans, C. P. *et al.* Thieno [2,3-c] Isoquinolin-5-one, a potent poly (ADP-ribose) polymerase inhibitor , promotes atherosclerotic plaque regression in high-fat diet-fed apolipoprotein E-deficient mice: Effects on inflammatory markers and lipid content. *J. Pharmacol. Exp. Ther.* **329,** 150–158 (2009).
105. O'Connor, M. J. Targeting the DNA damage response in cancer. *Mol. Cell* **60,** 547–560 (2015).
106. Lupo, B. & Trusolino, L. Inhibition of poly(ADP-ribosyl)ation in cancer: Old and new paradigms revisited. *Biochim. Biophys. Acta - Rev. Cancer* **1846,** 201–215 (2014).
107. Ferraris, D. V. Evolution of poly(ADP-ribose) polymerase-1 (PARP-1) inhibitors. from concept to clinic. *J. Med. Chem.* **53,** 4561–4584 (2010).
108. Curtin, N. J. & Szabo, C. Therapeutic applications of PARP inhibitors: Anticancer therapy and beyond. *Mol. Aspects Med.* **34,** 1217–12561.

109. Galindo, M. *et al.* Enhancing tumor-targeting monoclonal antibodies therapy by PARP inhibitors. *Oncoimmunology* **5,** 1–9 (2016).
110. Liscio, P., Camaioni, E., Carotti, A., Pellicciari, R. & Macchiarulo, A. From polypharmacology to target specificity: the case of PARP inhibitors. *Curr Top. Med. Chem.* **13,** 2939–2954 (2013).
111. Dedes, K. J. *et al.* Synthetic lethality of PARP inhibition in cancers lacking BRCA1 and BRCA2 mutations. *Cell Cycle* **10,** 1192–1199 (2011).
112. Comen, E. & Robson, M. Poly(ADP-Ribose) polymerase inhibitors in triple-negative breast cancer. *Cancer J.* **16,** 48–52 (2010).
113. Turner, N., Tutt, A. & Ashworth, A. Hallmarks of 'BRCAness' in sporadic cancers. *Nat. Rev. Cancer* **4,** 814–819 (2004).
114. Weston, V. J. *et al.* The PARP inhibitor olaparib induces significant killing of ATM -deficient lymphoid tumor cells in vitro and in vivo. *Blood* **116,** 4578–4587 (2010).
115. Bryant, H. E. *et al.* Specific killing of BRCA2-deficient tumours with inhibitors of poly(ADP-ribose) polymerase. *Nature* **434,** 913–917 (2005).
116. McCabe, N. *et al.* Deficiency in the repair of DNA damage by homologous recombination and sensitivity to poly(ADP-ribose) polymerase inhibition. *Cancer Res.* **66,** 8109–8115 (2006).
117. Lord, C. J., McDonald, S., Swift, S., Turner, N. C. & Ashworth, A. A high-throughput RNA interference screen for DNA repair determinants of PARP inhibitor sensitivity. *DNA Repair (Amst).* **7,** 2010–2019 (2010).
118. Livraghi, L. & Garber, J. E. PARP inhibitors in the management of breast cancer: current data and future prospects. *BMC Med.* **13,** 188 (2015).
119. Edwards, S. L. *et al.* Resistance to therapy caused by intragenic deletion in BRCA2. *Nature* **451,** 1111–1115 (2008).
120. Gameiro, J., Nagib, P. & Verinaud, L. The thymus microenvironment in regulating thymocyte differentiation. *Cell Adhes. Migr.* **4,** 382–390 (2010).
121. Schwarz, B. a & Bhandoola, A. Circulating hematopoietic progenitors with T lineage potential. *Nat. Immunol.* **5,** 953–960 (2004).
122. Pelayo, R. *et al.* Lymphoid progenitors and primary routes to becoming cells of the immune system. *Curr. Opin. Immunol.* **17,** 100–107 (2005).
123. Shortman, K. & Wu, L. Early T lymphocyte progenitors. *Annu. Rev. Immunol.* **14,** 29–47 (1996).
124. Porritt, H. E. *et al.* Heterogeneity among DN1 prothymocytes reveals multiple progenitors with different capacities to generate T cell and non-T cell lineages. *Immunity* **20,** 735–745 (2004).
125. Boudil, A. *et al.* IL-7 coordinates proliferation, differentiation and Tcra recombination during thymocyte β-selection. *Nat. Immunol.* **16,** 397–405 (2015).
126. Bhandoola, A., von Boehmer, H., Petrie, H. T. & Zúñiga-Pflücker, J. C. Commitment and developmental potential of extrathymic and intrathymic T cell precursors: Plenty to choose from. *Immunity* **26,** 678–689 (2007).
127. Petrie, H. T., Livak, F., Burtrum, D. & Mazel, S. T cell receptor gene recombination patterns and mechanisms: cell death, rescue, and T cell production. *J. Exp. Med.* **182,** 121–7 (1995).
128. Yannoutsos, N. *et al.* The role of recombination activating gene (RAG) reinduction in thymocyte development in vivo. *J. Exp. Med.* **194,** 471–480 (2001).

129. Xiong, J., Parker, B. L., Dalheimer, S. L. & Yankee, T. M. Interleukin-7 supports survival of T-cell receptor-β-expressing CD4-CD8- double-negative thymocytes. *Immunology* **138,** 382–391 (2013).
130. Rothenberg, E. V. & Taghon, T. Molecular genetics of T cell development. *Annu. Rev. Immunol.* **23,** 601–649 (2005).
131. Guo, J. *et al.* Regulation of the TCRalpha repertoire by the survival window of CD4(+)CD8(+) thymocytes. *Nat. Immunol.* **3,** 469–76 (2002).
132. Capone, M., Hockett, R. D. & Zlotnik, A. Kinetics of T cell receptor beta, gamma, and delta rearrangements during adult thymic development: T cell receptor rearrangements are present in CD44(+)CD25(+) Pro-T thymocytes. *Proc. Natl. Acad. Sci. U. S. A.* **95,** 12522–12527 (1998).
133. McBlane, J. F. *et al.* Cleavage at a V(D)J recombination signal requires only RAG1 and RAG2 proteins and occurs in two steps. *Cell* **83,** 387–395 (1995).
134. Zha, S. *et al.* Ataxia telangiectasia-mutated protein and DNA-dependent protein kinase have complementary V(D)J recombination functions. *Proc. Natl. Acad. Sci. U. S. A.* **108,** 2028–2033 (2011).
135. Kim, D. R., Park, S. J. & Oettinger, M. A. V(D)J recombination: site-specific cleavage and repair. *Mol. Cells* **10,** 367–374 (2000).
136. Rabenstein, H. *et al.* Differential kinetics of antigen dependency of CD4+ and CD8+ T cells. *J. Immunol.* **192,** 3507–3517 (2014).
137. Koji Eshima, H. S. and N. S. Cross-positive selection of thymocytes expressing a single TCR by multiple major histocompatibility complex molecules of both classes: Implications for CD4 + versus CD8 + lineage commitment. *J. Immunol.* (2006).
138. Belizário, J. E., Brandão, W., Rossato, C. & Peron, J. P. Thymic and postthymic regulation of naïve CD4 + T-cell lineage fates in humans and mice models. *Mediators Inflamm.* **2016** (2016).
139. Germain, R. N. T-cell development and the CD4-CD8 lineage decision. *Nat. Rev. Immunol.* **2,** 309–322 (2002).
140. Xing, Y. & Hogquist, K. A. T-cell tolerance: Central and peripheral. *Cold Spring Harb. Perspect. Biol.* **4,** 1–15 (2012).
141. Han, B. Y. *et al.* Zinc finger protein Zfp335 is required for the formation of the naïve T cell compartment. *Elife* **3,** 1–28 (2014).
142. Xu, X. & Ge, Q. Maturation and migration of murine CD4 single positive thymocytes and thymic emigrants. *Comput. Struct. Biotechnol. J.* **9,** e201403003 (2014).
143. Hsu, F.-C., Pajerowski, A. G., Nelson-Holte, M., Sundsbak, R. & Shapiro, V. S. NKAP is required for T cell maturation and acquisition of functional competency. *J. Exp. Med.* **208,** 1291–1304 (2011).
144. Boursalian, T. E., Golob, J., Soper, D. M., Cooper, C. J. & Fink, P. J. Continued maturation of thymic emigrants in the periphery. *Nat. Immunol.* **5,** 418–425 (2004).
145. Jameson, S. C. Maintaining the norm: T-cell homeostasis. *Nat. Rev. Immunol.* **2,** 547–556 (2002).
146. Takada, K. & Jameson, S. C. Naive T cell homeostasis: from awareness of space to a sense of place. *Nat. Rev. Immunol* **9,** 823–832 (2009).
147. Tan, J. T. *et al.* IL-7 is critical for homeostatic proliferation and survival of naive T cells. *Proc. Natl. Acad. Sci. U. S. A.* **98,** 8732–8737 (2001).

148. Bradley, L. M., Haynes, L. & Swain, S. L. IL-7: Maintaining T-cell memory and achieving homeostasis. *Trends Immunol.* **26,** 172–176 (2005).
149. Vivien, L., Benoist, C. & Mathis, D. T lymphocytes need IL-7 but not IL-4 or IL-6 to survive in vivo. *International immunology* **13,** 763–768 (2001).
150. Goldrath, A. W. *et al.* Cytokine requirements for acute and basal homeostatic proliferation of naive and memory CD8+ T cells. *J. Exp. Med.* **195,** 1515–1522 (2002).
151. Blander, J. M. *et al.* A Pool of central memory-like CD4 T cells contains effector memory precursors. *J. Immunol.* **170,** 2940–2948 (2003).
152. Littman, D. R. & Rudensky, A. Y. Th17 and regulatory T cells in mediating and restraining inflammation. *Cell* **140,** 845–858 (2010).
153. Zhou, L., Chong, M. M. W. & Littman, D. R. Plasticity of CD4+ T cell lineage differentiation. *Immunity* **30,** 646–655 (2009).
154. Weinmann, A. S. Regulatory mechanisms that control T-follicular helper and T-helper 1 cell flexibility. *Immunol. Cell Biol.* **92,** 34–39 (2014).
155. Wang, X. & Mosmann, T. In vivo priming of CD4 T cells that produce interleukin (IL)-2 but not IL-4 or interferon (IFN)-gamma, and can subsequently differentiate into IL-4- or IFN-gamma-secreting cells. *J. Exp. Med.* **194,** 1069–1080 (2001).
156. Caza, T. & Landas, S. Functional and phenotypic plasticity of CD4+ T cell subsets. *Biomed Res. Int.* **2015** (2015).
157. Vladar, E. K., Lee, Y. L., Stearns, T. & Axelrod, J. D. $CD4^{+}$ $CD44^{v.low}$ cells are unique peripheral precursors that are distinct from recent thymic emigrants and stem cell-like memory cells. *Cell Immunol.* **296,** 37–54 (2015).
158. Bettelli, E. *et al.* Reciprocal developmental pathways for the generation of pathogenic effector TH17 and regulatory T cells. *Nature* **441,** 235–238 (2006).
159. Crotty, S. T Follicular helper cell differentiation, function, and roles in disease. *Immunity* **41,** 529–542 (2014).
160. Vignali, D. a, Collison, L. W. & Workman, C. J. How regulatory T cells work. *Nat. Rev. Immunol.* **8,** 523–532 (2009).
161. Curotto de Lafaille, M. A. & Lafaille, J. J. Natural and adaptive Foxp3+ regulatory T cells: More of the same or a division of labor? *Immunity* **30,** 626–635 (2009).
162. Fontenot, J. D., Gavin, M. A. & Rudensky, A. Y. Foxp3 programs the development and function of CD4+CD25+ regulatory T cells. *Nat. Immunol.* **4,** 330–336 (2003).
163. Craft, J. E. Follicular helper T cells in immunity and systemic autoimmunity. *Nat. Rev. Rheumatol.* **8,** 337–347 (2012).
164. Büttcher, J. P. *et al.* IL-6 trans-Signaling-dependent rapid development of cytotoxic CD8+ T cell function. *Cell Rep.* **8,** 1318–1327 (2014).
165. Curtsinger, J. M., Lins, D. C., Johnson, C. M. & Mescher, M. F. Signal 3 tolerant CD8 T cells degranulate in response to antigen but lack granzyme B to mediate cytolysis. *J. Immunol.* **175,** 4392–9 (2005).
166. MacLeod, M. K. L. *et al.* Vaccine adjuvants aluminum and monophosphoryl lipid A provide distinct signals to generate protective cytotoxic memory CD8 T cells. *Proc. Natl. Acad. Sci. U. S. A.* **108,** 7914–7919 (2011).
167. CD8+ T cells: Foot soldiers of the immune system. *Immunity* **35,** 161–168 (2011).

168. Yélamos, J. *et al.* PARP-2 deficiency affects the survival of CD4+CD8+ double-positive thymocytes. *EMBO J.* **25,** 4350–4360 (2006).
169. Saenz, L. *et al.* Transcriptional regulation by poly(ADP-ribose) polymerase-1 during T cell activation. *BMC Genomics* **9,** 171 (2008).
170. Zhang, P. *et al.* PARP-1 controls immunosuppressive function of regulatory T cells by destabilizing Foxp3. *PLoS One* **8,** e71590 (2013).
171. Luo, X. *et al.* Poly(ADP-ribosyl)ation of FOXP3 protein mediated by PARP-1 protein regulates the function of regulatory T cells. *J. Biol. Chem.* **290,** 28675–28682 (2015).
172. Nasta, F., Laudisi, F., Sambucci, M., Rosado, M. M. & Pioli, C. Increased Foxp3+ regulatory T cells in poly(ADP-ribose) polymerase-1 deficiency. *J. Immunol.* **184,** 3470–3477 (2010).
173. Olabisi, O. a *et al.* Regulation of transcription factor NFAT by ADP-ribosylation. *Mol. Cell. Biol.* **28,** 2860–2871 (2008).
174. Valdor, R. *et al.* Regulation of NFAT by poly(ADP-ribose) polymerase activity in T cells. *Mol. Immunol.* **45,** 1863–1871 (2008).
175. Sambucci, M. *et al.* Effects of PARP-1 deficiency on Th1 and Th2 cell differentiation. *Sci. World J.* **2013** (2013).
176. Thoren, F. B., Romero, A. I. & Hellstrand, K. Oxygen radicals induce poly(ADP-ribose) polymerase-dependent cell death in cytotoxic lymphocytes. *J. Immunol.* **176,** 7301–7307 (2006).
177. Ambrose, H. E. *et al.* Poly(ADP-ribose) polymerase-1 (Parp-1)-deficient mice demonstrate abnormal antibody responses. *Immunology* **127,** 178–186 (2009).
178. Aldinucci, a *et al.* A key role for poly(ADP-ribose) polymerase-1 activity during human dendritic cell maturation. *J. Immunol* **179,** 305–312 (2007).
179. Lee, P. P. *et al.* A critical role for Dnmt1 and DNA methylation in T cell development, function, and survival. *Immunity* **15,** 763–774 (2001).
180. Schreiber, R. I. E., Muller, S., Masson, M. & Niedergang, C. XRCC1 is specifically associated with poly (ADP-ribose) polymerase and negatively regulates its activity following DNA damage. *Mol. Cell Biol.* **18,** 3563–3571 (1998).
181. Seder, R. A. & Ahmed, R. Similarities and differences in CD4+ and CD8+ effector and memory T cell generation. *Nat. Immunol* .**4,** 835–842 (2003).
182. Prlic, M., Lefrancois, L. & Jameson, S. C. Multiple choices: regulation of memory CD8 T cell generation and homeostasis by interleukin (IL) -7 and IL-15. *J. Exp. Med.* **195,** 17–20 (2002).
183. Kaech, S. M. *et al.* Selective expression of the interleukin 7 receptor identifies effector CD8 T cells that give rise to long-lived memory cells. *Nat. Immunol.* **4,** 1191–1198 (2003).
184. Peschon, B. J. J. *et al.* Early lymphocyte expansion is severely impaired in interleukin 7 receptor-deficient mice. *J. Exp. Med.* **180,** 6–11 (1994).
185. Kondo, M., Weissman, I. L. & Akashi, K. Identification of clonogenic common lymphoid progenitors in mouse bone marrow. *Cell* **91,** 661–672 (1997).
186. Fernandez-Capetillo, O., Lee, A., Nussenzweig, M. & Nussenzweig, A. H2AX: The histone guardian of the genome. *DNA Repair (Amst).* **3,** 959–967 (2004).

187. Kuo, L. J. & Yang, L.-X. Gamma-H2AX - a novel biomarker for DNA double-strand breaks. *In Vivo* **22,** 305–9 (2008).
188. Affar, E. B. *et al.* Caspase-3-mediated processing of poly (ADP-ribose) glycohydrolase during apoptosis. **276,** 2935–2942 (2001).
189. Crotty, S. Follicular helper CD4 T cells (TFH). *Annu. Rev. Immunol.* **29,** 621–663 (2011).
190. Grossman, Z. & Paul, W. E. Dynamic tuning of lymphocytes: physiological basis, mechanisms, and function. *Annu. Rev. Immunol.* **33,** 677–713 (2015).
191. Prochazkova, J., Sakaguchi, S., Owusu, M. & Mazouzi, A. DNA repair cofactors ATMIN and NBS1 are required to suppress T cell cctivation. *PLoS Genet.* **11,** 1–26 (2015).
192. Akashi, K., Kondo, M., Freeden-jeffry, U. Von, Murray, R. & Weissman, I. L. Bcl-2 rescues T lymphopoiesis in interleukin-7 receptor – deficient mice. **89,** 1033–1041 (1997).
193. Schmidt-supprian, M. *et al.* Mature T cells depend on signaling through the IKK complex. **19,** 377–389 (2003).
194. Sibon, D. *et al.* HTLV-1 propels untransformed CD4 + lymphocytes into the cell cycle while protecting CD8 + cells from death. *Immunity* **19,** 377-389 (2006).
195. Choi, J. *et al.* Genomic landscape of cutaneous T cell lymphoma. *Nat. Genet.* **47,** 1011–1019 (2015).
196. Palomero, T. *et al.* Recurrent mutations in epigenetic regulators RHOA and FYN kinase in peripheral T cell lymphomas. *Nat. Genet.* **46,** 166–170 (2014).
197. Papers, J. B. C., Jeang, K. & Giam, C. Life, death, and tax : Role of HTLV-I oncoprotein in genetic instability and cellular transformation. *J. Biol. Chem.* **279,** 51–55 (2004).
198. Sinclair, C., Bains, I., Yates, A. J. & Seddon, B. Asymmetric thymocyte death underlies the CD4 : CD8 T-cell ratio in the adaptive immune system. (2013). *Proc. Natl. Acad. Sci. U.S.A.* **110,** 2905-2914 (2013).
199. Ernst, B., Lee, D. S., Chang, J. M., Sprent, J. & Surh, C. D. The peptide ligands mediating positive selection in the thymus control T cell survival and homeostatic proliferation in the periphery. *Immunity* **11,** 173–181 (1999).
200. Cho, B. B. K., Rao, V. P., Ge, Q., Eisen, H. N. & Chen, J. Homeostasis-stimulated proliferation drives naive T cells to differentiate directly into memory T cells. *J. Exp. Med.* **192,** 549-556 (2000).
201. Weston, V. J. *et al.* The PARP inhibitor olaparib induces significant killing of ATM -deficient lymphoid tumor cells in vitro and in vivo. *Blood* **116,** 4578–4588 (2016).
202. Kubota, E. *et al.* Low ATM protein expression and depletion of p53 correlates with olaparib sensitivity in gastric cancer cell lines. *Cell Cycle* **13,** 2129–2137 (2014).
203. Moudry, P. *et al.* TOPBP1 regulates RAD51 phosphorylation and chromatin loading and determines PARP inhibitor sensitivity. *J. Cell Biol.* **212,** 2129-2137(2016).
204. Williamson, C. T. *et al.* Enhanced cytotoxicity of PARP inhibition in mantle cell lymphoma harbouring mutations in both ATM and p53. *EMBO Mol. Med.* **4,** 515–527 (2012).

205. Sonnenblick, A., de Azambuja, E., Azim Jr, H. A. & Piccart, M. An update on PARP inhibitors moving to the adjuvant setting. *Nat. Rev. Clin. Oncol.* **12,** 27–41 (2015).
206. Wahlberg, E. *et al.* Family-wide chemical profiling and structural analysis of PARP and tankyrase inhibitors. *Nat. Biotech* **30,** 283–288 (2012).
207. Macchiarulo, A. PARP inhibitors: polypharmacology versus selective inhibition. *FEBS J.* **280,** 3563–3575 (2013).